RIGA TECHNICAL UNIVERSITY

Faculty of Computer Science and Information Technology

Department of Engineering Mathematics

Sergejs NAZAROVS

Ph. D. student of Mathematical Modelling program

LINEAR AND WEAKLY NON-LINEAR STABILITY ANALYSIS OF SHALLOW FLUID FLOWS IN OPEN SYSTEMS

Ph. D. Thesis

Scientific supervisor

Dr. Math., Prof.

A. Koliskins

Rīga 2008

Contents

1 ABSTRACT

The present thesis considers stability of shallow shear flows in open channels. Shallow shear flows are widespread in nature and engineering, so it is important to know factors that are affecting flow stability.

A flow is shallow when it's transverse scale is much larger than fluid depth. Limited depth strongly influences behavior of perturbation, so it differs from the one in deep flows. Development of three-dimensional perturbations is impossible due to small vertical scale of the flow. Two-dimensional instabilities are supressed by bottom friction that becomes a major factor affecting the flow.

Shear flows have transverse velocity gradient. Difference in velocities between adjacent layers leads to shear stresses that may cause lateral motion of the fluid and become an onset of instabilities. Wake flows, mixing layers, jets are examples of shear flows that are abundant in nature.

Stability of shear shallow flows is affected by many factors. Vertical non-uniformity of velocity, fluctuation of depth, presence of particles, change of flow profile downstream are some of them, that are considered in the thesis.

Fluctuation of depth is usually omited in stability analysis of shallow flows. A "rigid-lid" assumption is often applied that implies the flow depth is constant. However application of the "rigid-lid" assumption may introduce some error in the results. The error that may arise due to omiting possible depth fluctuations is analyzed in this thesis. Froude number is used to characterize flow deviation from the "rigid-lid" assumption. It is found that for values of the Froude number typical for natural shallow flows the error due to the "rigid-lid" assumption is small and can be neglected.

As shallow flow model is based on equations that are depth-averaged, vertical non-uniformity of velocity components is not taken into account. The thesis considers how velocity non-uniformity affects results of linear stability analysis and evaluates the error due to neglection of velocity non-uniformity. The vertical velocity profile deviation from uniform is expressed with momentum

correction coefficients. It is found that for values of momentum correction coefficients, that are typical for flows abundant in nature, the error that arise if the vertical non-uniformity of velocty is neglected may reach significant values. So, it might be important to use momentum correction coefficients for analysis of shallow shear flows.

Linear analysis allows to define conditions when the transition from stable to unstable flow takes place. Linear analysis however does not give a clue about further evolution of perturbation.

Weakly non-linear analysis is employed to track development of perturbation. A perturbation amplitude function is used that is weakly dependent on time and coordinate. As a result of weakly-nonlinear stability analysis the Ginzburg-Landau equation is derived that governs growth of perturbation. Numerical methods allowing to calculate coefficients of the Ginzburg-Landay equations have also been developed. The Ginzburg-Landau equation contains a coefficient, often referred to as ”the Landau constant”, that defines if perturbation amplitude saturation and appearance of the secondary flow is possible.

Stability of two-phase flow is also considered in the thesis by means of linear and weakly non-linear method. Examples of two-phase flows are gas-particle flow, gas-droplet flow, liquid-particle flow. A particle loading parameter that envolves concentration and mass of the particles as well as drag on particles and particle response time is used in order to include influence of particles into the model. Linear stability analysis results clearly indicate that presence of particles or droplets in a gas flow enhance flow stability. Weakly non-linear analysis results show that perturbation amplitude is governed by the Ginzburg-Landay equation. The coefficients of the Ginzburg-Landau equation are calculated and calculation results indicate that perturbation finite-amplitude equilibrium is possible. The effect of particle loading parameter on finite perturbation amplitude is evaluated. It is shown, that presence of particles leads to finite amplitude decrease. In addition, it is shown that pure periodic solutions of the Ginzburg-Landau equation are unstable (and, therefore, not observable).

Stability analysis is usually performed under the assumption that the transverse velocity profile of the flow is not changing downstream. This is not the case, however, for real flows. Therefore an approach to stability analysis of a shallow flow with slowly altering velocity profile has been developed in the thesis. As a result a leading order approximation to the perturbation stream function has been derived. The approximation contains three terms. Important conclusions can

be drawn by looking at the form of the leading order approximation. First, all the three terms contain information related to the amplitude and phase of the perturbation. Second, the growth rate and phase speed of the perturbation at any given downstream station depends on the choice of the perturbed quantities (e. g. velocity components). Finally, the growth rate and phase speed depend even on the location where these quantities were calculated.

2 ANOTĀCIJA

Promocijas darbā ir apskatīta seklo bīdes plūsmu stabilitātes analīze atklātās hidrodinamiskās sistēmās. Seklās bīdes plūsmas ir plaši izplatītas dabā un inženierpielietojumos, tāpēc ir svarīgi zināt, kādi faktori ietekmē plūsmas stabilitāti. Seklā plūsma ir plūsma ar sķērsvirziena mērogu daudz lielāku par plūsmas dziļumu. Ierobežots dziļums stipri ietekmē perturbācijas attīstības veidu, tāpēc tas atšķiras no perturbācijas attīstības veida dziļajā ūdenī. Trīsdimensiju perturbāciju attīstība nav iespējama mazā ūdens dziļuma dēļ. Divdimensiju perturbāciju attīstība ir apgrūtināta plūsmas gultnes berzes dēļ, kas kļūst par nozīmīgu faktoru, kas ietekmē plūsmu.

Bīdes plūsmas ir plūsmas ar šķērsvirziena ātruma gradientu. Blakusslāņu ātrumu starpība var veicināt bīdes spriegumu veidošanos, kas izsauc fluīda pārvietošanos šķērsvirzienā un var kļūt par nestabilitātes avotu. Plūsmas aiz šķēršļiem, strūklas ir tipiski bīdes plūsmu piemēri dabā.

Seklo bīdes plūsmu stabilitāti ietekmē daudzi faktori. Ātruma vertikālā profila nevienmērība, plūsmas dziļuma fluktuācijas, daliņu klātbūtne, plūsmas ātruma šķērsvirziena profila izmaiņas lejup pa straumi ir daži faktori, kas var ietekmēt plūsmas stabilitāti, un šo faktoru ietekme ir analizēta promocijas darbā.

Plūsmas dziļuma fluktuācijas parasti tiek ignorētas, veicot stabilitātes analīzi. Bieži pielieto ”cietā vāka” pieņēmumu . Tas nozīmē, ka plūsmas dziļums tiek pieņemts par konstantu. ”Cietā vāka” pieņēmums var radīt kļūdas stabilitātes analīzes rezultātos. Promocijas darbā tiek analizēta kļūda, kas var parādīties plūsmas dziļuma fluktuāciju neievērošanas dēļ. Frude skaitli izmanto, lai raksturotu plūsmas novirzi no ”cietā vāka” pieņēmuma. Analīzes rezultātā konstatēts, ka kļūda, kas rodas pie Frude skaitļa vērtībām, kas ir sastopamas dabā, ir neliela un to var ignorēt.

Seklās plūsmas modelis balstās uz vienādojumiem, kuros izmanto plūsmas ātruma komponenšu vidējās vērtības. Vetikālā ātruma profila nevienmerība netiek ņemta vērā. Promocijas darbā veikta analīze ar mērķi noskaidrot, kā ātruma nevienmērība vertikālā virzienā var ietekmēt stabilitātes analīzes rezultātus. Tiek novērtēta arī kļūda, kas rodas vidējo vērtību izmanotšanas dēļ. Veicot analīzi, ātruma profila nevienmerība tiek izteikta, izmantojot impulsa korekcijas koefi-

cientus. Tika konstatēts, ka pie impulsa korekcijas koeficientu vērtībām, kas ir sastopamas dabā un inženierpielietojumos, kļūda, kas parādās, ja ātruma nevienmērība tiek ignorēta, var sasniegt nozīmīgu līmeni. Tātad ir svarīgi pielietot impulsa korekcijas koeficientus, veicot seklo bīdes plūsmu stabilitātes analīzi.

Lineārā analīze ļauj noteikt nosacījumus, pie kādiem plūsma maina stabilitāti. No otras puses, lineārā analīze nedod iespēju modelēt talāko perturbācijas attīstību.

Vāji nelineārā analīze ir pielietota, lai sekotu līdzi perturbācijas augšanai. Ir izmantota perturbācijas amplitūdas funkcija, kas ir vāji atkarīga no laika un koordinātas. Vāji nelineārās analīzes veikšanas rezultātā tika iegūts Ginzburga-Landau vienādojums, kas apraksta perturbācijas attīstību. Tika izveidotas arī skaitliskās metodes, kas atļauj izrēķināt Ginzburga - Landau vienādojuma koeficientus. Ginzburga - Landau vienādojums satur koeficientu, ko bieži sauc par "Landau konstanti", kas nosaka, vai ir iespējami perturbācijas amplitūdas piesātinājums un sekundārās plūsmas stabilizēšana.

Promocijas darbā ir arī analizēta divfāzu plūsmas stabilitāte. Divfāzu plūsmas piemēri ir ūdens vai gāzes plūsmas, kas satur cietas daliņas, kā arī gāzes plūsmas, kas satur šķidruma pilienus. Lai aprakstītu daļiņu ietekmi vienādojumos, tika pielietots daļiņu koncentrācijas parametrs, kas ietver sevī daļiņu koncentrāciju, masu, daliņu reakcijas laiku. Lineārās stabilitātes analīzes rezultāti parāda, ka daliņas palielina fluīda plūsmas stabilitāti. Vāji nelineārās analīzes rezultāts parāda, ka perturbācijas amplitūdu apraksta Gizburga-Landau vienādojums. Ginzburga-Landau vienādojuma koeficienti ir aprēķināti, un rezultāti parāda, ka ir iespējams amplitūdas piesātinājums un sekundārās plūsmas stabilizēšana. Ir novērtēta daļiņu koncentrācijas parametra ietekme uz galīgo amplitūdas vērtību. Redzams, ka, daļiņu koncentrācijas parametram pieaugot, galīgā amplitūdas vērtība samazinas. Ir arī parādīts, ka plakana viļņa atrisinājums Ginzburga - Landau vienādojumam nav stabils, tas nozīmē, ka sekundārai plūsmai ir sarežģītāka struktūra.

Stabilitātes analīze parasti tiek veikta, izmantojot pieņēmumu, ka plūsmas ātruma profils nav atkarīgs no gareniskās koordinātas. Reālām plūsmām, tomēr profils ir atkarīgs. Tapēc tika izstrādāta stabilitātes analīzes metode, ko var pielietot plūsmām ar ātruma profilu, kas ir vāji atkarīgs no gareniskās koordinātas. Ir iegūta risinājuma vadošās kārtas aproksimācija, kas satur trīs locekļus. Pēc tās formas, var secināt, ka, pirmkārt, visi trīs labās puses locekļi satur informāciju, kas attiecas uz amplitūdu un fāzi, otrkārt, perturbācijas augšanas ātrums ir atkarīgs no tā, kāds loceklis

ir perturbēts, un, galvenokārt, tas ir atkarīgs arī no koordinātas.

3 INTRODUCTION

3.1 Shear flows

A shear flow is a flow with transverse velocity gradient. The existence of the gradient leads to appearance of viscous forces. The faster layer is slowed down by interaction with slower layer, but the velocity of the slower layer is increased according to the third law of Newton. This is the way momentum is transferred from one layer to another. Viscous forces acting in shear flows may lead to transverse movement which in turn can lead to fluid instabilities. Shear flows are widespread in nature and engineering. The two typical examples of shear flows are wake flows and mixing layers. A wake flow is a flow downstream of a body immersed in a stream or the flow behind a body propagating through a fluid. Wakes are narrow elongated regions, usually filled with large and small eddies. Examples of wake flows are eddies of a bridge pier immersed in a river stream, or of a ship propelled through the water. Velocity profile of the wake flow is not uniform thus leading to shear stresses. The wake flow velocity profile can be approximated by a hyperbolic secant function (see Figure 3.1). Chen and Jirka [2] suggested the following formula for approximating wake flow velocity profile:

$$U(y) = \breve{u}(1 - R + 2R\,sech^2(\frac{y}{l})), \tag{3.1}$$

where y is transverse coordinate, l is characteristic dimension of the wake (wake half-width), $\breve{u} = \frac{1}{2}(u_c + u_\infty)$, u_c is flow velocity at the line parallel to the flow and going through the center of the bluff body, u_∞ is ambient flow velocity and parameter R describes non-uniormity of the profile, related to u_c and u_∞ by means of the following formula: $R = \frac{u_c - u_\infty}{u_c + u_\infty}$.

Wakes are usually sustained for very large distances downstream of a body. Ship wakes retain their turbulent character for miles behind a vessel and can be detected by special satellites hours after their generation. Similarly, condensation in the wake of aircraft sometimes makes it look like a narrow braided cloud, traversing the sky. Turbulence in the wake of bluff bodies in some cases

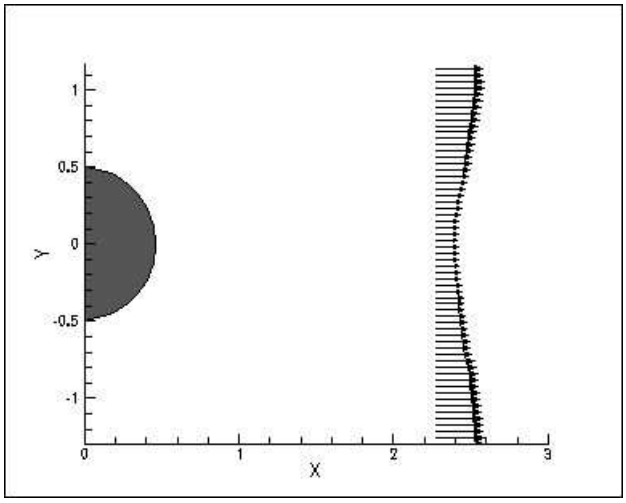

Figure 3.1: Hyperbolic secant velocity profile of a wake flow.

may consist of all sizes of eddies, which interact with each other in their unruly motion. However, eddies may organize themselves into coherent structures where large groups of eddies form a well-ordered sequence of vortices. In this case the sense of rotation of these vortices alternates but their spacing may be quite regular. As a result, they can drive a structure that they encounter, or they can exert on the body that created them a force alternating in sign with the same frequency as that of the formation of the vortices. Such forces can impose on structures unwanted vibrations which often lead to serious damage. Flow-induced forces can be catastrophic if they are in tune with the frequency of vibration of the structure. Water circulation behind a bluff body may strongly depend on the size and structure of eddies. In some case areas with poor water circulation can appear in the wake that can result in deposition of sediments and trapping of pollutants.

Mixing layer flow is a flow downstream of junction of two streams of different velocities. Merge of two different streams leads to shear stresses between them that in turn may lead to formation of vortices. Mixing layer flow is usually approximated by a hyperbolic tangent function (see Figure 3.2). The velocity profile may be expressed by the formula:

$$u = 1 + \bar{R}\tanh(y).$$

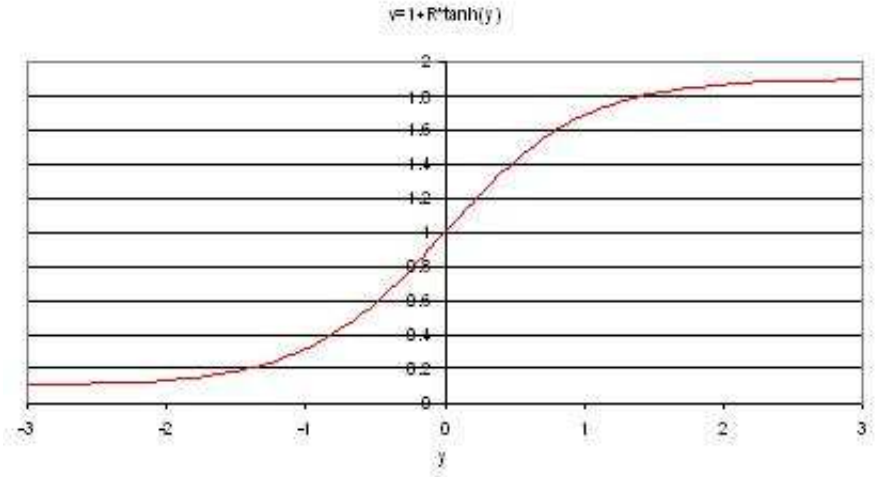

Figure 3.2: Hyperbolic tangent velocity profile of a mixing layer flow

3.2 Shallow flows

Shallow flows are flows with the transverse scale of the flow being much larger than the vertical scale (water depth). Experiments show that development of instabilities in shallow water significantly differs from the development of wakes in deep water. Vortex structures observed in shallow water in many cases may resemble flow patterns in deep water, but in shallow water case the corresponding flow patterns can be observed at much larger values of the Reynolds number. For example, photograph Nr. 173 by Van Dyke [38] shows formation of eddies organized into a vortex street behind an obstacle in shallow water although the Reynolds number for this case is 10^7. Note that vortex street pattern in unbounded flows is limited to significantly smaller Reynolds numbers. This fact demonstrates that different approach is required for shallow flow modelling and stability analysis.

Shallow flows are widespread in nature and engineering and include wake flows and mixing layer flows as well as jets. Therefore shallow flows may be subjected to shear stress. Shear stresses in shallow flows are caused by non-uniformity of the velocity profile and frequently gives rise to perturbations. As the abundance of shallow flows in nature is quite high, there is a need in establishing of a comprehensive model for shallow water flows as well as development of methods that would enable us to perform stability analysis and to track evolution of perturbation. Understanding of mass, momentum and energy exchange in shallow flows is also important. Shallow wake

flows, in particular flows behind islands in rivers and bays, are an object of growing interest from environmental point of view. Complex flows created by eddies can trap pollutants. Poor water circulation in a wake may lead to deposition of sediments. These two factors can result in poor water quality on the sheltered side of an island. Increased concentration of sediments and contaminants might affect marine culture causing, for example, fish disease and mortality. It is believed that the trapping of low-salinity Pearl river water in the sheltered areas led to intense stratification and resulted in deaths of marine inhabitants in Hong Kong in 1994 [14].

Keeping all above-said in mind it is clear that it is essential to know factors influencing flow patterns and, as a result, water circulation in shallow shear flows.

The main factor that affects perturbations and makes them evolve in shallow flows in a different way than in deep flows is bottom friction [20]. Due to shallowness of water, bottom friction has much bigger effect on stability of the flow. In particular, the growth of transverse perturbations is suppressed. Another factor influencing shallow flow stability is limited water depth. Evolution of three-dimensional instabilities is prevented in shallow water leaving space only for two-dimensional perturbations.

One of the main assumptions which is usually made in shallow water theory in order to facilitate the analysis is the independence of the flow characteristics on the vertical coordinate since shallow water equations are depth-averaged equations. There are many cases, however, where this assumption may not valid. Changes in flow geometry, flow regimes or roughness of the bottom boundary can lead to large deviations from the above-mentioned assumption [40], [43]. Momentum correction coefficients are applied by several authors [40], [43] in order to take into account the non-uniformity of the velocity distribution. In particular, momentum correction coefficients are used in [16] for linear stability analysis of shallow mixing layers.

3.3 Mathematical model

A widely-used model for fluid flow is the Navier-Stokes equations:

$$\frac{\partial u}{\partial x}+\frac{\partial v}{\partial y}+\frac{\partial \omega}{\partial z}=0, \tag{3.2}$$

$$\frac{\partial u}{\partial t}+u\frac{\partial u}{\partial x}+v\frac{\partial u}{\partial y}+\omega\frac{\partial u}{\partial z}=g_x-\frac{1}{\rho}\frac{\partial p}{\partial x}+\frac{\mu}{\rho}\nabla^2 u, \tag{3.3}$$

$$\frac{\partial v}{\partial t}+u\frac{\partial v}{\partial x}+v\frac{\partial v}{\partial y}+\omega\frac{\partial v}{\partial z}=g_y-\frac{1}{\rho}\frac{\partial p}{\partial y}+\frac{\mu}{\rho}\nabla^2 v, \tag{3.4}$$

$$\frac{\partial \omega}{\partial t}+u\frac{\partial \omega}{\partial x}+v\frac{\partial \omega}{\partial y}+\omega\frac{\partial \omega}{\partial z}=g_z-\frac{1}{\rho}\frac{\partial p}{\partial z}+\frac{\mu}{\rho}\nabla^2 w, \tag{3.5}$$

where $\vec{g}=(g_x,g_y,g_z)$ is the gravitational force per unit mass, $\vec{u}=(u,v,\omega)$ is the velocity vector, p is pressure, ρ is fluid density, μ us the dynamic viscosity. Integrating the equations over the flow depth enables us to obtain the depth-averaged equations. Integrating the continuity equation (3.2) we get:

$$\int_{Z_b}^{Z}\frac{\partial u}{\partial x}\,dz+\int_{Z_b}^{Z}\frac{\partial v}{\partial y}\,dz+\int_{Z_b}^{Z}\frac{\partial \omega}{\partial z}\,dz=0 \tag{3.6}$$

or

$$\int_{Z_b}^{Z}\frac{\partial u}{\partial x}\,dz+\int_{Z_b}^{Z}\frac{\partial v}{\partial y}\,dz+\omega(Z)-\omega(Z_b)=0, \tag{3.7}$$

where Z and Z_b are the z-coordinates of the water surface and the channel bottom. Respectively, $Z=Z(x,y,t)$, $Z_b=Z_b(x,y)$.

It is known that

$$\frac{\partial}{\partial x}\int_{Z_b}^{Z}u\,dz=\int_{Z_b}^{Z}\frac{\partial u}{\partial x}\,dz+u(Z)\frac{\partial Z}{\partial x}-u(Z_b)\frac{\partial Z_b}{\partial x}, \tag{3.8}$$

$$\frac{\partial}{\partial y}\int_{Z_b}^{Z}v\,dz=\int_{Z_b}^{Z}\frac{\partial v}{\partial y}\,dz+v(Z)\frac{\partial Z}{\partial y}-v(Z_b)\frac{\partial Z_b}{\partial y}. \tag{3.9}$$

Using (3.8) and (3.9) we can rewrite the integrals $\int_{Z_b}^{Z}\frac{\partial u}{\partial x}\,dz$ and $\int_{Z_b}^{Z}\frac{\partial v}{\partial y}\,dz$ as follows:

$$\int_{Z_b}^{Z}\frac{\partial u}{\partial x}\,dz=\frac{\partial}{\partial x}\int_{Z_b}^{Z}u\,dz-u(Z)\frac{\partial Z}{\partial x}+u(Z_b)\frac{\partial Z_b}{\partial x}, \tag{3.10}$$

$$\int_{Z_b}^{Z}\frac{\partial v}{\partial x}\,dz=\frac{\partial}{\partial y}\int_{Z_b}^{Z}v\,dz-v(Z)\frac{\partial Z}{\partial y}+u(Z_b)\frac{\partial Z_b}{\partial y}. \tag{3.11}$$

If the function Z(x,y,t) specifies the z-coordinate of the free-water surface and if it is assumed that any particle on the surface does not leave it, then the vertical velocity of a particle on the water surface, $\omega(z)$, is given by:

$$\begin{aligned}\omega(Z) &= \frac{DZ}{\partial t} = \frac{\partial Z}{\partial t} + \frac{\partial Z}{\partial x}\frac{\partial x}{\partial t} + \frac{\partial Z}{\partial y}\frac{\partial y}{\partial t} \\ &= \frac{\partial Z}{\partial t} + u(Z)\frac{\partial Z}{\partial x} + v(Z)\frac{\partial Z}{\partial y}. \end{aligned} \tag{3.12}$$

Similarly, if the bottom of the channel is rigid, then $F_b = Z_b(x,y) - z = 0$. Hence,

$$w(Z_b) = \frac{DF_b}{\partial t} = u(Z_b)\frac{\partial Z_b}{\partial x} + v(Z_b)\frac{\partial Z_b}{\partial y}. \tag{3.13}$$

Substituting (3.10) - (3.13) into (3.7) we obtain:

$$\begin{aligned}\frac{\partial}{\partial x}\int_{Z_b}^{Z} u\,dz - u(Z)\frac{\partial Z}{\partial x} + u(Z_b)\frac{\partial Z_b}{\partial x} + \frac{\partial}{\partial y}\int_{Z_b}^{Z} v\,dz \\ -v(Z)\frac{\partial Z}{\partial y} + v(Z_b)\frac{\partial Z_b}{\partial y} + \frac{\partial Z}{\partial t} + u(Z)\frac{\partial Z}{\partial x} \\ +v(Z)\frac{\partial Z}{\partial y} - u(Z_b)\frac{\partial Z_b}{\partial x} - v(Z_b)\frac{\partial Z_b}{\partial y} = 0 \end{aligned} \tag{3.14}$$

or

$$\frac{\partial}{\partial x}\int_{Z_b}^{Z} u\,dz + \frac{\partial}{\partial y}\int_{Z_b}^{Z} v\,dz + \frac{\partial Z}{\partial t} = 0. \tag{3.15}$$

Introducing depth-averaging velocities

$$\bar{u} = \frac{1}{d}\int_{Z_b}^{Z} u\,dz$$

and

$$\bar{v} = \frac{1}{d}\int_{Z_b}^{Z} v\,dz,$$

that are the mean values over the depth of the channel, where $d = Z - Z_b$ is the water depth measured normal to the bottom of the channel, we obtain:

$$\frac{\partial Z}{\partial t} + \frac{\partial(\bar{u}d)}{\partial x} + \frac{\partial(\bar{v}d)}{\partial y} = 0. \tag{3.16}$$

We are assuming the vertical acceleration to neglible ($\frac{D\omega}{Dt} \approx 0$, $\mu\nabla^2\omega \approx 0$). Hence, the equation (3.5) reduces to:

$$g_z - \frac{1}{\rho}\frac{\partial p}{\partial z} = 0. \tag{3.17}$$

By integrating the equation (3.17) in the z-direction and considering the atmospheric pressure to be zero, we obtain

$$\int_Z^z g_z\, dz = \frac{1}{\rho}\int_Z^z \frac{\partial p}{\partial z}\, dz$$

or

$$g_z(z-Z) = \frac{1}{\rho}p\Big|_Z^z.$$

so that the distribution of pressure is hydrostatic:

$$p = \rho g_z(z-Z). \tag{3.18}$$

It follows from (3.18) that

$$-\frac{1}{\rho}\frac{\partial p}{\partial x} = g_z\frac{\partial Z}{\partial x}, \tag{3.19}$$

$$-\frac{1}{\rho}\frac{\partial p}{\partial y} = g_z\frac{\partial Z}{\partial y}. \tag{3.20}$$

Multiplying (3.2) by u, we obtain

$$u\frac{\partial u}{\partial x} + u\frac{\partial v}{\partial y} + u\frac{\partial \omega}{\partial z} = 0. \tag{3.21}$$

We add (3.3) and (3.21) and use (3.19) - (3.20):

$$\frac{\partial u}{\partial t} + u\frac{\partial u}{\partial x} + u\frac{\partial v}{\partial y} + u\frac{\partial \omega}{\partial z} + u\frac{\partial u}{\partial x} + v\frac{\partial u}{\partial y} + \omega\frac{\partial u}{\partial z}$$

$$= g_x + g_z \frac{\partial Z}{\partial x} + \frac{\mu}{\rho}\nabla^2 u \tag{3.22}$$

or

$$\frac{\partial u}{\partial t} + \frac{\partial}{\partial x}(u^2) + \frac{\partial}{\partial y}(uv) + \frac{\partial}{\partial z}(u\omega) = g_x + g_z \frac{\partial Z}{\partial x} + \frac{\mu}{\rho}\nabla^2 u. \tag{3.23}$$

Similarly, multiplying equation (3.2) by v, adding to it (3.4) and using (3.19) - (3.20) we obtain

$$\frac{\partial v}{\partial t} + \frac{\partial}{\partial x}(uv) + \frac{\partial}{\partial y}(v^2) + \frac{\partial}{\partial z}(v\omega) = g_y + g_z \frac{\partial Z}{\partial y} + \frac{\mu}{\rho}\nabla^2 v. \tag{3.24}$$

We integrate (3.23) with respect to z from from Z_b to Z:

$$\frac{\partial}{\partial t}\int_{Z_b}^{Z} u\,dz = \int_{Z_b}^{Z} \frac{\partial u}{\partial t}\,dz + u(Z)\frac{\partial Z}{\partial t} - u(Z_b)\frac{\partial Z_b}{\partial t}. \tag{3.25}$$

It follows that

$$\int_{Z_b}^{Z} \frac{\partial u}{\partial t}\,dz = \frac{\partial}{\partial t}\int_{Z_b}^{Z} u\,dz - u(Z)\frac{\partial Z}{\partial t}, \tag{3.26}$$

$$\frac{\partial}{\partial x}\int_{Z_b}^{Z} u^2\,dz = \int_{Z_b}^{Z} \frac{\partial}{\partial x}u^2\,dz + u^2(Z)\frac{\partial Z}{\partial x} - u^2(Z_b)\frac{\partial Z_b}{\partial x}, \tag{3.27}$$

$$\frac{\partial}{\partial y}\int_{Z_b}^{Z} uv\,dz = \int_{Z_b}^{Z} \frac{\partial}{\partial y}(uv)\,dz + u(Z)v(Z)\frac{\partial Z}{\partial y} - u(Z_b)v(Z_b)\frac{\partial Z_b}{\partial y}, \tag{3.28}$$

$$\frac{\partial}{\partial z}\int_{Z_b}^{Z} u\omega\,dz = \int_{Z_b}^{Z} \frac{\partial}{\partial z}(u\omega)\,dz + u(Z)\omega(Z)\frac{\partial Z}{\partial z} - u(Z_b)\omega(Z_b)\frac{\partial Z_b}{\partial z}. \tag{3.29}$$

Hence,

$$\begin{aligned}
&\int_{Z_b}^{Z} \left(\frac{\partial u}{\partial t} + \frac{\partial}{\partial x}(u^2) + \frac{\partial}{\partial y}(uv) + \frac{\partial}{\partial z}(u\omega)\right) dz \\
&= \frac{\partial}{\partial t}\int_{Z_b}^{Z} u\,dz - u(Z)\frac{\partial Z}{\partial t} + \frac{\partial}{\partial x}\int_{Z_b}^{Z} u^2\,dz - u^2(Z)\frac{\partial Z}{\partial x} \\
&\quad + u^2(Z_b)\frac{\partial Z_b}{\partial x} + \frac{\partial}{\partial y}\int_{Z_b}^{Z} (uv)\,dz - u(Z)v(Z)\frac{\partial Z}{\partial y} \\
&\quad + u(Z_b)v(Z_b)\frac{\partial Z_b}{\partial y} + u(Z)\omega(Z) - u(Z_b)\omega(Z_b).
\end{aligned} \tag{3.30}$$

As $u(Z) = u(Z_b)$ and $v(Z) = v(Z_b)$, we get:

$$\frac{\partial}{\partial t}\int_{Z_b}^{Z} u\,dz = \frac{\partial}{\partial t}(\frac{1}{d}\int_{Z_b}^{Z} ud\,dz) = \frac{\partial}{\partial t}(\overline{u}d), \tag{3.31}$$

$$\frac{\partial}{\partial x}\int_{Z_b}^{Z} u^2\,dz = \frac{\partial}{\partial x}(\overline{u^2}d), \tag{3.32}$$

$$\frac{\partial z}{\partial y}\int_{Z_b}^{Z} (uv)\,dz = \frac{\partial}{\partial y}(\overline{uv}d), \tag{3.33}$$

$$\begin{aligned} -u(z)\frac{\partial Z}{\partial t} - u^2(Z)\frac{\partial Z}{\partial x} + u^2(Z_b)\frac{\partial Z_b}{\partial x} - u(Z)v(Z)\frac{\partial Z}{\partial y} \\ +u(Z_b)v(Z_b)\frac{\partial Z_b}{\partial y} = -u(Z)(\frac{\partial Z}{\partial t} + u(Z)\frac{\partial Z}{\partial x} \\ +v(Z)\frac{\partial Z}{\partial y}) + u(Z_b)(u(Z_b)\frac{\partial Z_b}{\partial x} + v(Z_b)\frac{\partial Z_b}{\partial y}). \end{aligned} \tag{3.34}$$

Taking into account the relationship

$$\frac{\partial Z}{\partial t} + u(Z)\frac{\partial Z}{\partial x} + v(Z)\frac{\partial Z}{\partial y} = \omega(Z),$$

$$u(Z_b)\frac{\partial Z_b}{\partial x} + v(Z_b)\frac{\partial Z_b}{\partial y} = \omega(Z_b),$$

the left-hand side of equation (3.30) can be simplified to

$$\frac{\partial}{\partial t}(\overline{u}d) + \frac{\partial}{\partial x}(\overline{u^2}d) + \frac{\partial}{\partial y}(\overline{uv}d). \tag{3.35}$$

Similarly, the right-hand side of (3.24) becomes:

$$\frac{\partial}{\partial t}(\overline{v}d) + \frac{\partial}{\partial x}(\overline{uv}d) + \frac{\partial}{\partial y}(\overline{v^2}d). \tag{3.36}$$

By integrating, the right-hand sides of (3.23) and (3.24) are transformed to the form:

$$(g_x + g_z\frac{\partial Z}{\partial x})d + \int_{Z_b}^{Z} \frac{\mu}{\rho}\nabla^2 u\,dz,$$

$$(g_y + g_z\frac{\partial Z}{\partial y})d + \int_{Z_b}^{Z} \frac{\mu}{\rho}\nabla^2 v\,dz.$$

We have $\dfrac{\partial Z}{\partial x} = \dfrac{\partial(Z_b + d)}{\partial x} = \dfrac{\partial d}{\partial x}$, since $Z_b = const$.

Similarly,

$$\frac{\partial Z}{\partial y} = \frac{\partial d}{\partial y}.$$

Now, let us consider the shear stress terms. In turbulent flow the dynamic viscosity is replaced by an eddy viscosity coefficient. Moreover, a distinction is made between the stresses acting in the $x-y$ plane and the stresses acting in the $x-z$ and $y-z$ planes. For example, the shear-stress term of the momentum equation in the x-direction may be written as

$$\varepsilon_{xy}(\frac{\partial^2 u}{\partial x^2} + \frac{\partial^2 u}{\partial y^2}) + \varepsilon_{zx}\frac{\partial^2 u}{\partial z^2}. \tag{3.37}$$

It is assumed that the effective stresses are dominated by the bottom shear stresses. This means that the first term in (3.37) is neglible as compared to the second term. Integrating the term $\varepsilon_{zx}\frac{\partial^2 u}{\partial Z^2}$ with respect to Z we obtain

$$\int_{Z_b}^{Z} \varepsilon_{zx}\frac{\partial^2 u}{\partial z}\, dz = \varepsilon_{zx}(\frac{\partial u}{\partial z})\mid_{z=Z} - \varepsilon_{zx}(\frac{\partial u}{\partial z})\mid_{z=Z_b} = \tau_{sx} - \tau_{bx},$$

in which τ_{sx} and τ_{bx} are the shear stresses at the water surface and at the channel bottom acting in the x-direction. Similarly, the shear stress for the second equation reduces to

$$\tau_{sy} - \tau_{by}.$$

The shear stresses acting at the water surface due to wind velocity, τ_{sx} and τ_{sy} are neglected and the shear stresses at the channel bottom, τ_{bx} and τ_{by} are evaluated by using empirical formulas. For example, the Chezy formula gives [37]:

$$\tau_b = \frac{\rho g}{c^2}V^2,$$

where $V = \sqrt{\bar{u}^2 + \bar{v}^2}$ and c is Chezy coefficient. Hence

$$\tau_{bx} = \frac{\rho g}{c^2}\bar{u}\bar{V},\ \tau_{by} = \frac{\rho g}{c^2}\bar{v}\bar{V}.$$

Hence, the momentum equations become

$$\frac{\partial}{\partial t}(\bar{u}d) + \frac{\partial}{\partial x}(\bar{u}^2 d) + \frac{\partial}{\partial y}(\overline{uv}d) = (g_x + g_z\frac{\partial d}{\partial x})d - \frac{g\bar{u}}{c^2}\sqrt{\bar{u}^2 + \bar{v}^2}, \tag{3.38}$$

$$\frac{\partial}{\partial t}(\bar{v}d) + \frac{\partial}{\partial x}(\overline{uv}d) + \frac{\partial}{\partial y}(\bar{v}^2 d) = (g_y + g_z\frac{\partial d}{\partial y})d - \frac{g\bar{v}}{c^2}\sqrt{\bar{u}^2 + \bar{v}^2}. \tag{3.39}$$

Denoting d by h we get:

$$\frac{\partial}{\partial t}(\overline{u}\overline{h}) + \frac{\partial}{\partial x}(\overline{u^2}h) + \frac{\partial}{\partial y}(\overline{uv}h) = (g_x + g_z\frac{\partial h}{\partial x})h - \frac{g\overline{u}}{c^2}\sqrt{\overline{u^2}+\overline{v^2}}, \tag{3.40}$$

$$\frac{\partial}{\partial t}(\overline{v}\overline{h}) + \frac{\partial}{\partial x}(\overline{uv}h) + \frac{\partial}{\partial y}(\overline{v^2}h) = (g_y + g_z\frac{\partial h}{\partial y})h - \frac{g\overline{v}}{c^2}\sqrt{\overline{u^2}+\overline{v^2}}. \tag{3.41}$$

Using algebraic transformations we obtain:

$$\begin{aligned} h\frac{\partial\overline{u}}{\partial t} + \overline{u}\frac{\partial h}{\partial t} + \overline{u}\frac{\partial}{\partial x}(\overline{u}\overline{h}) \\ +\overline{u}\overline{h}\frac{\partial\overline{u}}{\partial x} + \overline{v}h\frac{\partial\overline{u}}{\partial y} + \overline{u}\frac{\partial}{\partial y}(\overline{v}\overline{h}) = (g_x + g_z\frac{\partial h}{\partial x})h - \frac{g\overline{u}}{c^2}\sqrt{\overline{u^2}+\overline{v^2}}, \end{aligned} \tag{3.42}$$

$$\begin{aligned} h\frac{\partial\overline{v}}{\partial t} + \overline{v}\frac{\partial h}{\partial t} + \overline{v}\frac{\partial}{\partial x}(\overline{u}\overline{h}) \\ +\overline{u}\overline{h}\frac{\partial\overline{v}}{\partial x} + \overline{v}\frac{\partial}{\partial y}(\overline{v}\overline{h}) + \overline{v}h\frac{\partial v}{\partial y} = (g_y + g_z\frac{\partial h}{\partial y})h - \frac{g\overline{v}}{c^2}\sqrt{\overline{u^2}+\overline{v^2}}. \end{aligned} \tag{3.43}$$

Taking into account that $\frac{\partial h}{\partial t} + \frac{\partial}{\partial x}(\overline{u}\overline{h}) + \frac{\partial}{\partial y}(\overline{v}\overline{h}) = 0$ and dividing (3.42), (3.43) by h we get:

$$\frac{\partial\overline{u}}{\partial t} + \overline{u}\frac{\partial\overline{u}}{\partial x} + \overline{v}\frac{\partial\overline{u}}{\partial y} + = (g_x + g_z\frac{\partial h}{\partial x}) - \frac{g\overline{u}}{hc^2}\sqrt{\overline{u^2}+\overline{v^2}}, \tag{3.44}$$

$$\frac{\partial\overline{v}}{\partial t} + \overline{u}\frac{\partial\overline{v}}{\partial x} + \overline{v}\frac{\partial v}{\partial y} = (g_y + g_z\frac{\partial h}{\partial y}) - \frac{g\overline{v}}{hc^2}\sqrt{\overline{u^2}+\overline{v^2}}. \tag{3.45}$$

Integration of the Navier-Stokes equations along the vertical coordinate means that the non-uniformity of vertical velocity distribution is no more taken into account. The velocity components u and v are considered to be independent on vertical coordinate and at every point of the flow are constant across the flow depth.

In order to compensate for the possible error that may arise from non-uniform vertical velocity distribution of a real flow, momentum correction coefficients β_1, β_2 and β_3 are used (see [43]). The meaning of the coefficients can be explained as follows.

The approach of considering velocity to be uniformly distributed accross the vertical coordinate is satisfied if the following relation holds:

$$\sum mu = (\sum m)U,$$

where u is the velocity of the fluid, m is the mass of the fluid passing through a small cross-section element, U is averaged (mean) velocity.

Let us consider a small cross-sectional area element $\Delta A = \Delta y \Delta z$. The discharge (volume passing through the area element ΔA in a second) is $Q = u\Delta A = u\Delta y\Delta z$. The mass flow rate through the element ΔA is $M = \rho u \Delta A = \rho u \Delta y \Delta z$.

The momentum I passing through the cross-sectional area element ΔA can be calculated from the formula

$$I = \rho u^2 \Delta y \Delta z.$$

By integration of the momentum equation from z_1 to z_2 with respect to z we obtain:

$$I = \int_{z_1}^{z_2} \rho u^2 \Delta y \, dz = \rho \Delta y \int_{z_1}^{z_2} u^2 \, dz.$$

If we consider velocity U to be uniform over the cross-section, then the momentum passing through the element ΔA is

$$\hat{I} = (\rho U) U \Delta y h.$$

In order to compensate for the error introduced by the assumption of uniform velocity distribution across the vertical coordinate a momentum correction coefficient β is used, defined by the expression

$$\beta \hat{I} = I$$

or

$$\beta(\rho U) U \Delta h = \rho \Delta y \int_{z_1}^{z_2} u^2 \, dz.$$

The momentum correction coefficient can be explicitly expressed as follows:

$$\beta = \frac{1}{hU^2} \int_{z_1}^{z_2} u^2 \, dz.$$

Similar to [43] the momentum correction coefficients used in this thesis are defined by formulas:

$$\beta_1 = \frac{1}{hu^2} \int_{z_1}^{z_2} \tilde{u}^2 \, dz, \tag{3.46}$$

$$\beta_2 = \frac{1}{huv} \int_{z_1}^{z_2} \tilde{u}\tilde{v} \, dz, \tag{3.47}$$

$$\beta_3 = \frac{1}{hv^2} \int_{z_1}^{z_2} \tilde{v}^2 \, dz. \tag{3.48}$$

where $\tilde{u}$ and $\tilde{v}$ are the velocity components in the x and y directions respectively.

It is assumed that the coefficients β_1, β_2 and β_3 are independent on the spatial coordinates x and y.

3.4 Stability analysis

Water circulation in a shear flow may depend on stability of the flow. Unstable flows may have better water circulation and better mixing due to formation of large eddies [34].

Stability analysis considers response of the flow to a small disturbance. If the disturbance amplitude decays and the flow returns to its original state, then the flow is defined as stable. However, if the perturbation grows with time and flow changes to a different state then the flow is unstable [33].

By means of stability analysis one can track evolution of disturbances superimposed on the base flow. Ususally it is assumed that the disturbance or perturbation is small; that allows to obtain a linear equation governing the disturbance. However, one needs to keep in mind that in case disturbance velocities reach a couple of percent of the base flow, linear analysis is no more valid as non-linear effects become significant. Although the linear equations have a limited range where they can accurately predict evolution of disturbance, they are important tool that enables detection of physical growth mechanisms and identification of dominant disturbance types [33].

The essence of the stability analysis is well described in [8]. The undisturbed flow, also referred to as the base flow, can be described by a velocity field as well as other fields (like pressure, temperature etc.) that are needed to specify the flow at each point of space and time. If the perturbation is imposed on the flow, the perturbation may be inhibited, stay at the same level or grow to the scale when the flow considerably alters it's structure. The three types of perturbations can be referred to as stable, neutrally stable and unstable respectively [8].

The stability analysis can be performed in the following way. First, a small perturbation is imposed on the flow. The solution with perturbation is substituted into initial non-linear equations. Quadratic terms containing disturbances are neglected so the equations are linearized. Thereby a linear homogeneous system of partial differential equations and boundary conditions is obtained. According to [8] the solution of the system can be expressed as a superposition of components,

each component varying with time like e^{st} for some complex number $s = \sigma + i\omega$. The linear system will determine values of s and the spatial variation of corresponding components as eigenvalues and eigenfunctions. This is effectively the method of normal modes, whereby small disturbances are resolved into modes. Each mode can be analyzed separately, as they all satisfy the linear system.

If $\sigma > 0$ for a mode, then the perturbation is amplified and the mode is said to be unstable. If $\sigma = 0$, the mode is neutrally stable, and the mode is stable if $\sigma < 0$. In this thesis the solution of perturbation is sought as a superposition of functions of transverse coordinate, each of them propagating in lengthwise direction as a wave with certain complex frequency and wavenumber. The wave is represented in the form $\exp(ik(x-ct))$. By denoting ikc as the complex frequency λ we can rewrite the wave expression in the form $\exp(-\lambda t + ikx)$.

The method of normal modes allows to obtain a system of ordinary differential equations.

Under rigid-lid assumption it is possible to introduce a flow function that allows to reduce the system of equations to single ordinary differential equation. The equation, governing the perturbation, is often referred to as Rayleigh equation.

As a system of equations or a single equation for the perturbation has been derived, eigenvalues of the equation are to be examined as they control development of perturbations.

3.5 Previous studies

Due to high abundance in nature and engineering as well as enviromental significance, shallow water flows are object of growing interest. Several authors analyzed stability of shallow flows both experimentally and theoretically [2], [10], [13], [34].

The effect of bottom friction on stability of shallow wake flows is investigated in [2], [4], [34], [35]. According to [35], two-dimentional structures in the flow can be associated with three stability classes. If a small perturbation imposed on the flow increases with time at certain fixed point of the flow and reaches a defined threshold, the flow is said to be absolutely unstable. In case a small perturbation grows at moving point of the flow (is convected downstream) up to certain threshold, the flow is convectively unstable. If a small perturbation decays with time and grows neither at fixed nor at moving point, the flow is said to be hydrodynamically stable. Different flow

patterns correspond to the three stability classes. Chen&Jirka [2] classify them as vortex street, unsteady bubble and steady bubble. The vortex street pattern is observed in an absolutely unstable flow and is characterized by large eddes that arise at the endpoint of the obstacle and propagate downstream. The unsteady bubble wake, typical for convectively unstable flows, has no expressed eddies, although the flow pattern is twisting. Steady bubble wake has smooth pattern free of eddies. The type of a stability class of a flow is ascribed to a value of stability parameter, defined by expression:

$$S = c_f \frac{l}{h},$$

where c_f is bottom friction coefficient, l is characteristic diameter of the obstacle and h is water depth. The distinction between absolute and convective instability can be made by analyzing growth rate of perturbation at points where group velocity is equal to zero. If absolute growth rate is positive at a point where the condition of zero group velocity is satisfied, there exist some modes that will travel upstream, so the flow is absolutely unstable. If absolute growth rate is negative, the flow is convectively unstable.

Grubisic&Smith [18] applied shallow-water equations for mountain-induced flow modeling. The authors investigated influence of bottom friction on stability of wake flow in atmosphere and studied effect of bottom friction on creating and dissipating vorticity. They found that stability of mountain wakes is affected by bottom friction and correlated to the surface drag parameter r that represents ratio of bottom friction to advection. The parameter r is expressed as

$$r = \frac{c_f a}{h(g'h)^{(1-n)/2}},\ n = 0\ or\ 1.$$

Here c_f is a surface drag coefficient, a is half-width of obstacle, h is upstream fluid depth for the vertical scale, g' is reduced gravity, defined as $g' = g\Delta\rho/\rho$ where $\Delta\rho$ is the density difference between layers. The value of n depends on whether only Rayleigh friction is taken into account ($n = 0$) or surface stress is calculated using the bulk aerodynamic friction formula. Grubisic&Smith [18] found that bottom friction has a strong impact on the mean-flow characteristics. Both absolute and convective growth rates are reduced as bottom friction is increased. The bottom friction parameter r controls the stability of the flow: the larger the r parameter is, the more stable the wake will be.

Ghidaoui&Kolyshkin [14] tested validity of rigid-lid assumption for linear stability analysis of shallow wake flows. Rigid-lid assumption is often used under shallow water model. The idea is to replace the original flow by a flow between two parallel plates. The bottom plate has the friction coefficient equal to the one of original channel; the boundary between the top plate and the flow is inviscid. The rigid-lid assumption enables to reduce the system of equations governing the flow to a single equation that remarcably elaborates calculations. The authors found that using the rigid-lid assumption for linear stability analysis will not result in any serious error. Ghidaoui&Kolyshkin also found the stability analysis results to be quite sensitive to the shape of velocity profile. The authors applied weakly non-linear analysis in order to describe evolution of perturbation in shallow wake flows. The Ginzburg-Landau equation has been derived as a governing equation for evolution of perturbation for shallow wake flows.

Crighton&Gaster [6] analyzed stability of slowly diverging jet flow. The authors showed that both theories for diverging flow and for parallel flow agree well with experiment.

Ghidaoui&Kolyshkin [13] analyzed stability of transverse shear flows. The authors evaluated influence of different factors such as Froude number, velocity profile, turbulence and chosen resistance formula on stability analysis results. The Froude number defines how much energy is stored in gravity waves. The authors found that if Froude number is close to zero, the results are close to results obtained under the rigid-lid assumption. On other hand, if the value of Froude number is higher than two, the stability analysis results are no more valid, so non-linear analysis should be applied. The authors studied stability of the flow for two velocity profiles: hyperbolic secant and hyperbolic tangent profile. It is shown that size and shape of the stability domain is affected by the velocity profile as well as non-uniformity of base flow. The choice of the resistance formula has been found to have some effect on stability analysis results. Generally speaking, the friction of the floodplain is the major factor stabilizing the flow. Turbulence dissipation is contributing to the stability too, but its influence diminishes with growing Reynolds number.

The stability of two-phase flows (fluid-particle, gas-fluid and gas-particle flows) has been considered by many authors [7], [39], [41], [42].

Yang et al. [41] analyzed the effect of particles on spatial stability of two-phase gas-particle mixing layers. The results indicate that particles enhance stability of the flow and attenuate the most unstable modes. The maximal spatial amplification rate decreases linearly with the increase

of particle loading parameter, which takes into account the magnitude of shear, particle/fluid density ratio, flow and particle characteristic response time, and ratio of particle drag to Stokes drag. However, the angular frequency of the most unstable mode is relatively unaffected by presence of particles. The numerical simulation was performed under the assumptions that mean velocity profile of the two-phase flow corresponds to the one of the single-phase flow and the particles are initially in dynamic equilibrium with the fluid flow.

Dimas et al [7] include a term describing a dynamic interaction between the fluid and the particle phase. Dynamic particle phase has been found to attenuate the spatial growth rate of instabilities. The attenuation depends on the mean particle loading parameter and particle responsivness parameter. It has been found that for small values of the mean particle loading parameter representing the flow with no dynamic particle motion the growth rate of instabilities linearly decreases with increase of particle loading that is consistent with analysis results of authors (e. g. Yang et al [41]) who neglected the dynamic interation of the particles. For higher values of the mean particle loading parameter the growth rate dependence on particle loading deviates from linear preventing complete stabilization of the flow.

Most of the authors perform analysis of shallow water flows based on equations that are integrated with respect to vertical coordinate. So, the non-uniformity of flow characteristics accross the vertical coordinate is not taken into account and it assumed that vertical velocity distribution is uniform. In some cases, however, this assumption may not be valid. Changes in roughness of the bottom boundary or flow regimes can lead to large deviations from the above-mentioned assumption [40], [43]. Momentum correction coefficients [40], [43] are sometimes used in order to take into account the non-uniformity of the velocity distribution with respect to the vertical coordinate. In particular, momentum correction coefficients are used in [16] for linear stability analysis of shallow mixing layers and in [22] for weakly nonlinear analysis of shallow wakes.

Xia et al [40] explored influence of averaging coefficients including pressure and momentum correction coefficients on the solution of the Saint-Venant equations. Pressure deviation from hydrostatic and flow velocity distribution deviation from uniform have been considered. Simulations were made for the two cases:

- No downstream backwater effect as there is no downstream boundary restriction.
- The flow depth at downstream boundary is unchanged.

The authors found that in absence of downstream backwater effect, the influence of pressure correction coefficient is neglible with no downstream backwater effect. The same statement is correct for momentum correction coefficient. However, is backwater effect is present (and it is always present for a real flow), the value of pressure correction coefficient has a remarkable effect on solution. The momentum correction coefficient has been found to have some influence too, but it is less expressed. In both cases the error increases as a correction coefficient (either pressure or momentum) goes higher. Error grows with increased backwater effect too. The authors state that although the common concept of correction coefficient contribution being minor for steady-flow solutions, for accurate unsteady-flow solutions it might be necessary to take the correction coefficients into account.

Yen [43] states that the assumptions usually made for derivation of open-channel equations are to be re-examined. The author presents an attempt to obtain generalized open-flow equations suitable for examining the assumptions involved in commonly used open-flow equations. As a result equations for unsteady turbulent viscous nonhomogenious flow with free surface have been derived. The derivation technique was based on integration of point form equations of continuity, momentum and energy over a cross-sectional area of the channel. As the distribution of flow characteristics over the cross section is usually not known in details, the resulting equations involve quantities averaged over cross-section. Correction coefficients like mass flux correction factor and momentum correction factor are used to compensate for the deviation arising from averaged approach. Similar correction coefficients are used also in [44]. The derived one-dimensional equations can be employed for engineering applications as they take into account density variation, lateral flow and other factors.

Another assumption that is widely applied for stability analyses of shallow wake flows is that the base flow is assumed to be parallel. The assumption has been used in, for example, [2], [4], [14]. Experimental data, however, show that the width of shallow wake [3] and the width of the mixing layer [31] are slowly changing with respect to the longitudinal coordinate. The slow divergence of the base flow in the downstream direction allows one to construct an asymptotic scheme which takes non-parallelism of shallow water flows into account. Such formulations have been applied in the past to the spatial stability analysis of slowly diverging shear flows in deep water [6], [12]. Recently such a scheme has also been applied to shallow wakes [15].

El-Hady [9] applies a correction due to non-parallelism of the flow on the spatial growth rate. The spatial growth rate σ is sought in the form $\sigma = -\alpha_i - \varepsilon\hat{\alpha}_i + \varepsilon(\frac{1}{\xi_n}\frac{\partial \xi_n}{\partial x_1})_r$. The first term reflects spatial growth rate of a parallel flow. The second term is the nonparallel correction. The third term is correction due to the distortion of the eigenfunction. The curves depicting variation of the spatial growth rates with frequency are presented for different Mach numbers of the flow. The author considers three cases: purely parallel flow (only the first term in the expression of spatial growth rate is used, the second and the third terms are neglected), the flow with non-parallelity correction (the first and the second terms are used), and the flow with both nonparallelity and eigenfunction disturbance correction (all terms are applied). The results indicate that for subsonic Mach numbers the second term tends to overestimate the effect of non-parallelism. If the distortion of eigenfunction is also considered, the non-parallel curve goes close to the curve for parallel case. However, as the Mach number grows, the non-parallel curve moves away from the parallel curve demonstrating strong effect of the non-parallelism. The obtained dependence curves of spatial growth rate on frequency are compared with experimental data. The author shows that application of non-parallelity correction enhances the agreement between the theory and experiment at least for high Mach numbers.

Some authors imposed known controlled disturbances on a flow that favoured study of instabilities. Disturbances were introduced either by mechanical devices such as a vibrating ribbon or by acoustic influence. Forcing a flow in a controlled way hopefully would provide basis for construction of a representative model of instabilities and large-scale structures that occur in shear layer flows.

Gaster et al. [12] performed theoretical and experimental analysis of deep mixing layers. The authors pursued the goal to find the limit where large-scale vortex structure that develops in turbulent mixing layer can still be described by an inviscid model. In their experiments a mixing layer was formed by two uniform flows of different velocities separated by a splitter plate. At the end of separating plate the flows are combined into one flow. At the merging point the flow was disturbed by a periodic motion of a small flap to make formation of large-scale vortices more regular. Theoretical analysis in the paper is based on linearized theory that took into account slow deviation of the mean flow from parallel. The leading term of the asymptotic expansion of the solution is obtained by the WKB method. According to the paper the mixing layer velocity profile

is close to hyperbolic tangent function. The thickness of the mixing layer increases downstream almost linearly. Experimental results in terms of magnitude and phase of velocity fluctuations are in good agreement with theoretical predictions.

4 STABILITY ANALYSIS OF FLOWS WITH FREE SURFACE

The present chapter considers stability of a flow with free unbounded surface. Effect of momentum corrections coefficients and the Froude number on stability analysis results has been evaluated in order to estimate influence of flow velocity vertical non-uniformity and flow deviation from ”rigid-lid” assumption. It has been found that neglection of momentum correction coefficients may lead to significant errors in results. Application of the ”rigid-lid” assumption, in it’s turn, has minor influence on results, therefore use of the assumption is justified [30].

4.1 Introduction

Two main assumptions are usually made in order to facilitate the analysis under the shallow water model:

1. The ”rigid-lid” assumption.
2. Vertical velocity uniformity assumption.
3. Parallel flow assumption (the flow profile is not altered downstream).

The essence of the first assumption is that the free surface of the flow is not perturbed and acts as ”rigid-lid”. According to the second assumption, the velocity is considered to be independent on vertical coordinate. This assumption complies with the fact that the governing equations for shallow flow are the depth-averaged.

In some cases, however, the two assumptions may not be appropriate. Fluctuations of bottom friction coefficient and changes in flow geometry can result in appreciable deviation of the real flow from above-mentioned assumptions.

Momentum correction coefficients were applied by several authors [40], [43] in order to compensate for the deviation arisen by the vertical non-uniformity of a real flow. However, ”rigid-lid”

assumption brings some error into the results as well. The magnitude of the error is not yet known well enough.

An attempt to evaluate the influence of both "rigid-lid" and uniform velocity distribution assumptions on the stability analysis of shallow wake flows is presented in this chapter. The evaluaton is done in the following way

- The influence of vertical velocity uniformity assumption is tested by calculating stability of the flow for different values of momentum correction coefficients and comparing the results.
- The "rigid-lid" assumption is tested by performing stability analysis and comparing the results for various values of the Froude number Fr_H.

The latter point requires some elaboration. The Froude number is defined by the expression $Fr_H = \frac{U}{\sqrt{gH_0}}$, where U is flow velocity, g is acceleration due to gravity and H_0 is water depth. The Froude number represents the ratio of inertia and gravity forces. It is shown in [13] that when the Froude number tends to zero, the stability analysis results coinside with the results obtained under the "rigid-lid" assumption. So, by calculating the stability of the flow at different values of the Froude number and comparing the results to "rigid-lid" results, we can get an estimate of the error, arising for the flow with specific Froude number due to simplification of the analysis by applying the "rigid-lid" assumption. The Froude number Fr_H, however, is not included into the equations in an explicit way, so the Froude-like number Fr defined by the expression $Fr = \frac{U_0}{\sqrt{gb}}$ is used. The Fr number is linked to the Froude number Fr_H by means of formula:

$$Fr_H = Fr\sqrt{\frac{b}{H_0}}. \tag{4.1}$$

The stability analysis results are performed for a range of values of the Fr number and $\frac{b}{H_0}$ ratio, where b is characteristic width (e. g. half-width of the wake). The Froude number can be calculated for any given set of Fr and $\frac{b}{H_0}$ values using (4.1).

4.2 Problem Formulation

The governing equations for shallow flow are obtained by integrating Euler equations with respect to vertical coordinate (for an example refer to the introduction chapter where (3.38) - (3.39) are

derived). In case momentum correction coefficients are used, the resuling equations have the form [43]:

$$\frac{\partial h}{\partial t}+\frac{\partial}{\partial x}(uh)+\frac{\partial}{\partial y}(vh) = 0, \tag{4.2}$$

$$\begin{aligned}\frac{\partial u}{\partial t}+(2\beta_1-1)u\frac{\partial u}{\partial x}+[(\beta_1-1)\frac{u^2}{h}+g]\frac{\partial h}{\partial x}\\ +(\beta_2-1)u\frac{\partial v}{\partial y}+(\beta_2-1)\frac{uv}{h}\frac{\partial h}{\partial y}\\ +\beta_2 v\frac{\partial u}{\partial y}-gS_{0x}+\frac{c_f u\sqrt{u^2+v^2}}{2h}-F(y) &= 0,\end{aligned} \tag{4.3}$$

$$\begin{aligned}\frac{\partial v}{\partial t}+\beta_2 u\frac{\partial v}{\partial x}+(\beta_2-1)v\frac{\partial u}{\partial x}\\ +(\beta_2-1)\frac{uv}{h}\frac{\partial h}{\partial x}+(2\beta_3-1)v\frac{\partial v}{\partial y}\\ +[(\beta_3-1)\frac{v^2}{h}+g]\frac{\partial h}{\partial y}\\ -gS_{0y}+\frac{c_f v\sqrt{u^2+v^2}}{2h} &= 0,\end{aligned} \tag{4.4}$$

where x and y are spatial coordinates, t is time, u and v are depth-averaged velocity components in the x and y directions respectively, h is water depth, g is acceleration due to gravity, $F(y)$ is the forcing function, $S_{0x}=-\frac{\partial z_b(x,y)}{\partial x}$ and $S_{0y}=-\frac{\partial z_b(x,y)}{\partial y}$ are the bed slopes, z_b is distance from the bottom, c_f is the friction coefficient defined by the equation

$$\frac{1}{\sqrt{c_f}}=A_s+B_s\ln(Re\sqrt{c_f}), \tag{4.5}$$

where A_s and B_s are coefficients defined in [37], Re is the Reynolds number of the flow. In fact (4.5) is often used in practice to calculate the friction coefficient for the flow with a given Re. Formula (4.5) is used when the wall is smooth. Similar formulas for the case of rough surfaces can be found in [37]. Shear stress at the boundary is modelled by the Chezy formula $\tau_{wx}=\frac{1}{2}c_f\rho u\sqrt{u^2+v^2}$ and $\tau_{wy}=\frac{1}{2}c_f\rho v\sqrt{u^2+v^2}$, where ρ is density, τ_{wx} and τ_{wy} are wall shear stresses along the x and y directions respectively.

The coefficients β_1, β_2, and β_3 in equations (4.2-4.4) are the momentum correction coefficients defined by formulas (3.46) - (3.48) which are introduced in order to take into account non-uniformity of velocity distribution in the vertical direction.

Introducing characteristic length (e. g. halfwidth of the wake for wake flows) b and the characteristic velocity U_a, we choose the measure of time in the form b/U_a. Denoting dimensionless functions by subscripts d we define the terms as follows: $u = u_d U_a$, $v = v_d U_a$, $t = \frac{t_d b}{U_a}$, $x = x_d b$, $h = h_d b$, $y = y_d b$, $F = \frac{\tilde{F} U_a^2}{b}$.

Transforming (4.2) - (4.4) to dimensionless variables and dropping the subscript "d" we get

$$\frac{\partial h}{\partial t} + h\frac{\partial u}{\partial x} + u\frac{\partial h}{\partial x} + h\frac{\partial v}{\partial y} + v\frac{\partial h}{\partial y} = 0, \tag{4.6}$$

$$\begin{aligned} &\frac{\partial u}{\partial t} + (2\beta_1 - 1)u\frac{\partial u}{\partial x} + (\beta_1 - 1)\frac{u^2}{h}\frac{\partial h}{\partial x} \\ &+\frac{1}{Fr^2}(\frac{\partial h}{\partial x} - S_{0x}) + \beta_2 v\frac{\partial u}{\partial y} + (\beta_2 - 1)u\frac{\partial v}{\partial y} \\ &+(\beta_2 - 1)\frac{uv}{h}\frac{\partial h}{\partial y} + \frac{c_f u\sqrt{u^2+v^2}}{2h} - \tilde{F}(y) = 0, \end{aligned} \tag{4.7}$$

$$\begin{aligned} &\frac{\partial v}{\partial t} + \beta_2 u\frac{\partial v}{\partial x} + (\beta_3 - 1)\frac{v^2}{h}\frac{\partial h}{\partial y} \\ &+\frac{1}{Fr^2}(\frac{\partial h}{\partial y} - S_{0y}) + (\beta_2 - 1)v\frac{\partial u}{\partial x} + (\beta_2 - 1)\frac{uv}{h}\frac{\partial h}{\partial x} \\ &+(2\beta_3 - 1)v\frac{\partial v}{\partial y} + \frac{c_f v\sqrt{u^2+v^2}}{2h} = 0. \end{aligned} \tag{4.8}$$

We seek a perturbed solution for equations (4.6 - 4.8) in the form:

$$u = U(y) + \hat{u}(y)e^{-\lambda t + ikx}, \tag{4.9}$$

$$v = \hat{v}(y)e^{-\lambda t + ikx}, \tag{4.10}$$

$$h = \frac{H_0}{b} + \hat{h}(y)e^{-\lambda t + ikx}. \tag{4.11}$$

The structure of the expressions (4.9) - (4.10) suggests that the velocity functions are sought in a form of superposition of base flow $U = U(y)$ and perturbations, propagating in the lengthwise direction x as a wave packet. The wave packet consists of modes; each mode is represented by the function $e^{-\lambda t + ikx}$, where k is the wavenumber and $\lambda = \lambda_r + i\lambda_i$ is the complex eigenvalue.

Formula (4.11) assumes that periodic perturbations are imposed on the surface; H_0 is undisturbed water depth.

Calculating the partial derivatives of the functions u, v and h in (4.9-4.11) and substituting the derivatives into (4.6-4.8), we obtain

$$
\begin{aligned}
&-\lambda\hat{h}e^{-\lambda t+ikx}+(\frac{H_0}{b}+\hat{h}(y)e^{-\lambda t+ikx})ik\hat{u}e^{-\lambda t+ikx}\\
&+(U(y)+\hat{u}(y)e^{-\lambda t+ikx})ik\hat{h}e^{-\lambda t+ikx}\\
&+(\frac{H_0}{b}+\hat{h}(y)e^{-\lambda t+ikx})\frac{\partial\hat{v}}{\partial y}e^{-\lambda t+ikx}+\hat{v}(y)e^{-\lambda t+ikx}\frac{\partial\hat{h}}{\partial y}e^{-\lambda t+ikx}=0,\\
&-\lambda\hat{u}e^{-\lambda t+ikx}+(2\beta_1-1)(U(y)+\hat{u}(y)e^{-\lambda t+ikx})ik\hat{u}e^{-\lambda t+ikx}\\
&+(\beta_1-1)\frac{(U(y)+\hat{u}(y)e^{-\lambda t+ikx})^2}{\frac{H_0}{b}+\hat{h}(y)e^{-\lambda t+ikx}}ik\hat{h}e^{-\lambda t+ikx}\\
&+\frac{1}{Fr^2}(ik\hat{h}e^{-\lambda t+ikx}-S_{0x})+\beta_2\hat{v}(y)e^{-\lambda t+ikx}(\frac{\partial U}{\partial y}+\frac{\partial\hat{u}}{\partial y}e^{-\lambda t+ikx})\\
&+(\beta_2-1)(U(y)+\hat{u}(y)e^{-\lambda t+ikx})\frac{\partial\hat{v}}{\partial y}e^{-\lambda t+ikx}\\
&+(\beta_2-1)\frac{(U(y)+\hat{u}(y)e^{-\lambda t+ikx})\hat{v}(y)e^{-\lambda t+ikx}}{\frac{H_0}{b}+\hat{h}(y)e^{-\lambda t+ikx}}\frac{\partial\hat{h}}{\partial y}e^{-\lambda t+ikx}\\
&+\frac{c_f(U(y)+\hat{u}(y)e^{-\lambda t+ikx})}{2(\frac{H_0}{b}+\hat{h}(y)e^{-\lambda t+ikx})}\sqrt{(U(y)+\hat{u}(y)e^{-\lambda t+ikx})^2+(\hat{v}(y)e^{-\lambda t+ikx})^2}\\
&-\tilde{F}(y)=0,\\
&-\lambda\hat{v}e^{-\lambda t+ikx}+\beta_2(U(y)+\hat{u}(y)e^{-\lambda t+ikx})ik\hat{v}e^{-\lambda t+ikx}\\
&+(\beta_3-1)\frac{(\hat{v}(y)e^{-\lambda t+ikx})^2}{\frac{H_0}{b}+\hat{h}(y)e^{-\lambda t+ikx}}\frac{\partial\hat{h}}{\partial y}e^{-\lambda t+ikx}\\
&+\frac{1}{Fr^2}(\frac{\partial\hat{h}}{\partial y}e^{-\lambda t+ikx}-S_{0y})+(\beta_2-1)\hat{v}(y)e^{-\lambda t+ikx}ik\hat{u}e^{-\lambda t+ikx}\\
&+(\beta_2-1)\frac{(U(y)+\hat{u}(y)e^{-\lambda t+ikx})\hat{v}(y)e^{-\lambda t+ikx}}{\frac{H_0}{b}+\hat{h}(y)e^{-\lambda t+ikx}}ik\hat{h}e^{-\lambda t+ikx}\\
&+(2\beta_3-1)\hat{v}(y)e^{-\lambda t+ikx}\frac{\partial\hat{v}}{\partial y}e^{-\lambda t+ikx}\\
&+\frac{c_f(\hat{v}(y)e^{-\lambda t+ikx})}{2(\frac{H_0}{b}+\hat{h}(y)e^{-\lambda t+ikx})}\sqrt{(U(y)+\hat{u}(y)e^{-\lambda t+ikx})^2+(\hat{v}(y)e^{-\lambda t+ikx})^2}=0.
\end{aligned}
$$

We perform linearization in the neighborhood of the base flow, neglecting quadratic terms. Linearization of square root terms is performed in the folowing way:

$$
\begin{aligned}
&(U+\hat{u}e^{-\lambda t+ikx})\sqrt{(U+\hat{u}e^{-\lambda t+ikx})^2+(\hat{v}e^{-\lambda t+ikx})^2}\\
&=(U+\hat{u}e^{-\lambda t+ikx})\sqrt{(U^2+2U\hat{u}e^{-\lambda t+ikx}+\hat{u}^2e^{-2\lambda t+2ikx}+\hat{v}^2e^{-2\lambda t+2ikx}}\\
&=(U+\hat{u}e^{-\lambda t+ikx})\sqrt{(U^2+2U\hat{u}e^{-\lambda t+ikx}}\\
&=(U+\hat{u}e^{-\lambda t+ikx})U(1+\frac{2\hat{u}}{U}e^{-\lambda t+ikx})^{\frac{1}{2}}
\end{aligned}
$$

$$= |(1+\varepsilon)^{\alpha} = 1+\alpha\varepsilon+...| = (U+\hat{u}e^{-\lambda t+ikx})(1+\frac{1}{2}\frac{2\hat{u}}{U}e^{-\lambda t+ikx})U$$
$$= (U+\hat{u}e^{-\lambda t+ikx})(U+\hat{u}e^{-\lambda t+ikx}) = U^2+2U\hat{u}e^{-\lambda t+ikx}+\hat{u}^2e^{-2\lambda t+2ikx}$$
$$= U^2+2U\hat{u}e^{-\lambda t+ikx}.$$

So, the term

$$\frac{c_f(U(y)+\hat{u}(y)e^{-\lambda t+ikx})}{2(\frac{H_0}{b}+\hat{h}(y)e^{-\lambda t+ikx})}\sqrt{(U(y)+\hat{u}(y)e^{-\lambda t+ikx})^2+(\hat{v}(y)e^{-\lambda t+ikx})^2}$$

can be linearized as follows:

$$\frac{c_f(U(y)+\hat{u}(y)e^{-\lambda t+ikx})}{2(\frac{H_0}{b}+\hat{h}(y)e^{-\lambda t+ikx})}\sqrt{(U(y)+\hat{u}(y)e^{-\lambda t+ikx})^2+(\hat{v}(y)e^{-\lambda t+ikx})^2}$$
$$= \frac{c_f(U(y)^2+2U(y)\hat{u}(y)e^{-\lambda t+ikx})}{2(\frac{H_0}{b}+\hat{h}(y)e^{-\lambda t+ikx})}.$$

The term

$$\frac{c_f(\hat{v}(y)e^{-\lambda t+ikx})}{2(\frac{H_0}{b}+\hat{h}(y)e^{-\lambda t+ikx})}\sqrt{(U(y)+\hat{u}(y)e^{-\lambda t+ikx})^2+(\hat{v}(y)e^{-\lambda t+ikx})^2}$$

is linearized in the following way:

$$\frac{c_f(\hat{v}(y)e^{-\lambda t+ikx})}{2(\frac{H_0}{b}+\hat{h}(y)e^{-\lambda t+ikx})}\sqrt{(U(y)+\hat{u}(y)e^{-\lambda t+ikx})^2+(\hat{v}(y)e^{-\lambda t+ikx})^2}$$
$$= \frac{c_f(\hat{v}(y)e^{-\lambda t+ikx})}{2(\frac{H_0}{b}+\hat{h}(y)e^{-\lambda t+ikx})}(U+\hat{u}e^{-\lambda t+ikx}) = \frac{c_f(U(y)\hat{v}(y)e^{-\lambda t+ikx})}{2(\frac{H_0}{b}+\hat{h}(y)e^{-\lambda t+ikx})}.$$

So, we get

$$-\lambda\hat{h}e^{-\lambda t+ikx}+\frac{H_0}{b}ik\hat{u}e^{-\lambda t+ikx}+U(y)ik\hat{h}e^{-\lambda t+ikx}+\frac{H_0}{b}\frac{\partial\hat{v}}{\partial y}e^{-\lambda t+ikx} = 0,$$
$$-\lambda\hat{u}e^{-\lambda t+ikx}+(2\beta_1-1)U(y)ik\hat{u}e^{-\lambda t+ikx}$$
$$+(\beta_1-1)\frac{U(y)^2}{\frac{H_0}{b}+\hat{h}(y)e^{-\lambda t+ikx}}ik\hat{h}e^{-\lambda t+ikx}+\frac{1}{Fr^2}(ik\hat{h}e^{-\lambda t+ikx}-S_{0x})$$
$$+\beta_2\hat{v}(y)e^{-\lambda t+ikx}\frac{\partial U}{\partial y}+(\beta_2-1)U(y)\frac{\partial\hat{v}}{\partial y}e^{-\lambda t+ikx}$$
$$+\frac{c_f(U(y)^2+2U(y)\hat{u}(y)e^{-\lambda t+ikx})}{2(\frac{H_0}{b}+\hat{h}(y)e^{-\lambda t+ikx})}-\tilde{F}(y) = 0,$$
$$-\lambda\hat{v}e^{-\lambda t+ikx}+\beta_2U(y)ik\hat{v}e^{-\lambda t+ikx}+\frac{1}{Fr^2}(\frac{\partial\hat{h}}{\partial y}e^{-\lambda t+ikx}-S_{0y})$$

$$+\frac{c_f U(y)\hat{v}(y)e^{-\lambda t+ikx}}{2(\frac{H_0}{b}+\hat{h}(y)e^{-\lambda t+ikx})}=0.$$

The term $\frac{1}{\frac{H_0}{b}+\hat{h}(y)e^{-\lambda t+ikx}}$ is linearized in the following way:

$$\begin{aligned}\frac{1}{\frac{H_0}{b}+\hat{h}(y)e^{-\lambda t+ikx}}&=\frac{1}{\frac{H_0}{b}}\frac{1}{1+\frac{b\hat{h}(y)}{H_0}e^{-\lambda t+ikx}}\\&=\frac{1}{\frac{H_0}{b}}(1+\frac{b\hat{h}(y)}{H_0}e^{-\lambda t+ikx})^{-1}=|\frac{h(y)}{H_0}\to 0|\\&=|(1+\varepsilon)^{\alpha}=1+\alpha\varepsilon+...|=\frac{1}{\frac{H_0}{b}}(1-\frac{b\hat{h}(y)}{H_0}e^{-\lambda t+ikx})\\&=\frac{b}{H_0}(1-\frac{b\hat{h}(y)}{H_0}e^{-\lambda t+ikx}).\end{aligned}$$

The term $\frac{U(y)^2}{\frac{H_0}{b}+\hat{h}(y)e^{-\lambda t+ikx}}ik\hat{h}e^{-\lambda t+ikx}$ becomes

$$\begin{aligned}&\frac{U(y)^2}{\frac{H_0}{b}+\hat{h}(y)e^{-\lambda t+ikx}}ik\hat{h}e^{-\lambda t+ikx}=U(y)^2\frac{1}{\frac{H_0}{b}+\hat{h}(y)e^{-\lambda t+ikx}}ik\hat{h}e^{-\lambda t+ikx}\\&=U(y)^2\frac{b}{H_0}(1-\frac{b\hat{h}(y)}{H_0}e^{-\lambda t+ikx})ik\hat{h}e^{-\lambda t+ikx}=U(y)^2\frac{b}{H_0}ik\hat{h}e^{-\lambda t+ikx},\end{aligned}$$

and the term $\frac{c_f(U(y)^2+2U(y)\hat{u}(y)e^{-\lambda t+ikx})}{2(\frac{H_0}{b}+\hat{h}(y)e^{-\lambda t+ikx})}$ changes to

$$\begin{aligned}&\frac{c_f(U(y)^2+2U(y)\hat{u}(y)e^{-\lambda t+ikx})}{2(\frac{H_0}{b}+\hat{h}(y)e^{-\lambda t+ikx})}\\&=\frac{1}{2}c_f(U(y)^2+2U(y)\hat{u}(y)e^{-\lambda t+ikx})\frac{1}{\frac{H_0}{b}+\hat{h}(y)e^{-\lambda t+ikx}}\\&=c_f(U(y)^2+2U(y)\hat{u}(y)e^{-\lambda t+ikx})\frac{b}{2H_0}(1-\frac{b\hat{h}(y)}{H_0}e^{-\lambda t+ikx})\\&=c_fU(y)^2\frac{b}{2H_0}-c_fU(y)^2\frac{b}{2H_0}\frac{b\hat{h}(y)}{H_0}e^{-\lambda t+ikx}\\&\quad+c_f2U(y)\hat{u}(y)e^{-\lambda t+ikx}\frac{b}{2H_0}\\&=\frac{c_fU(y)^2b}{2H_0}-\frac{c_fU(y)^2bb\hat{h}(y)e^{-\lambda t+ikx}}{2H_0H_0}+\frac{c_fU(y)\hat{u}(y)be^{-\lambda t+ikx}}{H_0}.\end{aligned}$$

We get

$$
\begin{aligned}
-\lambda\hat{h}e^{-\lambda t+ikx}+\frac{H_0}{b}ik\hat{u}e^{-\lambda t+ikx}+U(y)ik\hat{h}e^{-\lambda t+ikx}\\
+\frac{H_0}{b}\frac{\partial\hat{v}}{\partial y}e^{-\lambda t+ikx}=0,\\
-\lambda\hat{u}e^{-\lambda t+ikx}+(2\beta_1-1)U(y)ik\hat{u}e^{-\lambda t+ikx}+(\beta_1-1)U(y)^2\frac{b}{H_0}ik\hat{h}e^{-\lambda t+ikx}\\
+\frac{1}{Fr^2}(ik\hat{h}e^{-\lambda t+ikx}-S_{0x})+\beta_2\hat{v}(y)e^{-\lambda t+ikx}\frac{\partial U}{\partial y}+(\beta_2-1)U(y)\frac{\partial\hat{v}}{\partial y}e^{-\lambda t+ikx}\\
+\frac{c_fU(y)^2b}{2H_0}-\frac{c_fU(y)^2bb\hat{h}(y)e^{-\lambda t+ikx}}{2H_0H_0}+\frac{c_fU(y)\hat{u}(y)be^{-\lambda t+ikx}}{H_0}-\tilde{F}(y)=0,\\
-\lambda\hat{v}e^{-\lambda t+ikx}+\beta_2U(y)ik\hat{v}e^{-\lambda t+ikx}+\frac{1}{Fr^2}(\frac{\partial\hat{h}}{\partial y}e^{-\lambda t+ikx}-S_{0y})\\
+\frac{c_fbU(y)\hat{v}(y)e^{-\lambda t+ikx}}{2H_0}=0.
\end{aligned}
$$

Assuming that $\tilde{F}(y)=\frac{c_fU(y)^2b}{2H_0}-\frac{S_{0x}}{Fr^2}$, taking into account that the slope in transverse direction S_{0y} is zero, dividing by $e^{-\lambda t+ikx}$ and introducting the stability parameter s denoted as

$$s=c_f\frac{b}{H_0},$$

we obtain the system of ordinary differential equations

$$
\begin{aligned}
-\lambda\hat{h}+\frac{H_0}{b}ik\hat{u}+U(y)ik\hat{h}+\frac{H_0}{b}\frac{\partial\hat{v}}{\partial y}=0,\\
-\lambda\hat{u}+(2\beta_1-1)U(y)ik\hat{u}+(\beta_1-1)U(y)^2\frac{b}{H_0}ik\hat{h}+\frac{1}{Fr^2}ik\hat{h}\\
+\beta_2\hat{v}(y)\frac{\partial U}{\partial y}+(\beta_2-1)U(y)\frac{\partial\hat{v}}{\partial y}-\frac{sU(y)^2b\hat{h}(y)}{2H_0}+sU(y)\hat{u}(y)=0,\\
-\lambda\hat{v}+\beta_2U(y)ik\hat{v}+\frac{1}{Fr^2}\frac{\partial\hat{h}}{\partial y}+\frac{sU(y)\hat{v}(y)}{2}=0,
\end{aligned}
$$

or, grouping the terms,

$$\frac{H_0}{b} ik\hat{u} + ikU\hat{h} + \frac{H_0}{b}\frac{d\hat{v}}{dy} - \lambda\hat{h} = 0, \tag{4.12}$$

$$[(2\beta_1 - 1)ikU + sU]\hat{u} + [(\beta_1 - 1)\frac{ikU^2 b}{H_0} + \frac{ik}{Fr^2} - \frac{sU^2 b}{2H_0}]\hat{h} + (\beta_2 - 1)U\frac{d\hat{v}}{dy} + \beta_2 \nu \frac{\partial U}{\partial y} - \lambda\hat{u} = 0, \tag{4.13}$$

$$\frac{1}{Fr^2}\frac{d\hat{h}}{dy} + (ik\beta_2 U + \frac{s}{2}U)\hat{v} - \lambda\hat{v} = 0, \tag{4.14}$$

with the boundary conditions

$$\hat{v}(\pm\infty) = 0, \tag{4.15}$$

where $\hat{u} = \hat{u}(y)$, $\hat{v} = \hat{v}(y)$, $\hat{h} = \hat{h}(y)$ and $U = U(y)$.

Numerical solution of (4.12) - (4.15) is explained in detail in the Chapter 5.

4.3 Results and discussion

This chapter presents an attempt to evaluate the influence of "rigid-lid" assumption and momentum correction coefficients on stability analysis results. The rigid-lid assumption is evaluated by solving problems (4.12) - (4.15) numerically for different values of Froude-like number $Fr = \frac{U_0}{\sqrt{gb}}$ as well as $\frac{b}{H_0}$ parameter. The $\frac{b}{H_0}$ parameter is the ratio of characteristic length of the flow (e. g. halfwidth of the wake for wake flows) and water depth.

As it has been said in the introduction section, the solution is sought as a supersposition of modes, each mode propagating in the x direction (that is the direction of the flow) as a wave having a form of $e^{-\lambda t + ikx}$ where λ is the complex frequency of the mode and k is the wavenumber. It is seen that λ is an eigenvalue of the problem (4.12-4.15) and determines stability of the flow. If the real parts of eigenvalues λ for all modes are positive then perturbations decay with time and flow is said to be stable. If the real part of a λ is negative for at least one mode then the mode will amplify and the flow is unstable. By solving the problem (4.12-4.15) for different values of

Table 4.1: Values of parameters Fr, $\frac{b}{H_0}$, β_1, β_2.

Fr	0.0001	0.1	0.2
$\frac{b}{H_0}$	5	50	
β_1	1.00	1.05	1.10
β_1	1.00	1.05	1.10

wavenumber k and stability parameter s we can get a set of points on (k,s) plane for which one mode has the real part of the eigenvalue λ equal to zero while other modes have λ with positive real parts. The points define a stability curve: the boundary between stable and unstable flow. All points above the curve form the stability domain, where the flow is stable. The points below the curve correspond to unstable flow. The value of the stability parameter s at the top of the curve is called "critical value" and is denoted s_c.

By solving problem (4.12-4.15) for different values of Fr, $\frac{b}{H_0}$ and constructing stability curves we are able to evaluate influence of these two parameters on the critical values s_c of the stability parameter s. The assumption of uniform velocity distribution across the vertical coordinate for a flow with free surface is evaluated by solving problems (4.12-4.15) for different values of the momentum correction coefficients β_1 and β_2.

The values of s_c have been calculated for the values of the parameters Fr, $\frac{b}{H_0}$, β_1, and β_2 presented in Table 4.1. The values of the parameters have been selected to match the range observed in nature and experiments [34], [40].

Figure 4.1 presents stability curves obtained for different values of momentum correction coefficients for the free surface flow with Fr close to zero and characteristic length to depth ratio $\frac{b}{H_0} = 5$. Figure 4.2 shows stability curves for $Fr = 0.2$, and $\frac{b}{H_0} = 5$.

Figure 4.3 presents stability analysis results for the case when $Fr = 0.2$ and $\frac{b}{H_0} = 50$.

Effect of variation of momentum correction coefficients on the critical value s_c of the stability parameter s in terms of percentage difference is shown in Figure 4.4.

Figure 4.5 depicts the dependence of the critical stability parameter s_c on the parameters Fr and $\frac{b}{H_0}$.

The results are compared to the case when the Fr (and, therefore Fr_H) is close to zero. Ac-

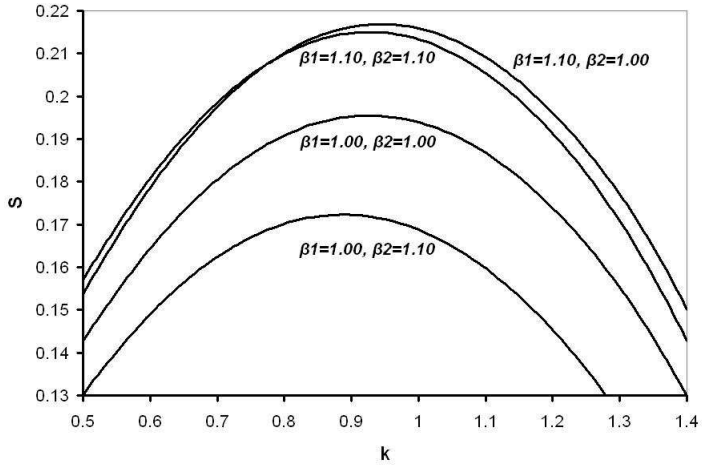

Figure 4.1: Stability curves for various values of momentum correction coefficients obtained at $Fr = 0.0001$, $\frac{b}{H_0} = 5$.

cording to [13] stability characteristics for flows with free surface tend to the stability characteristics obtained under rigid-lid assumption when the Froude number approaches zero. The Froude number Fr_H (based on the undisturbed water depth) is related to Fr by means of the formula $Fr_H = Fr\sqrt{\frac{b}{H_0}}$.

The two values of the parameter $\frac{b}{H_0}$ are chosen since the condition $\frac{b}{H_0} \gg 1$ is consistent with the shallow water approximation.

It can be seen from Figures 4.1 - 4.3 that the critical value s_c of the stability parameter is decreasing for higher Fr numbers and higher $\frac{b}{H_0}$ values. So, higher Fr has a stabilizing effect on the flow.

Figure 4.5 shows that although the stability boundary is sensitive to variations of Fr, the error in determining the s_c parameter is below 6% if Fr is less than 0.2 for the case $\frac{b}{H_0}$=5, and if the Fr is less than 0.1 for the case $\frac{b}{H_0}$=50.

Socolofsky&Jirka [34] performed shallow water experiments with flows around bluff bodies. The experimental results were compared with theoretical stability analysis performed under the rigid-lid assumption. Two experiments are described in [34]. The Fr and $\frac{b}{H_0}$ values (if half-width of an obstacle is taken as b) for the first experiment are about 0.2 and 1.8 respectively. The second

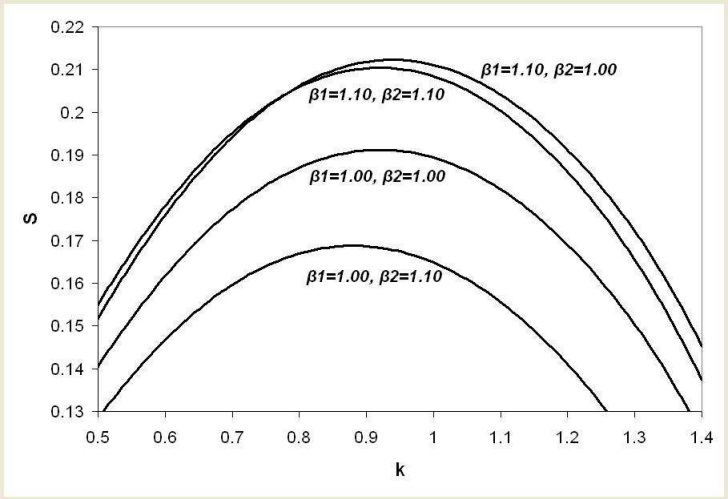

Figure 4.2: Stability curves for various vaules of momentum correction coefficients obtained at $Fr = 0.2$, $\frac{b}{H_0} = 5$.

experiment has Fr close to 0.1 and $\frac{b}{H_0}$ close to 15. According to Figure 4.5, the use of rigid-lid assumption is justified for both experiments, as resulting error will be relatively small (in the range of 2-3%).

The Froude number Fr_H for real island wakes is in the range of 0.1-0.2 [14]. Given that the flow is shallow (which means $\frac{b}{H_0}$ is much higher than unity and is equal to, let's say, 50), the Fr parameter will be no larger than 0.03. Figure 4.5 clearly shows, that the error will be in the 2% range.

So, the "rigid-lid" assumption is precise enough for calculation of the s_c parameter for the range of Froude numbers typical for shallow flows. However, for large Froude numbers application of "rigid-lid" may lead to underestimation of the stability of the flow.

Figure 4.4 presents results of the comparison of the s_c parameter calculated from (4.12) - (4.15) for different values of momentum correction coefficients β_1 and β_2. The results are compared to the values of s_c calculated for β_1=1.00 and β_2=1.00 that corresponds to the case when the velocity non-uniformity across the vertical coordinate is not taken into account.

As it can be seen from Figure 4.4 for some combination of the values of β_1 and β_2 the relative error can reach 10%. The increase of β_1 leads to growth of s_c, so the flow becomes more unstable. The β_2 coefficient has, in turn, stabilizing effect on the flow, but its influence diminishes with the

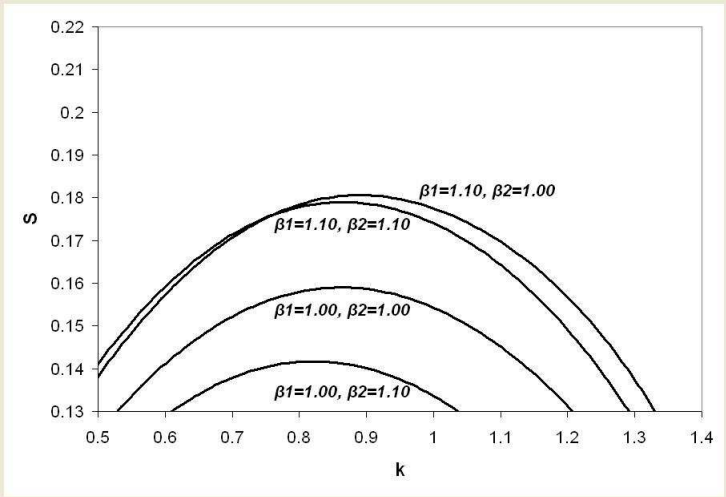

Figure 4.3: Stability curves for various vaules of momentum correction coefficients obtained at $Fr = 0.2$, $\frac{b}{H_0} = 50$.

growth of β_1. Unfortunately, the values of coefficients β_1 and β_2 for real island wakes are not known. However, as the error in determining the s_c parameter may grow with increased values of β_1 or β_2 it might be important to know the values of β_1 and β_2 for analyzed shallow flows.

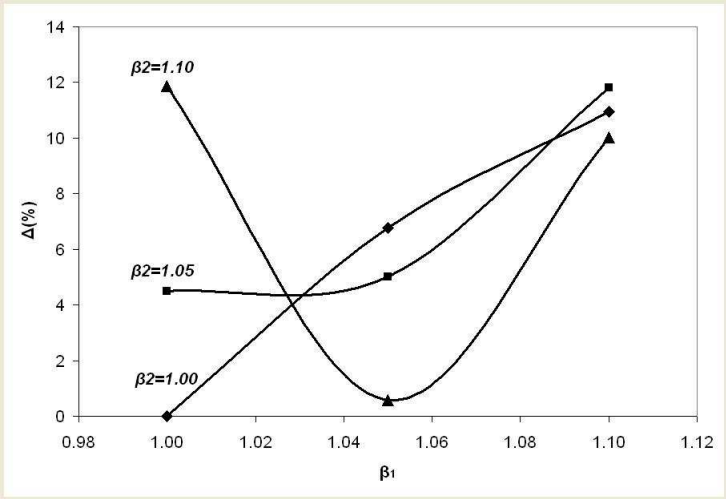

Figure 4.4: The percentage difference Δ between the values of the s_c for depth-averaged equations ($\beta_1 = 1$, $\beta_2 = 1$) and equations with correction factors ($\beta_1 > 1$, $\beta_2 > 1$).

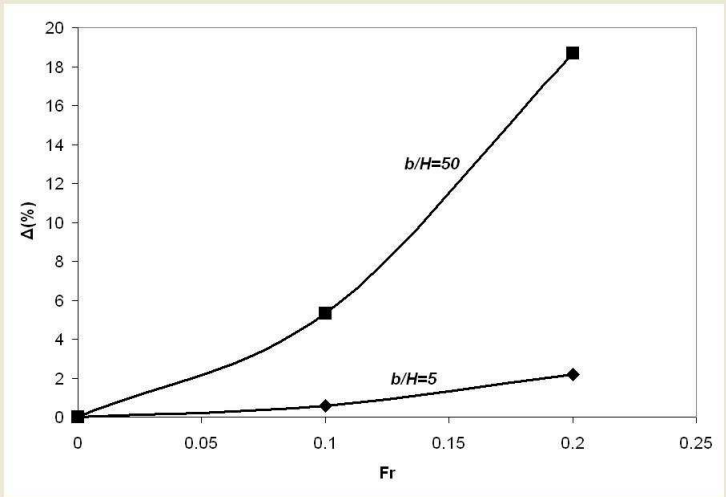

Figure 4.5: The percentage difference Δ between the values of the s_c with and without the rigid-lid assumption for the case $\frac{b}{H_0}$=5 and $\frac{b}{H_0}$=50.

5 RIGID-LID ASSUMPTION. LINEAR STABILITY ANALYSIS

The present chapter considers stability of a shallow flow. The stability analysis is performed under the ”rigid-lid” assumption that allows to reduce the model to a single equation. Influence of vertical non-uniformity of flow velocity in terms of momentum correction coefficients on stability analysis results is considered. It is shown that an error of 10%-12% may arise if the coefficients are neglected [21] [22].

5.1 Introduction

The ”rigid-lid” assumption is widely used under the shallow flow model in order to facilitate analysis. The idea of ”rigid-lid” assumption is to model gravity-driven free surface flow as a pressure-driven flow between two parallel plates. The top plate is assumed to have zero friction coefficient while the bottom plate has friction coefficient equal to the one of the original channel. In other words, one considers a flow with constant depth.

Application of ”rigid-lid” assumption enables to eliminate pressure and introduce a stream function into the governing equations. The system of equations is therefore replaced by a single partial differential equation containing only one unknown function: the stream function.

Besides the ”rigid-lid” assumption there are other assumptions used under the shallow flow model:

They are:

1. The velocity is independent from vertical coordinate.

2. The flow profile does not depend on the lengthwise coordinate (parallel flow assumption).

The assumption of velocity independence on vertical coordinate is tested in this chapter.

The assumption complies with the fact that the shallow-flow equations are obtained by integrating Euler equations with respect to vertical coordinate, so the vertical velocity distribution profile is replaced by some average value.

Figure 5.1 demonstrates vertical velocity distribution profiles for turbulent and averaged flows. In other words, the vertical velocity distribution is considered to be uniform in a shallow flow model.

In some cases, however, vertical velocity profile may deviate from uniform. In order to compensate for possible deviations, momentum correction coefficients are introduced.

The present chapter's objective is to evaluate influence of the values of momentum correction coefficients on stability analysis results, obtained under the "rigid-lid" assumption. Stability analysis results is performed for different values of momentum correction coefficients and are compared to ones obtained for unity values.

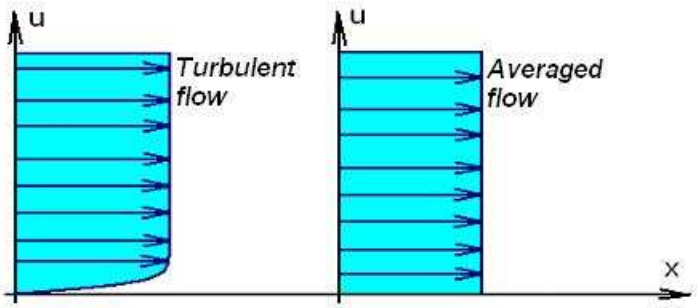

Figure 5.1: Vertical velocity distribution profiles for turbulent and averaged flow

5.2 Governing Equations for "rigid-lid" assumption

The governing equations for shallow flow are derived from Euler equations by integrating them with respect to vertical coordinate [43]. The resulting equations, frequently referred to as Saint–Venant equations, are:

$$\begin{aligned} \frac{\partial H_0}{\partial t} &+ \frac{\partial}{\partial x}(uH_0) + \frac{\partial}{\partial y}(vH_0) = 0, \\ \frac{\partial u}{\partial t} &+ (2\beta_1 - 1)u\frac{\partial u}{\partial x} + [(\beta_1 - 1)\frac{u^2}{H_0} + g]\frac{\partial H_0}{\partial x} \\ &+ (\beta_2 - 1)u\frac{\partial v}{\partial y} + (\beta_2 - 1)\frac{uv}{H_0}\frac{\partial H_0}{\partial y} \end{aligned} \tag{5.1}$$

$$+ \quad \beta_2 v\frac{\partial u}{\partial y} - gS_{0x} + \frac{c_f u\sqrt{u^2+v^2}}{2H_0} - F(y) = 0, \tag{5.2}$$

$$\begin{aligned}\frac{\partial v}{\partial t} &+ \beta_2 u\frac{\partial v}{\partial x} + (\beta_2 - 1)v\frac{\partial u}{\partial x} \\ &+ (\beta_2 - 1)\frac{uv}{H_0}\frac{\partial H_0}{\partial x} + (2\beta_3 - 1)v\frac{\partial v}{\partial y} \\ &+ [(\beta_3 - 1)\frac{v^2}{H_0} + g]\frac{\partial H_0}{\partial y} - gS_{0y} + \frac{c_f v\sqrt{u^2+v^2}}{2H_0} = 0,\end{aligned} \tag{5.3}$$

where H_0 is water depth, u and v are flow velocities in x (lengthwise) and y (transverse) directions respectively, g is acceleration due to gravity, S_{0x} and S_{0y} are slopes in x and y directions, c_f is the friction coefficient defined by the equation [14]:

$$\frac{1}{\sqrt{c_f}} = -4\log(\frac{1.25}{4Re\sqrt{c_f}}),$$

where Re is the Reynolds number.

Shear stress at the boundary is modeled by the Chezy formula

$$\tau_{wx} = \frac{1}{2}c_f \rho u\sqrt{u^2+v^2}$$

and

$$\tau_{wy} = \frac{1}{2}c_f \rho v\sqrt{u^2+v^2},$$

where ρ is density, τ_{wx} and τ_{wy} are wall shear stresses along the x and y directions respectively.

The coefficients β_1, β_2, and β_3 in equations (5.4) - (5.6) are the momentum correction coefficients defined by (3.46) - (3.47) which are used in order to take into account non-uniformity of velocity distribution in the vertical direction. The effect of β_1, β_2 and β_3 variation on the stability of the flow is evaluated in this chapter.

By assuming water depth H_0 to be constant in (5.1) - (5.3), introducing measures of length, time and velocity given by b, $\frac{b}{U_a}$ and U_a respectively, transforming the equations to dimensionless form, and replacing gravity-drive flow by pressure-driven flow, namely $\frac{\partial p}{\partial x} = -\frac{S_{0x}}{Fr^2} - \frac{F(y)b}{U_a^2}$, $\frac{\partial p}{\partial y} = -\frac{S_{0y}}{Fr^2}$ we get

$$\frac{\partial u}{\partial x} + \frac{\partial v}{\partial y} = 0, \tag{5.4}$$

$$\frac{\partial u}{\partial t} + (2\beta_1 - 1)u\frac{\partial u}{\partial x} + (\beta_2 - 1)u\frac{\partial v}{\partial y} + \beta_2 v\frac{\partial u}{\partial y}$$

$$= -\frac{\partial p}{\partial x} - \frac{c_f}{2h} u\sqrt{u^2+v^2}, \tag{5.5}$$

$$\frac{\partial v}{\partial t} + (\beta_2 - 1)v\frac{\partial u}{\partial x} + \beta_2 u\frac{\partial v}{\partial x} + (2\beta_3 - 1)v\frac{\partial v}{\partial y} = -\frac{\partial p}{\partial y} - \frac{c_f}{2h} v\sqrt{u^2+v^2}, \tag{5.6}$$

where x and y are the spatial coordinates, t is the time, u and v are the depth-averaged velocity components in the x and y directions respectively, $h = \frac{H_0}{b}$ is dimensionless water depth, c_f is the friction coefficient defined by the equation [14]:

$$\frac{1}{\sqrt{c_f}} = -4\log(\frac{1.25}{4Re\sqrt{c_f}}),$$

where *Re* is the Reynolds number.

By denoting the partial derivatives by subscripts we can rewrite the equations (5.4) - (5.6) in the form:

$$u_x + u_y = 0, \tag{5.7}$$

$$u_t + (2\beta_1 - 1)uu_x + (\beta_2 - 1)uv_y + \beta_2 vu_y = -p_x - \frac{c_f}{2h} u\sqrt{u^2+v^2}, \tag{5.8}$$

$$v_t + (\beta_2 - 1)vu_x + \beta_2 uv_x + (2\beta_3 - 1)vv_y = -p_y - \frac{c_f}{2h} v\sqrt{u^2+v^2}. \tag{5.9}$$

In order to eliminate pressure we differentiate the equation (5.8) with respect to y and the equation (5.9) with respect to x. We obtain the following system of equations:

$$u_x + u_y = 0, \tag{5.10}$$

$$u_{yt} + (2\beta_1 - 1)u_y u_x + (2\beta_1 - 1)uu_{xy} + (\beta_2 - 1)u_y v_y + (\beta_2 - 1)uv_{yy} + \beta_2 v_y u_y + \beta_2 vu_{yy} = -p_{xy} - \frac{c_f}{2h} u_y\sqrt{u^2+v^2} - \frac{c_f}{2h} u\frac{1}{\sqrt{u^2+v^2}}(uu_y + vv_y), \tag{5.11}$$

$$v_{tx} + (\beta_2 - 1)v_x u_x + (\beta_2 - 1)vu_{xx} + \beta_2 u_x v_x + \beta_2 uv_{xx} + (2\beta_3 - 1)v_x v_y + (2\beta_3 - 1)vv_{yx} = -p_{xy} - \frac{c_f}{2h} v_x\sqrt{u^2+v^2} - \frac{c_f}{2h} v\frac{1}{\sqrt{u^2+v^2}}(uu_x + vv_x). \tag{5.12}$$

By subtracting (5.12) from (5.11) we obtain

$$u_x + u_y = 0, \tag{5.13}$$

$$\begin{aligned} &u_{yt} - v_{xt} + (2\beta_1 - 1)u_y u_x + (2\beta_1 - 1)uu_{xy} + (\beta_2 - 1)u_y v_y \\ &+(\beta_2 - 1)uv_{yy} + \beta_2 v_y u_y + \beta_2 vu_{yy} - (\beta_2 - 1)v_x u_x \\ &-(\beta_2 - 1)vu_{xx} - \beta_2 u_x v_x - \beta_2 uv_{xx} - (2\beta_3 - 1)v_x v_y - (2\beta_3 - 1)vv_{yx} \\ &+\frac{c_f}{2h}u_y\sqrt{u^2+v^2} - \frac{c_f}{2h}v_x\sqrt{u^2+v^2} + \frac{c_f}{2h}u\frac{1}{\sqrt{u^2+v^2}}(uu_y + vv_y) \\ &-\frac{c_f}{2h}v\frac{1}{\sqrt{u^2+v^2}}(uu_x + vv_x) = 0. \end{aligned} \tag{5.14}$$

Introducing the stream function $\psi(x,y,t)$ defined by the relations

$$u = \frac{\partial\psi}{\partial y}, v = -\frac{\partial\psi}{\partial x}, \tag{5.15}$$

we rewrite the equations (5.4) - (5.6) in the form:

$$u_x + u_y = 0, \tag{5.16}$$

$$\begin{aligned} &\psi_{yyt} + \psi_{xxt} + (2\beta_1 - 1)\psi_{yy}\psi_{yx} + (2\beta_1 - 1)\psi_y\psi_{yyx} - (\beta_2 - 1)\psi_{yy}\psi_{xy} \\ &-(\beta_2 - 1)\psi_y\psi_{xyy} - \beta_2\psi_{xy}\psi_{yy} - \beta_2\psi_x\psi_{yyy} + (\beta_2 - 1)\psi_{xx}\psi_{yx} \\ &+(\beta_2 - 1)\psi_x\psi_{yxx} + \beta_2\psi_{yx}\psi_{xx} + \beta_2\psi_y\psi_{xxx} - (2\beta_3 - 1)\psi_{xx}\psi_{xy} \\ &-(2\beta_3 - 1)\psi_x\psi_{xxy} + \frac{c_f}{2h}\psi_{yy}\sqrt{\psi_x^2+\psi_y^2} + \frac{c_f}{2h}\psi_{xx}\sqrt{\psi_y^2+\psi_x^2} \\ &+\frac{c_f}{2h}\psi_y\frac{1}{\sqrt{\psi_y^2+\psi_x^2}}(\psi_y\psi_{yy} + \psi_x\psi_{xy}) \\ &+\frac{c_f}{2h}\psi_x\frac{1}{\sqrt{\psi_y^2+\psi_x^2}}(\psi_y\psi_{yx} + \psi_x\psi_{xx}) = 0, \end{aligned} \tag{5.17}$$

or

$$\begin{aligned} &(\Delta\psi)_t + (2\beta_1 - \beta_2)(\psi_y\psi_{xy})_y - \beta_2(\psi_x\psi_{yy})_y + (\beta_2 - 1)(\psi_x\psi_{xy})_x \\ &+\beta_2(\psi_{xx}\psi_y)_x - (2\beta_3 - 1)(\psi_x\psi_{xx})_y + \frac{c_f}{2h}\Delta\psi\sqrt{\psi_x^2+\psi_y^2} \\ &+\frac{c_f}{2h\sqrt{\psi_x^2+\psi_y^2}}(\psi_y^2\psi_{yy} + 2\psi_x\psi_y\psi_{xy} + \psi_x^2\psi_{xx}) = 0, \end{aligned} \tag{5.18}$$

where Δ is the Laplacian in two dimensions and the subscripts indicate derivatives with respect to the variables x and y.

We suppose that the base flow

$$U = (U(y), 0), \tag{5.19}$$

is perturbed and the perturbed solution to the equation (5.18) is assumed to be of the form

$$\psi = \psi_0 + \varepsilon\psi_1 + ..., \tag{5.20}$$

where ε is a small parameter and $\psi_{0y} = U$. Substituting (5.19) and (5.20) into (5.18) we obtain

$$\begin{aligned}
&(\Delta\psi_0)_t + \varepsilon(\Delta\psi_1)_t + (2\beta_1 - \beta_2)((\psi_{0y} + \varepsilon\psi_{1y})(\psi_{0xy} + \varepsilon\psi_{1xy}))_y \\
&-\beta_2((\psi_{0x} + \varepsilon\psi_{1x})(\psi_{0yy} + \varepsilon\psi_{1yy}))_y \\
&+(\beta_2 - 1)((\psi_{0x} + \varepsilon\psi_{1x})(\psi_{0xy} + \varepsilon\psi_{1xy}))_x \\
&+\beta_2((\psi_{0xx} + \varepsilon\psi_{1xx})(\psi_{0y} + \varepsilon\psi_{1y}))_x \\
&-(2\beta_3 - 1)((\psi_{0x} + \varepsilon\psi_{1x})(\psi_{0xx} + \varepsilon\psi_{1xx}))_y \\
&+\frac{c_f}{2h}(\Delta\psi_0 + \varepsilon\Delta\psi_1)\sqrt{(\psi_{0x} + \varepsilon\psi_{1x})^2 + (\psi_{0y} + \varepsilon\psi_{1y})^2} \\
&+\frac{c_f}{2h\sqrt{(\psi_{0x} + \varepsilon\psi_{1x})^2 + (\psi_{0y} + \varepsilon\psi_{1y})^2}}((\psi_{0y} + \varepsilon\psi_{1y})^2(\psi_{0yy} + \varepsilon\psi_{1yy}) \\
&+2(\psi_{0x} + \varepsilon\psi_{1x})(\psi_{0y} + \varepsilon\psi_{1y})(\psi_{0xy} + \varepsilon\psi_{1xy}) \\
&+(\psi_{0x} + \varepsilon\psi_{1x})^2(\psi_{0xx} + \varepsilon\psi_{1xx})) = 0.
\end{aligned} \tag{5.21}$$

Keeping in mind that ψ_{0t} and ψ_{0x} are both equal to zero as $\psi_0 = \psi_0(y)$, and neglecting terms of ε^2 we are able to linearize equation (5.21) in the neighbourhood of base flow (5.19).

The terms containing square roots are linearized as follows:

$$\begin{aligned}
\sqrt{\psi_{0y}^2 + 2\varepsilon\psi_{0y}\psi_{1y}} &= (\psi_{0y}^2 + 2\varepsilon\psi_{0y}\psi_{1y})^{\frac{1}{2}} = \psi_{0y}(1 + 2\varepsilon\frac{\psi_{1y}}{\psi_{0y}})^{\frac{1}{2}} \\
&= |(1+\varepsilon)^\alpha = 1 + \alpha\varepsilon + ...| = \psi_{0y}(1 + \varepsilon\frac{\psi_{1y}}{\psi_{0y}}) = \psi_{0y} + \varepsilon\psi_{1y}
\end{aligned} \tag{5.22}$$

and

$$\frac{1}{\sqrt{\psi_{0y}^2 + 2\varepsilon\psi_{0y}\psi_{1y}}} = (\psi_{0y}^2 + 2\varepsilon\psi_{0y}\psi_{1y})^{-\frac{1}{2}} = \frac{1}{\psi_{0y}}(1 + 2\varepsilon\frac{\psi_{1y}}{\psi_{0y}})^{-\frac{1}{2}}$$

$$= |(1+\varepsilon)^{\alpha} = 1+\alpha\varepsilon+...| = \frac{1}{\psi_{0y}}(1-\varepsilon\frac{\psi_{1y}}{\psi_{0y}}) = \frac{\psi_{0y}-\varepsilon\psi_{1y}}{\psi_{0y}^2}. \tag{5.23}$$

Hence,

$$\begin{aligned}(\Delta\psi_0+\varepsilon\Delta\psi_1)\sqrt{\psi_{0y}^2+2\varepsilon\psi_{0y}\psi_{1y}} &= (\psi_{0yy}+\varepsilon\psi_{1xx}+\varepsilon\psi_{1yy})(\psi_{0y}\\ &+\varepsilon\psi_{1y}) = \psi_{0yy}\psi_{0y}+\varepsilon(\psi_{0y}\psi_{1xx}+\psi_{0y}\psi_{1yy}+\psi_{0yy}\psi_{1y})\end{aligned} \tag{5.24}$$

and

$$\begin{aligned}&\frac{1}{\sqrt{\psi_{0y}^2+2\varepsilon\psi_{0y}\psi_{1y}}}((\psi_{0y}+\varepsilon\psi_{1y})^2(\psi_{0yy}+\varepsilon\psi_{1yy})\\ &+2(\psi_{0x}+\varepsilon\psi_{1x})(\psi_{0y}+\varepsilon\psi_{1y})(\psi_{0xy}+\varepsilon\psi_{1xy})\\ &+(\psi_{0x}+\varepsilon\psi_{1x})^2(\psi_{0xx}+\varepsilon\psi_{1xx}))\\ =\ &\frac{1}{\sqrt{\psi_{0y}^2+2\varepsilon\psi_{0y}\psi_{1y}}}((\psi_{0y}+\varepsilon\psi_{1y})^2(\psi_{0yy}+\varepsilon\psi_{1yy}))\\ =\ &(\frac{\psi_{0y}-\varepsilon\psi_{1y}}{\psi_{0y}^2})(\psi_{0y}^2+2\varepsilon\psi_{0y}\psi_{1y})(\psi_{0yy}+\varepsilon\psi_{1yy})\\ =\ &\frac{1}{\psi_{0y}^2}(\psi_{0y}-\varepsilon\psi_{1y})(\psi_{0y}^2\psi_{0yy}+\varepsilon(2\psi_{0yy}\psi_{0y}\psi_{1y}+\psi_{0y}^2\psi_{1yy}))\\ =\ &\frac{1}{\psi_{0y}^2}(\psi_{0y}^3\psi_{0yy}+\varepsilon(2\psi_{0yy}\psi_{0y}^2\psi_{1y}+\psi_{0y}^3\psi_{1yy}-\psi_{0y}^2\psi_{0yy}\psi_{1y}))\\ &=\frac{1}{\psi_{0y}^2}(\psi_{0y}^3\psi_{0yy}+\varepsilon(\psi_{0y}^3\psi_{1yy}+\psi_{0yy}\psi_{0y}^2\psi_{1y}))\\ &=\psi_{0y}\psi_{0yy}+\varepsilon(\psi_{0y}\psi_{1yy}+\psi_{0yy}\psi_{1y}).\end{aligned} \tag{5.25}$$

We obtain linearized equation (5.21) in the form:

$$\begin{aligned}\varepsilon((\Delta\psi_1)_t+(2\beta_1-\beta_2)(\psi_{0y}\psi_{1xy})_y-\beta_2(\psi_{1x}\psi_{0yy})_y+\beta_2(\psi_{1xx}\psi_{0y})_x)\\ +\frac{c_f}{2h}(\psi_{0yy}\psi_{0y}+\varepsilon(\psi_{0y}\psi_{1xx}+\psi_{0y}\psi_{1yy}+\psi_{0yy}\psi_{1y}))\\ +\frac{c_f}{2h}(\psi_{0y}\psi_{0yy}+\varepsilon(\psi_{0y}\psi_{1yy}+\psi_{0yy}\psi_{1y}))=0.\end{aligned} \tag{5.26}$$

Denoting ψ_{0y} as U, we rewrite (5.26) as follows

$$\varepsilon(\psi_{1xxt}+\psi_{1yyt}+(2\beta_1-\beta_2)(U_y\psi_{1xy}+U\psi_{1xyy})$$

$$
\begin{aligned}
&-\beta_2(U_{yy}\psi_{1x}+U_y\psi_{1xy})+\beta_2 U\psi_{1xxx})\\
&+\frac{c_f}{2h}(U_yU+\varepsilon(U\psi_{1xx}+U\psi_{1yy}+U_y\psi_{1y}))\\
&+\frac{c_f}{2h}(UU_y+\varepsilon(U\psi_{1yy}+U_y\psi_{1y})=0. \qquad (5.27)
\end{aligned}
$$

Collecting the terms proportional to ε we get

$$
\begin{aligned}
&\psi_{1xxt}+\psi_{1yyt}+(2\beta_1-\beta_2)(U_y\psi_{1xy}+U\psi_{1xyy})-\beta_2(U_y\psi_{1xy}\\
&+U_{yy}\psi_{1x})+\beta_2 U\psi_{1xxx}+\frac{c_f}{2h}(U\psi_{1xx}+2U_y\psi_{1y}+2U\psi_{1yy})=0. \qquad (5.28)
\end{aligned}
$$

According to the method of normal modes we seek the perturbed component ψ_1 of the stream function in the form

$$\psi_1(x,y,t)=\phi_1(y)e^{ik(x-ct)}+c.c., \qquad (5.29)$$

where k is a wavenumber and $c=c_r+ic_i$ is a complex eigenvalue; "c.c." means "complex conjugate".

Substituting (5.29) into (5.28) we obtain the linearized stability equation (the modified Rayleigh equation) in the form:

$$
\begin{aligned}
&\phi_1''[(2\beta_1-\beta_2)U-c+\frac{c_f}{ikh}U]+U_y(2\beta_1-2\beta_2\\
&+\frac{c_f}{ikh})\phi_1'+(k^2c-\beta_2U_{yy}-k^2\beta_2U-\frac{c_f}{2ih}kU)\phi_1=0, \qquad (5.30)
\end{aligned}
$$

with the boundary conditions

$$\phi_1(\pm\infty)=0. \qquad (5.31)$$

The solution of (5.30) - (5.31) is a superposition of modes. Each mode propagates as a wave that can be described by function $e^{ik(x-ct)}$. The wave speed of a mode, c, is complex ($c=c_r+c_i$). Imaginary parts c_i determine the temporal stability of the flow. The flow is said to be linearly stable if all wave speeds have negative imaginary parts. All modes of a perturbation decay with time in this case. If the imaginary part of the wave speed of at least one mode is positive then the flow is said to be linearly unstable as the perturbation has a mode that grows with time. Solving the equation for different values of the wavenumber k and bottom friction coefficient c_f we are able to find a set of values for which one mode has the imaginary part of the wave speed c equal to zero while wave speeds of all other modes have negative imaginary parts. For convenience and

in order to enable comparison with the results obtained for flows with free surface and two-phase flows, the stability parameter value s is calculated for each value of the friction coefficient c_f. The stability parameter s is related to the friction coefficient c_f by means of formula $s = \frac{c_f b}{H_0}$, where b is characteristic scale of the flow (e. g. halfwidth of the wake for wake flows, see [14]) and H_0 is water depth (keep in mind that dimensionless water depth h is defined by the expression $h = \frac{H_0}{b}$).

If we plot the points corresponding to values meeting the above-mentioned condition (one mode has c_i equal to zero) on the (k,s) plane, we obtain a so-called neutral stability curve. The neutral stability curve is effectively a boundary between the stablity region where perturbations decay with time and the instability region where perturbations have one or more amplifying modes (see Figure 5.2).

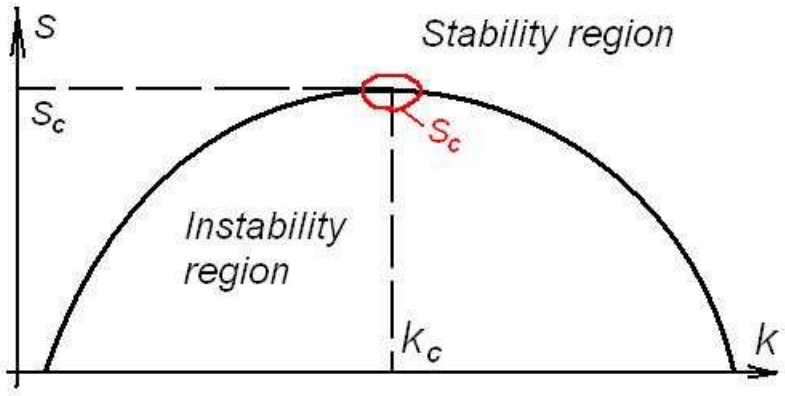

Figure 5.2: Neutral stability curve.

The value s_c of the stability parameter s at the top of the stability curve is called the critical value and is effectively a threshold separating stability and instability domains. If the bottom friction coefficient is above its critical value, then all the modes of a perturbation decay with time. For bottom friction coefficient values below critical some modes are unstable and the perturbation grows with time.

Calculations show that for sufficiently large values of the stability parameter s all eigenvalues have negative imaginary parts $(c_i < 0)$, so the flow is stable. By decreasing s for a given k it is possible to reach the point where at least one c_i becomes positive and the flow loses stability. The bisection method enables us to find the value of the stability parameter s for which at least one c_i is close to zero, while all other c_i are negative. This point lies on the ”border” between the

stability and instability regions of the flow. By repeating the process for different values of the wavenumber k we are able to build a neutral stability curve that is defined as a set of all points in the (k,s)-plane for which one c_m has the imaginary part equal to zero, while imaginary parts of all other c_m are negative. The neutral stability curve represents the boundary separating the stability domain (above the curve) from the instability domain (below the curve). The critical value, s_c of the parameter s is defined as the coordinate of the highest point of the curve, or $s_c = \max_k(s(k))$.

The s_c parameter is very important in linear stability analysis. The flow is stable for all k if the value of s is higher than s_c, and flow is unstable for some k if $s < s_c$.

The form of the stability curve and the critical value of the stability parameter depends on values of momentum correction coefficients.

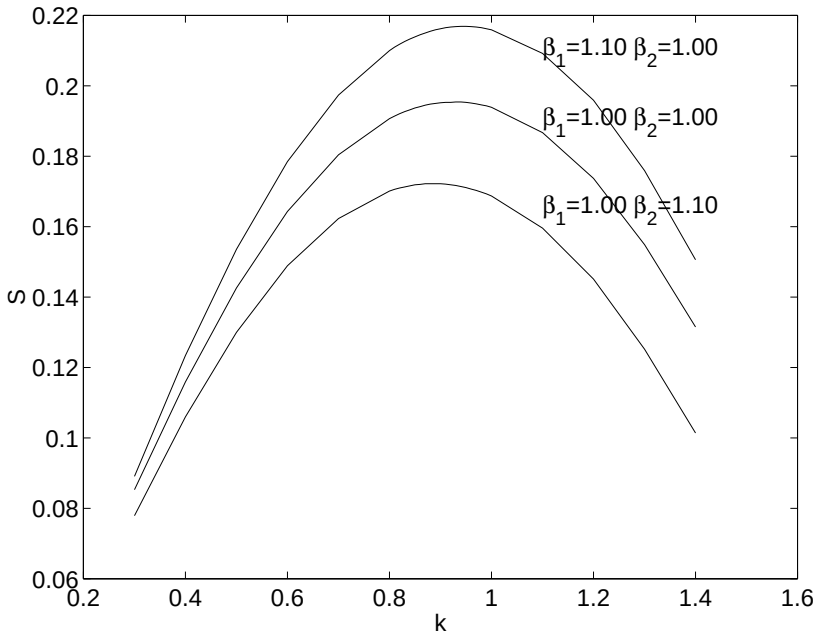

Figure 5.3: Neutral stability curves versus k for different values of momentum correction coefficients β_1 and β_2).

5.3 Results

The influence of momentum correction coefficients on the critical value of stability parameter s for the ”rigid-lid” case is analyzed in this section. The main objective is to determine how deviation of vertical velocity profile of a flow from uniform one affects the boundary between stable and

unstable flow. The influence is evaluated by solving problems (5.30)-(5.31) for different values of momentum correction coefficients β_1 and β_2. The threshold between the stable and unstable flow is represented by the critical value s_c of the parameter s. The s_c value of stability parameter is affected by variation of parameters β_1 and β_2. The linear stability results are presented for the classical (see Figure 3.1) hyperbolic secant wake profile. Numerical method used for computation is described in Chapter 5.

s_c has been calculated for the following β_1, and β_2 that are in the neighbourhood of experimentally determined values of momentum correction coefficients [40]:

$\beta_1 = 1.00, 1.05, 1.10,$

$\beta_2 = 1.00, 1.05, 1.10.$

These values have been chosen, as it is believed that values of momentum correction coefficients are not high for turbulent shallow flows due to good mixing of water. The flow profile does not differ much from uniform one with exception of domain near the bottom of the flow where the it is affected by bottom friction.

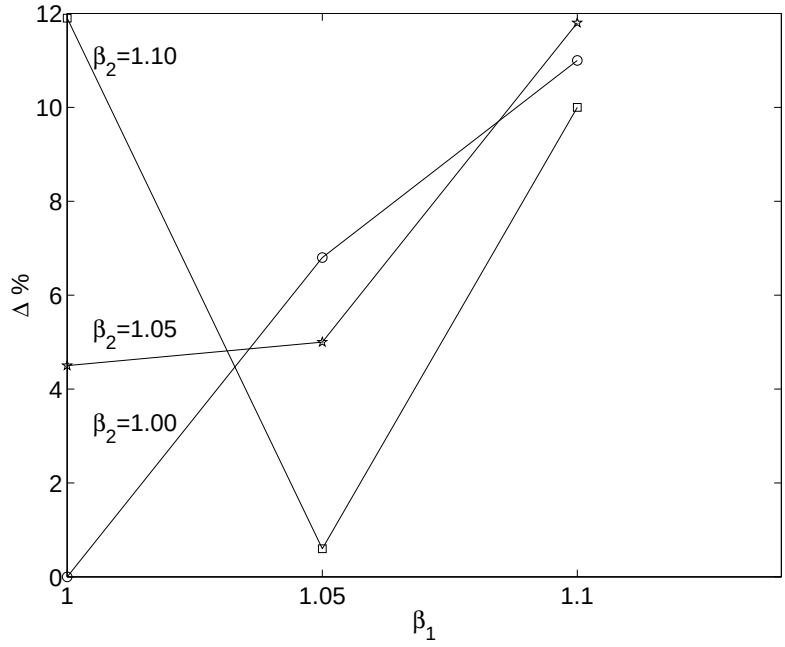

Figure 5.4: The percentage difference Δ between the values of the s_c for depth-averaged equations ($\beta_1 = 1$, $\beta_2 = 1$) and equations with correction factors ($\beta_1 > 1$,$\beta_2 > 1$).

The value of R of the wake profile in (3.1) is fixed at $R = -0.5$. The parameter N representing the number of terms in Chebyshev polynomial (refer to expression (7.4)) series is directly related to the accuracy of computations. Several values of N have been tried and effect of increase of N value on accuracy of computation has been analysed. It was found that the value $N = 50$ provides sufficient degree of accuracy and, therefore, all numerical results generated in the chapter are obtained for the case $N = 50$.

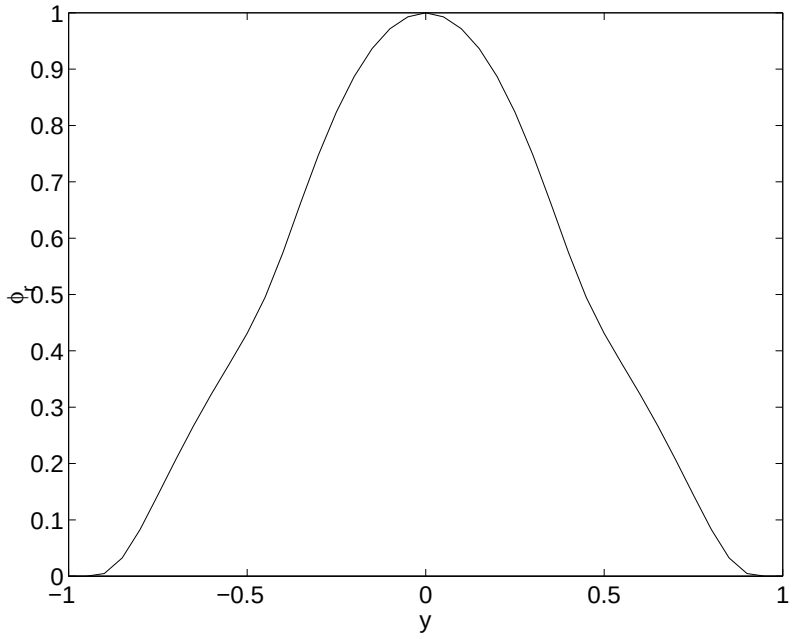

Figure 5.5: The real part of an eigenfunction obtained at $\beta_1 = 1$, $\beta_2 = 1$ and $R = -0.9$.

The stability curves obtained for various values of momentum correction coefficients β_1 and β_2 are presented in Figure 5.3. Each curve represents the boundary between the stability domain (above the curve) and the instability domain (below the curve). The ordinate of the top of the curve corresponds to the critical value of the parameter s. It can be seen that the coefficient β_1, reflecting influence of lengthwise velocity component non-uniformity, reduces stability of the flow. The instability domain grows as value of β_1 increases. The coeficient β_2 reflecting both lengthwise and transverse velocity components has, in its turn, stabilizing effect on the flow. The instability domain diminishes as β_2 grows.

Figure 5.4 presents results of the comparison of the s_c parameter calculated for different values of momentum correction coefficients β_1 and β_2. The results are compared to the values of s_c

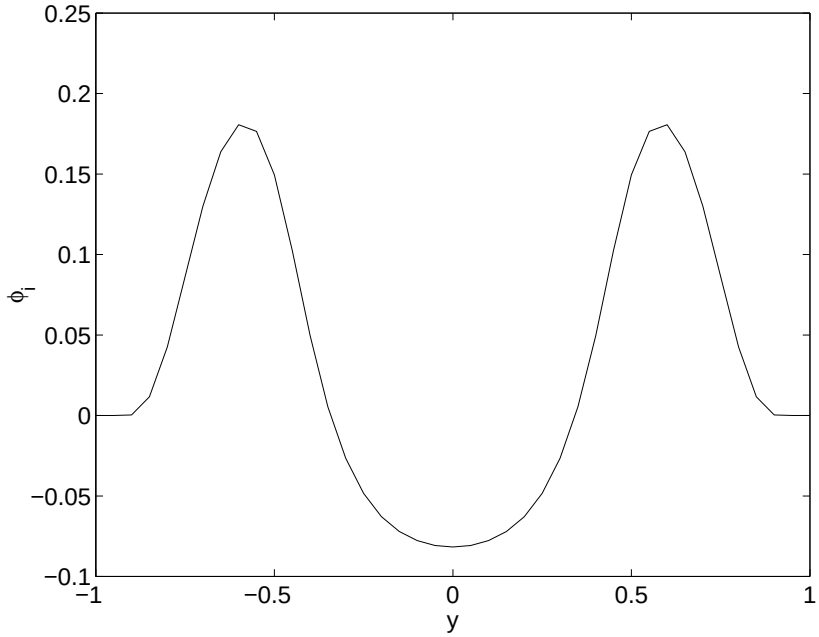

Figure 5.6: The imaginary part of an eigenfunction obtained at $\beta_1 = 1$, $\beta_2 = 1$ and $R = -0.9$.

that are calculated for β_1=1.00 and β_2=1.00. The case β_1=1.00 and β_2=1.00 corresponds to the approach when the velocity non-uniformity across the vertical coordinate is not taken into account.

As it can be seen, for some combinations of the values of β_1 and β_2 the relative error can reach 10%. The general trend is that error grows with values of the β_1 and β_2 coefficients. However, for a certain combination of the momentum correction coefficient values ($\beta_1 = 1.05$, $\beta_2 = 1.10$) the error is minimized.

The real and imaginary parts of the eigenfunction $\phi(x) = \phi_r(x) + i\phi_i(x)$ are shown in Figure 5.5 and Figure 5.6 for $R = -0.9$ and $\beta_1 = \beta_2 = 1.00$.

Unfortunately, the values of coefficients β_1 and β_2 for real island wakes are not known. It is assumed that for turbulent flow the values of the momentum correction coefficients should not be high, generally, they are expected be in the range of $1.00 - 1.10$ as turbulence of the flow favors momentum transfer between adjacent flow layers thus reducing the velocity non-uniformity in vertical direction. However, as the error in determining the s_c parameter may grow with increased values of β_1 (the stability boundary can be underestimated with increase of β_1) it might be important to know the values of β_1 and β_2 for the analyzed shallow flows.

6 WEAKLY NON-LINEAR ANALYSIS

The present chapter considers growth and development of a perturbation in shallow flows. Weakly non-linear analysis is employed to track evolution of perturbation. The analysis implies that the amplitude of a perturbation weakly depends on time and coordinate. The results indicate that perturbation amplitude is governed by the Ginzburg-Landau equation with complex coefficients [23] [24].

6.1 Introduction

Linear stability analysis is an effective tool for determining an onset of instability, that is the value of s at which a flow becomes unstable. However, linear stability analysis cannot predict how a perturbation will be evolving in time and space.

In other words linear stability analysis can tell that at a certain point perturbation is amplified but gives no clue about further development of instability. Indeed, the perturbation function is sought in a form:

$$\psi_1(x,y,t) = \phi_1(y)e^{ik(x-ct)} + c.c. \tag{6.1}$$

The eigenfunction $\phi_1(y)$ can be replaced by $C\phi_1(y)$ where C is arbitrary constant. The constant C cannot be specified by means of linear stability analysis.

The idea of weakly non-linear approach is to perform analysis in a domain that is slightly below s_c (see Figure 5.2). Effectively, the selected domain is defined by the expression

$$s = s_c(1-\varepsilon^2). \tag{6.2}$$

The point of considering a domain in the neighborhood of the s_c value is that the non-linearities grow slowly here and don't affect results so dramatically. Therefore the approach is called weakly non-linear.

The weakly non-linear approach implies that the function $\psi_1(x,y,t)$ is sought in the form:

$$\psi_1(x,y,t) = A(\xi,\tau)\phi_1(y)e^{ik(x-ct)} + c.c., \tag{6.3}$$

where A is slowly varying amplitude of perturbation. The function A depends on stretched lengthwise coordinate ξ and "slow" time τ. Parameters ξ and τ are defined by formulas (see [36]):

$$\tau = \varepsilon^2 t, \tag{6.4}$$

$$\xi = \varepsilon(x - c_g t). \tag{6.5}$$

The stretched coordinate ξ is moving with group velocity of the perturbation modes c_g.

The parameter ε is effectively a measure of how far the analysed domain spreads into the instability field (see (6.2)).

6.2 Derivation of modified Rayleigh equation

Let us consider equation (5.18). We seek perturbed solution of the equation (5.18) in a form of power series:

$$\psi = \psi_0 + \varepsilon\psi_1 + \varepsilon^2\psi_2 + \varepsilon^3\psi_3 + ..., \tag{6.6}$$

where ψ_{0y} is the base flow $U = U(0,y)$.

Substituting (6.6) into the equation (5.18) and collecting terms proportional to ε we obtain a linearized equation for function ψ_1:

$$L\psi_1 = 0, \tag{6.7}$$

where L is a linear operator defined by the expression:

$$\begin{aligned} L\phi = \phi_{xxt} + \phi_{yyt} + (2\beta_1 - \beta_2)(U_y\phi_{xy} + U\phi_{xyy}) - \beta_2(U_y\phi_{xy} + U_{yy}\phi_x) \\ + \beta_2 U\phi_{xxx} + \frac{c_f}{2h}(U\phi_{xx} + 2U_y\phi_y + 2U\phi_{yy}). \end{aligned} \tag{6.8}$$

The function ψ_1 satisfies the boundary conditions:

$$\psi_1(\pm\infty) = 0. \tag{6.9}$$

According to the method of normal modes we seek function ψ_1 in a form:

$$\psi_1(x,y,t) = \phi_1(y)e^{-\lambda t+ikx}. \tag{6.10}$$

Substituting (6.10) into (6.7) we obtain a modified Rayleigh equation for function ϕ_1

$$\begin{aligned}&(ik(2\beta_1-\beta_2)U_0+SU_0)\frac{d^2\phi_1}{dy^2}+(2ik(\beta_1-\beta_2)+s)\frac{dU_0}{dy}\frac{d\phi_1}{dy}\\&-\phi_1\left(ik\frac{d^2U_0}{dy^2}+ik^3U_0+\frac{s}{2}k^2U_0\right)-\lambda\left(\frac{d^2\phi_1}{dy^2}-k^2\phi_1\right)=0.\end{aligned} \tag{6.11}$$

As in case of linear analysis, s is the stability parameter here, defined by the expression

$$s = \frac{c_f b}{h},$$

where b is characteristic length and h is water depth.

Solving the modified Rayleigh equation we obtain a critical stability parameter value s_c that marks the boundary between stability and instability domains. If stability parameter s is below it's critical value, then the flow is unstable and vice versa.

6.3 Derivation of Ginzburg-Landau equation

In order to perform a weakly non-linear analysis we assume the stability parameter is a little bit below it's critical value (see (6.2)).

We introduce "slow" time $\tau = \varepsilon^2 t$, "stretched" coordinate $\xi = \varepsilon(x - c_g t)$ moving with a group velocity c_g, and seek function ψ_1 in the form (6.3).

According to the chain rule, partial derivatives (denoted by subscripts) for function $\psi(x,y,t,\xi,\tau)$ are denoted in the following way:

$$\psi_x \quad \rightarrow \quad \psi_x + \varepsilon\psi_\xi,$$

$$
\begin{aligned}
\psi_t &\rightarrow \psi_t - \varepsilon c_g \psi_\xi + \varepsilon^2 \psi_\tau, \\
\psi_{xy} &\rightarrow \psi_{xy} + \varepsilon \psi_{\xi y}, \\
\psi_{xx} &\rightarrow \psi_{xx} + 2\varepsilon \psi_{x\xi} + \varepsilon^2 \psi_{\xi\xi}, \\
\psi_{xxx} &\rightarrow \psi_{xxx} + 3\varepsilon \psi_{xx\xi} + 3\varepsilon^2 \psi_{x\xi\xi} + \varepsilon^3 \psi_{\xi\xi\xi}, \\
\psi_{xxy} &\rightarrow \psi_{xxy} + 2\varepsilon \psi_{xy\xi} + \varepsilon^2 \psi_{\xi\xi y}, \\
\psi_{xyy} &\rightarrow \psi_{xyy} + \varepsilon \psi_{yy\xi}.
\end{aligned} \tag{6.12}
$$

Substituting (6.6) into (5.18), we get:

$$
\begin{aligned}
&(\Delta(\psi_0 + \varepsilon\psi_1 + \varepsilon^2\psi_2 + \varepsilon^3\psi_3))_t + (2\beta_1 - \beta_2)((\psi_0 + \varepsilon\psi_1 + \varepsilon^2\psi_2 \\
&+\varepsilon^3\psi_3)_y(\psi_0 + \varepsilon\psi_1 + \varepsilon^2\psi_2 + \varepsilon^3\psi_3)_{xy})_y \\
&-\beta_2((\psi_0 + \varepsilon\psi_1 + \varepsilon^2\psi_2 + \varepsilon^3\psi_3)_x(\psi_0 \\
&+\varepsilon\psi_1 + \varepsilon^2\psi_2 + \varepsilon^3\psi_3)_{yy})_y + (\beta_2 - 1)((\psi_0 + \varepsilon\psi_1 + \varepsilon^2\psi_2 + \varepsilon^3\psi_3)_x(\psi_0 \\
&+\varepsilon\psi_1 + \varepsilon^2\psi_2 + \varepsilon^3\psi_3)_{xy})_x + \beta_2((\psi_0 + \varepsilon\psi_1 + \varepsilon^2\psi_2 + \varepsilon^3\psi_3)_{xx}(\psi_0 \\
&+\varepsilon\psi_1 + \varepsilon^2\psi_2 + \varepsilon^3\psi_3)_y)_x - (2\beta_3 - 1)((\psi_0 \\
&+\varepsilon\psi_1 + \varepsilon^2\psi_2 + \varepsilon^3\psi_3)_x(\psi_0 + \varepsilon\psi_1 + \varepsilon^2\psi_2 + \varepsilon^3\psi_3)_{xx})_y \\
&+\frac{c_f}{2h}\Delta(\psi_0 + \varepsilon\psi_1 + \varepsilon^2\psi_2 + \varepsilon^3\psi_3) \\
&\sqrt{(\psi_0 + \varepsilon\psi_1 + \varepsilon^2\psi_2 + \varepsilon^3\psi_3)_x^2 + (\psi_0 + \varepsilon\psi_1 + \varepsilon^2\psi_2 + \varepsilon^3\psi_3)_y^2} \\
&+\frac{c_f}{2h\sqrt{(\psi_0 + \varepsilon\psi_1 + \varepsilon^2\psi_2 + \varepsilon^3\psi_3)_x^2 + (\psi_0 + \varepsilon\psi_1 + \varepsilon^2\psi_2 + \varepsilon^3\psi_3)_y^2}} \\
&((\psi_0 + \varepsilon\psi_1 + \varepsilon^2\psi_2 + \varepsilon^3\psi_3)_y^2(\psi_0 + \varepsilon\psi_1 + \varepsilon^2\psi_2 + \varepsilon^3\psi_3)_{yy} \\
&+2(\psi_0 + \varepsilon\psi_1 + \varepsilon^2\psi_2 + \varepsilon^3\psi_3)_x(\psi_0 + \varepsilon\psi_1 \\
&+\varepsilon^2\psi_2 + \varepsilon^3\psi_3)_y(\psi_0 + \varepsilon\psi_1 + \varepsilon^2\psi_2 + \varepsilon^3\psi_3)_{xy} \\
&+(\psi_0 + \varepsilon\psi_1 + \varepsilon^2\psi_2 + \varepsilon^3\psi_3)_x^2(\psi_0 + \varepsilon\psi_1 + \varepsilon^2\psi_2 + \varepsilon^3\psi_3)_{xx}) = 0
\end{aligned} \tag{6.13}
$$

or

$$
\begin{aligned}
&\Delta(\psi_{0t} + \varepsilon\psi_{1t} + \varepsilon^2\psi_{2t} + \varepsilon^3\psi_{3t}) + (2\beta_1 - \beta_2)((\psi_{0y} + \varepsilon\psi_{1y} + \varepsilon^2\psi_{2y} \\
&+\varepsilon^3\psi_{3y})(\psi_{0xy} + \varepsilon\psi_{1xy} + \varepsilon^2\psi_{2xy} + \varepsilon^3\psi_{3xy}))_y \\
&-\beta_2((\psi_{0x} + \varepsilon\psi_{1x} + \varepsilon^2\psi_{2x} + \varepsilon^3\psi_{3x})(\psi_{0yy} \\
&+\varepsilon\psi_{1yy} + \varepsilon^2\psi_{2yy} + \varepsilon^3\psi_{3yy}))_y
\end{aligned}
$$

$$
\begin{aligned}
&+(\beta_2-1)((\psi_{0x}+\varepsilon\psi_{1x}+\varepsilon^2\psi_{2x}+\varepsilon^3\psi_{3x})(\psi_{0xy}\\
&+\varepsilon\psi_{1xy}+\varepsilon^2\psi_{2xy}+\varepsilon^3\psi_{3xy}))_x\\
&+\beta_2((\psi_{0xx}+\varepsilon\psi_{1xx}+\varepsilon^2\psi_{2xx}+\varepsilon^3\psi_{3xx})(\psi_{0y}\\
&+\varepsilon\psi_{1y}+\varepsilon^2\psi_{2y}+\varepsilon^3\psi_{3y}))_x-(2\beta_3-1)((\psi_{0x}\\
&+\varepsilon\psi_{1x}+\varepsilon^2\psi_{2x}+\varepsilon^3\psi_{3x})(\psi_{0xx}+\varepsilon\psi_{1xx}+\varepsilon^2\psi_{2xx}+\varepsilon^3\psi_{3xx}))_y\\
&+\frac{c_f}{2h}\Delta(\psi_0+\varepsilon\psi_1+\varepsilon^2\psi_2+\varepsilon^3\psi_3)\\
&\sqrt{(\psi_{0x}+\varepsilon\psi_{1x}+\varepsilon^2\psi_{2x}+\varepsilon^3\psi_{3x})^2+(\psi_{0y}+\varepsilon\psi_{1y}+\varepsilon^2\psi_{2y}+\varepsilon^3\psi_{3y})^2}\\
&+\frac{c_f}{2h\sqrt{(\psi_{0x}+\varepsilon\psi_{1x}+\varepsilon^2\psi_{2x}+\varepsilon^3\psi_{3x})^2+(\psi_{0y}+\varepsilon\psi_{1y}+\varepsilon^2\psi_{2y}+\varepsilon^3\psi_{3y})^2}}\\
&((\psi_{0y}+\varepsilon\psi_{1y}+\varepsilon^2\psi_{2y}+\varepsilon^3\psi_{3y})^2(\psi_{0yy}+\varepsilon\psi_{1yy}+\varepsilon^2\psi_{2yy}+\varepsilon^3\psi_{3yy})\\
&+2(\psi_{0x}+\varepsilon\psi_{1x}+\varepsilon^2\psi_{2x}+\varepsilon^3\psi_{3x})(\psi_{0y}+\varepsilon\psi_{1y}\\
&+\varepsilon^2\psi_{2y}+\varepsilon^3\psi_{3y})(\psi_{0xy}+\varepsilon\psi_{1xy}+\varepsilon^2\psi_{2xy}+\varepsilon^3\psi_{3xy})\\
&+(\psi_{0x}+\varepsilon\psi_{1x}+\varepsilon^2\psi_{2x}+\varepsilon^3\psi_{3x})^2(\psi_{0xx}\\
&+\varepsilon\psi_{1xx}+\varepsilon^2\psi_{2xx}+\varepsilon^3\psi_{3xx}))=0. \qquad (6.14)
\end{aligned}
$$

Taking into account that $\psi_0=\psi_0(y)$ and neglecting terms higher than ε^3 we get:

$$
\begin{aligned}
&(\varepsilon\psi_{1xxt}+\varepsilon^2\psi_{2xxt}+\varepsilon^3\psi_{3xxt})\\
&+(\varepsilon\psi_{1yyt}+\varepsilon^2\psi_{2yyt}+\varepsilon^3\psi_{3yyt})+(2\beta_1-\beta_2)(\varepsilon\psi_{0y}\psi_{1xy}+\varepsilon^2\psi_{1y}\psi_{1xy}\\
&+\varepsilon^3\psi_{2y}\psi_{1xy}+\varepsilon^2\psi_{0y}\psi_{2xy}+\varepsilon^3\psi_{1y}\psi_{2xy}+\psi_{0y}\varepsilon^3\psi_{3xy})_y\\
&-\beta_2(\varepsilon\psi_{0yy}\psi_{1x}+\varepsilon^2\psi_{0yy}\psi_{2x}+\varepsilon^3\psi_{0yy}\psi_{3x}\\
&+\varepsilon^2\psi_{1x}\psi_{1yy}+\varepsilon^3\psi_{2x}\psi_{1yy}+\varepsilon^3\psi_{1yy}\psi_{2x})_y\\
&+(\beta_2-1)(\varepsilon^2\psi_{1x}\psi_{1xy}+\varepsilon^3\psi_{2x}\psi_{1xy}+\varepsilon\psi_{1x}\psi_{2xy})_x\\
&\beta_2(\varepsilon\psi_{1xx}\psi_{0y}+\varepsilon^2\psi_{2xx}\psi_{0y}+\varepsilon^3\psi_{3xx}\psi_{0y}\\
&+\varepsilon^2\psi_{1xx}\psi_{1y}+\varepsilon^3\psi_{2xx}\psi_{1y}+\varepsilon^3\psi_{1xx}\psi_{2y})_x\\
&-(2\beta_3-1)(\varepsilon^2\psi_{1x}\psi_{1xx}+\varepsilon^3\psi_{2x}\psi_{1xx}+\varepsilon^3\psi_{1x}\psi_{2xx})_y\\
&+\frac{c_f}{2h}\Delta(\psi_0+\varepsilon\psi_1+\varepsilon^2\psi_2+\varepsilon^3\psi_3)\sqrt{u(\psi_0,\psi_1,\psi_2,\psi_3)}\\
&+\frac{c_f}{2h\sqrt{u(\psi_0,\psi_1,\psi_2,\psi_3)}}(\psi_{0y}^2\psi_{0yy}+\varepsilon\psi_{1y}\psi_{0y}\psi_{0yy}\\
&+\varepsilon^2\psi_{2y}\psi_{0y}\psi_{0yy}+2\varepsilon^3\psi_{3y}\psi_{0y}\psi_{0yy}\\
&+\varepsilon\psi_{0y}\psi_{1y}\psi_{0yy}+\varepsilon^2\psi_{1y}^2\psi_{0yy}+\varepsilon^3\psi_{2y}\psi_{1y}\psi_{0yy}+\varepsilon^2\psi_{0y}\psi_{2y}\psi_{0yy}\\
&+\varepsilon^3\psi_{1y}\psi_{2y}\psi_{0yy}+\varepsilon\psi_{0y}^2\psi_{1yy}+\varepsilon^2\psi_{1y}\psi_{0y}\psi_{1yy}
\end{aligned}
$$

$$+\varepsilon^3\psi_{2y}\psi_{0y}\psi_{1yy}+\varepsilon^2\psi_{0y}\psi_{1y}\psi_{1yy}+\varepsilon^3\psi_{1y}^2\psi_{1yy}+\varepsilon^3\psi_{0y}\psi_{2y}\psi_{1yy}$$
$$+\varepsilon^2\psi_{0y}^2\psi_{2yy}+\varepsilon^3\psi_{1y}\psi_{0y}\psi_{2yy}+\varepsilon^3\psi_{0y}\psi_{1y}\psi_{2yy}+\varepsilon^3\psi_{0y}^2\psi_{3yy}$$
$$+2(\varepsilon^2\psi_{1x}\psi_{0y}\psi_{1xy}+\varepsilon^3\psi_{2x}\psi_{0y}\psi_{1xy}+\varepsilon^3\psi_{1x}\psi_{1y}\psi_{1xy}+\varepsilon^3\psi_{1x}\psi_{0y}\psi_{2xy})$$
$$+\varepsilon^3\psi_{1x}^2\psi_{1xx})=0, \tag{6.15}$$

where

$$u(\psi_0,\psi_1,\psi_2,\psi_3)=\varepsilon^2\psi_{1x}^2+2\varepsilon^3\psi_{2x}\psi_{1x}+\psi_{0y}^2+2\varepsilon\psi_{1y}\psi_{0y}$$
$$+\varepsilon^2\psi_{2y}\psi_{0y}+\varepsilon^3\psi_{3y}\psi_{0y}+\varepsilon^2\psi_{1y}^2+\varepsilon^3\psi_{2y}\psi_{1y}$$
$$+\varepsilon^2\psi_{0y}\psi_{2y}+\varepsilon^3\psi_{1y}\psi_{2y}+\varepsilon^3\psi_{0y}\psi_{3y}. \tag{6.16}$$

Taking into account (6.12) and collecting terms proportional to ε^1 we obtain (5.26). Collecting terms proportional to ε^2 yelds:

$$\psi_{2xxt}-c_g\psi_{1xx\xi}+2\psi_{1x\xi t}+\psi_{2yyt}-c_g\psi_{1yy\xi}$$
$$+(2\beta_1-\beta_2)(U_y\psi_{2xy}+U_y\psi_{1\xi y}+\psi_{1yy}\psi_{1xy}+U\psi_{2xyy}$$
$$+U\psi_{1yy\xi}+\psi_{1y}\psi_{1xyy})-\beta_2(\psi_{1xy}\psi_{1yy}+U_y\psi_{2xy}+U_y\psi_{1\xi y}$$
$$+\psi_{1x}\psi_{1yyy}+U_{yy}\psi_{2x}+U_{yy}\psi_{1\xi})+(\beta_2-1)(\psi_{1xx}\psi_{1xy}$$
$$+\psi_{1x}\psi_{1xxy})+\beta_2(\psi_{1y}\psi_{1xxx}+U\psi_{2xxx}+3U\psi_{1xx\xi}$$
$$+\psi_{1xy}\psi_{1xx})-(2\beta_3-1)(\psi_{1xx}\psi_{1xy}+\psi_{1x}\psi_{1xxy})+\frac{c_f}{2h}(\psi_{1xx}\psi_{1y}$$
$$+U\psi_{2xx}+2U\psi_{1x\xi}+U_y\psi_{2y}+\psi_{1yy}\psi_{1y}+U\psi_{2yy}-UU_y)$$
$$+\frac{c_f}{2h}(U_y\psi_{2y}+\psi_{1y}\psi_{1yy}+U\psi_{2yy}+2\psi_{1x}\psi_{1xy}-UU_y)=0, \tag{6.17}$$

Assuming that $\beta_1=\beta_2=\beta_3=1$ we get

$$\psi_{2xxt}-c_g\psi_{1xx\xi}+2\psi_{1x\xi t}+\psi_{2yyt}-c_g\psi_{1yy\xi}$$
$$+(U_y\psi_{2xy}+U_y\psi_{1\xi y}+\psi_{1yy}\psi_{1xy}+U\psi_{2xyy}$$
$$+U\psi_{1yy\xi}+\psi_{1y}\psi_{1xyy})-(\psi_{1xy}\psi_{1yy}+U_y\psi_{2xy}+U_y\psi_{1\xi y}$$
$$+\psi_{1x}\psi_{1yyy}+U_{yy}\psi_{2x}+U_{yy}\psi_{1\xi})$$
$$+(\psi_{1y}\psi_{1xxx}+U\psi_{2xxx}+3U\psi_{1xx\xi}$$

$$
\begin{aligned}
&+\psi_{1xy}\psi_{1xx}) - (\psi_{1xx}\psi_{1xy} + \psi_{1x}\psi_{1xxy}) + \frac{c_f}{2h}(\psi_{1xx}\psi_{1y} \\
&+U\psi_{2xx} + 2U\psi_{1x\xi} + U_y\psi_{2y} + \psi_{1yy}\psi_{1y} + U\psi_{2yy} - UU_y) \\
&+\frac{c_f}{2h}(U_y\psi_{2y} + \psi_{1y}\psi_{1yy} + U\psi_{2yy} + 2\psi_{1x}\psi_{1xy} - UU_y) = 0.
\end{aligned} \tag{6.18}
$$

Collecting terms of order ε^3 we obtain:

$$
\begin{aligned}
&\psi_{3xxt} - c_g\psi_{2xx\xi} + \psi_{1xx\tau} + 2\psi_{2x\xi t} - 2c_g\psi_{1x\xi\xi} + \psi_{1\xi\xi t} + \psi_{3yyt} \\
&-c_g\psi_{2yy\xi} + \psi_{1yy\tau} + (2\beta_1 - \beta_2)(U_y\psi_{3xy} + U_y\psi_{2\xi y} + \psi_{1yy}\psi_{2xy} \\
&+\psi_{1yy}\psi_{1\xi y} + \psi_{2yy}\psi_{1xy} + U\psi_{3xyy} + U\psi_{2yy\xi} + \psi_{1y}\psi_{2xyy} \\
&+\psi_{1y}\psi_{1yy\xi} + \psi_{2y}\psi_{1xyy}) - \beta_2(\psi_{1xy}\psi_{2yy} + \psi_{2xy}\psi_{1yy} + U_y\psi_{3xy} \\
&+\psi_{1\xi y}\psi_{1yy} + U_y\psi_{2\xi y} + \psi_{1x}\psi_{2yyy} + \psi_{2x}\psi_{1yyy} + U_{yy}\psi_{3x} \\
&+\psi_{1\xi}\psi_{1yyy} + U_{yy}\psi_{2\xi}) + (\beta_2 - 1)(\psi_{1xx}\psi_{2xy} + \psi_{1xx}\psi_{1\xi y} \\
&+\psi_{2xx}\psi_{1xy} + 2\psi_{1x\xi}\psi_{1xy} + \psi_{1x}\psi_{2xxy} + 2\psi_{1x}\psi_{1xy\xi} + \psi_{2x}\psi_{1xxy} \\
&+\psi_{1\xi}\psi_{1xxy} + \psi_{2\xi}\psi_{1xxy}) + \beta_2(\psi_{2y}\psi_{1xxx} + \psi_{1y}\psi_{2xxx} + U\psi_{3xxx} \\
&+3\psi_{1y}\psi_{1xx\xi} + 3U\psi_{2xx\xi} + 3U\psi_{1x\xi\xi} + \psi_{1xx}\psi_{2xy} + \psi_{1xx}\psi_{1\xi y} \\
&+\psi_{2xx}\psi_{1xy} + 2\psi_{1x\xi}\psi_{1xy}) - (2\beta_3 - 1)(\psi_{1xx}\psi_{2xy} + \psi_{1xx}\psi_{1\xi y} \\
&+\psi_{2xx}\psi_{1xy} + 2\psi_{1x\xi}\psi_{1xy} + \psi_{1x}\psi_{2xxy} + 2\psi_{1x}\psi_{1xy\xi} + \psi_{2x}\psi_{1xxy} \\
&+\psi_{1\xi}\psi_{1xxy} + \psi_{2\xi}\psi_{1xxy}) + \frac{c_f}{2h}(\psi_{1xx}\psi_{2y} + \frac{\psi_{1xx}{\psi_{1x}}^2}{2U} \\
&+\psi_{2xx}\psi_{1y} + U\psi_{3xx} + 2\psi_{1x\xi}\psi_{1y} + 2U\psi_{2x\xi} + U\psi_{1\xi\xi} \\
&-\frac{U_y\psi_{1y}{\psi_{1x}}^2}{2U^2} + \frac{U_y\psi_{1x}\psi_{2x}}{U} + \frac{U_y\psi_{1x}\psi_{1\xi}}{U} + U_y\psi_{3y} \\
&+\psi_{1yy}\psi_{2y} + \frac{\psi_{1yy}{\psi_{1x}}^2}{2U} + \psi_{2yy}\psi_{1y} + U\psi_{3yy} - U\psi_{1xx} \\
&-U_y\psi_{1y} - U\psi_{1yy} + \frac{U_y\psi_{1y}{\psi_{1x}}^2}{2U^2} - \frac{U_y\psi_{1x}\psi_{2x}}{U} - \frac{U_y\psi_{1x}\psi_{1\xi}}{U} \\
&-U_y\psi_{3y} \\
&+\psi_{1yy}\psi_{2y} - \frac{\psi_{1yy}{\psi_{1x}}^2}{2U} + \psi_{1y}\psi_{2yy} + 2U_y\psi_{3y} \\
&+U\psi_{3yy} + 2\psi_{1x}\psi_{2xy} + 2\psi_{1x}\psi_{1\xi y} \\
&+2\psi_{2x}\psi_{1xy} + 2\psi_{1\xi}\psi_{1xy} + \frac{{\psi_{1x}}^2\psi_{1xx}}{U} - U_y\psi_{1y} - \psi_{1yy}U = 0.
\end{aligned} \tag{6.19}
$$

We can re-write equations (6.17) and (6.19) as nonhomogeneous equations with linear operator L defined by (6.8) on the left side.

The equation for the function ψ_2 is

$$
\begin{aligned}
L\psi_2 = c_g(\psi_{1xx\xi} + \psi_{1yy\xi}) - 2\psi_{1x\xi t} \\
-(2\beta_1 - \beta_2)(U_y\psi_{1\xi y} + \psi_{1yy}\psi_{1xy} \\
+U\psi_{1yy\xi} + \psi_{1y}\psi_{1xyy}) - \beta_2(\psi_{1xy}\psi_{1yy} + U_y\psi_{1\xi y} \\
+\psi_{1x}\psi_{1yyy} + U_{yy}\psi_{1\xi}) - (\beta_2 - 1)(\psi_{1xx}\psi_{1xy} \\
+\psi_{1x}\psi_{1xxy}) - \beta_2(\psi_{1y}\psi_{1xxx} - 3U\psi_{1xx\xi} \\
+\psi_{1xy}\psi_{1xx}) + (2\beta_3 - 1)(\psi_{1xx}\psi_{1xy} + \psi_{1x}\psi_{1xxy}) - \frac{c_f}{2h}(\psi_{1xx}\psi_{1y} \\
+2U\psi_{1x\xi} + \psi_{1yy}\psi_{1y} - UU_y \\
+\psi_{1y}\psi_{1yy} + 2\psi_{1x}\psi_{1xy} - UU_y). \qquad (6.20)
\end{aligned}
$$

The function ψ_3 satisfies the equation

$$
\begin{aligned}
L\psi_3 = c_g(\psi_{2xx\xi} + \psi_{2yy\xi} + 2\psi_{1x\xi\xi}) - \psi_{1xx\tau} - \psi_{1yy\tau} \\
-2\psi_{2x\xi t} - \psi_{1\xi\xi t} - (2\beta_1 - \beta_2)(U_y\psi_{2\xi y} + \psi_{1yy}\psi_{2xy} \\
+\psi_{1yy}\psi_{1\xi y} + \psi_{2yy}\psi_{1xy} + U\psi_{2yy\xi} + \psi_{1y}\psi_{2xyy} + \psi_{1y}\psi_{1yy\xi} \\
+\psi_{2y}\psi_{1xyy}) + \beta_2(\psi_{1xy}\psi_{2yy} + \psi_{2xy}\psi_{1yy} + \psi_{1\xi y}\psi_{1yy} \\
+U_y\psi_{2\xi y} + \psi_{1x}\psi_{2yyy} + \psi_{2x}\psi_{1yyy} + \psi_{1\xi}\psi_{1yyy} + U_{yy}\psi_{2\xi}) \\
-(\beta_2 - 1)(\psi_{1xx}\psi_{2xy} + \psi_{1xx}\psi_{1\xi y} + \psi_{2xx}\psi_{1xy} + 2\psi_{1x\xi}\psi_{1xy} \\
+\psi_{1x}\psi_{2xxy} + 2\psi_{1x}\psi_{1xy\xi} + \psi_{2x}\psi_{1xxy} + \psi_{1\xi}\psi_{1xxy} + \psi_{2\xi}\psi_{1xxy}) \\
-\beta_2(\psi_{2y}\psi_{1xxx} + \psi_{1y}\psi_{2xxx} + 3\psi_{1y}\psi_{1xx\xi} + 3U\psi_{2xx\xi} + 3U\psi_{1x\xi\xi} \\
+\psi_{1xx}\psi_{2xy} + \psi_{1xx}\psi_{1\xi y} + \psi_{2xx}\psi_{1xy} + 2\psi_{1x\xi}\psi_{1xy}) \\
+(2\beta_3 - 1)(\psi_{1xx}\psi_{2xy} + \psi_{1xx}\psi_{1\xi y} + \psi_{2xx}\psi_{1xy} + 2\psi_{1x\xi}\psi_{1xy} \\
+\psi_{1x}\psi_{2xxy} + 2\psi_{1x}\psi_{1xy\xi} + \psi_{2x}\psi_{1xxy} + \psi_{1\xi}\psi_{1xxy} + \psi_{2\xi}\psi_{1xxy}) \\
+\frac{c_f}{2h}(\psi_{1xx}\psi_{2y} + \frac{\psi_{1xx}{\psi_{1x}}^2}{2U} + \psi_{2xx}\psi_{1y} + 2\psi_{1x\xi}\psi_{1y} \\
+2U\psi_{2x\xi} + U\psi_{1\xi\xi} + \psi_{1yy}\psi_{2y} + \frac{\psi_{1yy}{\psi_{1x}}^2}{2U} \\
+\psi_{2yy}\psi_{1y} - U\psi_{1xx} - U_y\psi_{1y} - U\psi_{1yy} \\
+\psi_{1yy}\psi_{2y} - \frac{\psi_{1yy}{\psi_{1x}}^2}{2U} + \psi_{1y}\psi_{2yy} + 2\psi_{1x}\psi_{2xy} + 2\psi_{1x}\psi_{1\xi y} \\
+2\psi_{2x}\psi_{1xy} + 2\psi_{1\xi}\psi_{1xy} + \frac{{\psi_{1x}}^2\psi_{1xx}}{U} - U_y\psi_{1y} - \psi_{1yy}U. \qquad (6.21)
\end{aligned}
$$

Note that equations (6.20) and (6.21) are resonantly forced since the corresponding homo-

geneous equation (6.7) has a nontrivial solution. Thus, in accordance with the Fredholm alternative [45] equations (6.20) and (6.21) have solutions if and only if their right-hand sides are orthogonal to all eigenfunctions of the corresponding homogeneous adjoint problem.

We seek solution of equation (6.7) in the form

$$\psi_1 = A(\xi,\tau)\phi_1(y)e^{ik(x-ct)} + A^*{\phi_1}^* e^{-ik(x-ct)}. \tag{6.22}$$

The right-hand side of equation (6.20) suggests the solution has the form:

$$\psi_2 = AA^*{\phi_2}^{(0)}(y) + A_\xi \phi_2^{(1)}(y)e^{ik(x-ct)} + A^2\phi_2^{(2)}(y)e^{2ik(x-ct)} + c.c. \tag{6.23}$$

Substituting (6.22) and (6.23) into (6.20) and collecting terms proportional to AA^* we obtain

$$\begin{aligned}\frac{2c_f}{h}(U\phi_{2yy}^{(0)} + U_y\phi_{2y}^{(0)}) = ik\beta_2(\phi_{1y}\phi_{1yy}^* - \phi_{1y}^*\phi_{1yy} \\ +\phi_1\phi_{1yyy}^* - \phi_1^*\phi_{1yyy}) - \frac{c_f}{2h}(k^2\phi_1\phi_{1y}^* + k^2\phi_1^*\phi_{1y} \\ +2\phi_{1yy}\phi_{1y}^* + 2\phi_{1yy}^*\phi_{1y}).\end{aligned} \tag{6.24}$$

Collecting terms proportional to $A_\xi e^{ik(x-ct)}$ gives

$$\begin{aligned}ik^3c\phi_2^{(1)} - ikc\phi_{2yy}^{(1)} + (2\beta_1-\beta_2)ik(U_y\phi_{2y}^{(1)} + U\phi_{2yy}^{(1)}) \\ -ik\beta_2(U_y\phi_{2y}^{(1)} + U_{yy}\phi_2^{(1)} + k^2U\phi_2^{(1)}) + \frac{c_f}{2h}(-k^2U\phi_2^{(1)} + 2U_y\phi_{2y}^{(1)} \\ +2U\phi_{2yy}^{(1)}) = -2k^2c\phi_1 - k^2c_g\phi_1 + c_g\phi_{1yy} - (2\beta_1-\beta_2)(U_y\phi_{1y} \\ +U\phi_{1yy}) + \beta_2(U_y\phi_{1y} + U_{yy}\phi_1) + 3\beta_2k^2U\phi_1 - \frac{ikc_fU\phi_1}{h}.\end{aligned} \tag{6.25}$$

Finally, for terms proportional to $A^2e^{2ik(x-ct)}$ we acquire

$$\begin{aligned}8ik^3c\phi_2^{(2)} - 2ikc\phi_{2yy}^{(2)} + (2\beta_1-\beta_2)(2ikU_y\phi_{2y}^{(2)} + 2ikU\phi_{2yy}^{(2)}) \\ -\beta_2(2ikU_y\phi_{2y}^{(2)} + 2ikU_{yy}\phi_2^{(2)} + 8ik^3U\phi_2^{(2)}) \\ +\frac{c_f}{h}(-2k^2U\phi_2^{(2)} + U_y\phi_{2y}^{(2)} + U\phi_{2yy}^{(2)}) = -4ik(\beta_1-\beta_2)\phi_{1y}\phi_{1yy} \\ +ik\beta_2(\phi_{1y}\phi_{1yy} + \phi_1\phi_{1yyy}) - 2ik^3(\beta_2-1)\phi_1\phi_{1y}\end{aligned}$$

$$+2ik^3\beta_2\phi_1\phi_{1y} - 2ik^3(2\beta_3 - 1)\phi_1\phi_{1y} - \frac{c_f}{2h}(2\phi_{1y}\phi_{1yy} - 3k^2\phi_1\phi_{1y}). \tag{6.26}$$

Taking into account (6.8), equation (6.25) can be rewritten in the form

$$\begin{aligned} ikL\phi_2^{(1)} = -2k^2c\phi_1 - k^2c_g\phi_1 + c_g\phi_{1yy} - (2\beta_1 - \beta_2)(U_y\phi_{1y} \\ +U\phi_{1yy}) + \beta_2(U_y\phi_{1y} + U_{yy}\phi_1) + 3\beta_2k^2U\phi_1 - \frac{ikc_fU\phi_1}{h}. \end{aligned} \tag{6.27}$$

Equation (6.27) according to Fredholm alternative [45] has a solution if and only if its right-hand side is orthogonal to all eigenfunctions of the corresponding homogeneous adjoint problem, since corresponding homogeneous equation

$$ikL\phi_1 = 0$$

has a nontrivial solution.

We define adjoint operator and adjoint eigenfunction in the following way:

$$\int_{-\infty}^{+\infty} \phi_1^a L(\phi_1)dy = \int_{-\infty}^{+\infty} \phi_1 L^a(\phi_1^a)dy. \tag{6.28}$$

Performing integration of (6.7) by parts and taking into account (6.9), so that the terms containing ψ_1 are eliminated, we obtain the adjoint problem in the form:

$$\begin{aligned} L^a\phi_1^a \equiv (\phi_1^a)((2\beta_1 - \beta_2)U - c + \frac{c_f}{ikh}) \\ +(\phi_1^a)(2U_y(2\beta_1 - \beta_2 + \frac{c_f}{ikh}) - (2\beta_1 - \beta_2)U + c \\ -\frac{c_f}{ikh}U) + \phi_1^a(-U_y(2\beta_1 - \beta_2 + \frac{c_f}{ikh}) \\ +k^2c - \beta_2U_{yy} - k^2\beta_2U - \frac{c_f}{2ikh}U) = 0. \end{aligned} \tag{6.29}$$

So, solvability condition for equation (6.27) is

$$\begin{aligned} \int_{-\infty}^{+\infty} \phi_1^a(-k^2c_g\phi_1 + c_g\phi_{1yy} - 2k^2c\phi_1 - (2\beta_1 - \beta_2)(U_y\phi_{1y} \\ +U\phi_{1yy}) + \beta_2(U_y\phi_{1y} + U_{yy}\phi_1) + 3\beta_2K^2U\phi_1 - \frac{ikc_fU\phi_1}{h})dy = 0. \end{aligned} \tag{6.30}$$

This equation can be used for calculation of group velocity c_g.

The equation (6.21) allows us to determine the way how the amplitude A is growing with time. According to Fredholm alternative, the solvability condition for it is:

$$\begin{aligned}
\int_{-\infty}^{+\infty} \phi_1^a (c_g(\psi_{2xx\xi} + \psi_{2yy\xi} + 2\psi_{1x\xi\xi}) - \psi_{1xx\tau} \\
-\psi_{1yy\tau} - 2\psi_{2x\xi t} - \psi_{1\xi\xi t} - (2\beta_1 - \beta_2)(U_y\psi_{2\xi y} \\
+\psi_{1yy}\psi_{2xy} + \psi_{1yy}\psi_{1\xi y} + \psi_{2yy}\psi_{1xy} + U\psi_{2yy\xi} \\
+\psi_{1y}\psi_{2xyy} + \psi_{1y}\psi_{1yy\xi} + \psi_{2y}\psi_{1xyy}) + \beta_2(\psi_{1xy}\psi_{2yy} \\
+\psi_{2xy}\psi_{1yy} + \psi_{1\xi y}\psi_{1yy} + U_y\psi_{2\xi y} + \psi_{1x}\psi_{2yyy} \\
+\psi_{2x}\psi_{1yyy} + \psi_{1\xi}\psi_{1yyy} + U_{yy}\psi_{2\xi}) - (\beta_2 - 1)(\psi_{1xx}\psi_{2xy} \\
+\psi_{1xx}\psi_{1\xi y} + \psi_{2xx}\psi_{1xy} + 2\psi_{1x\xi}\psi_{1xy} + \psi_{1x}\psi_{2xxy} \\
+2\psi_{1x}\psi_{1xy\xi} + \psi_{2x}\psi_{1xxy} + \psi_{1\xi}\psi_{1xxy} + \psi_{2\xi}\psi_{1xxy}) \\
-\beta_2(\psi_{2y}\psi_{1xxx} + \psi_{1y}\psi_{2xxx} + 3\psi_{1y}\psi_{1xx\xi} + 3U\psi_{2xx\xi} \\
+3U\psi_{1x\xi\xi} + \psi_{1xx}\psi_{2xy} + \psi_{1xx}\psi_{1\xi y} + \psi_{2xx}\psi_{1xy} + 2\psi_{1x\xi}\psi_{1xy}) \\
+(2\beta_3 - 1)(\psi_{1xx}\psi_{2xy} + \psi_{1xx}\psi_{1\xi y} + \psi_{2xx}\psi_{1xy} + 2\psi_{1x\xi}\psi_{1xy} \\
+\psi_{1x}\psi_{2xxy} + 2\psi_{1x}\psi_{1xy\xi} + \psi_{2x}\psi_{1xxy} + \psi_{1\xi}\psi_{1xxy} + \psi_{2\xi}\psi_{1xxy}) \\
+\frac{c_f}{2h}(\psi_{1xx}\psi_{2y} + \frac{\psi_{1xx}{\psi_{1x}}^2}{2U} + \psi_{2xx}\psi_{1y} + 2\psi_{1x\xi}\psi_{1y} + 2U\psi_{2x\xi} + U\psi_{1\xi\xi} \\
+\psi_{1yy}\psi_{2y} + \frac{\psi_{1yy}{\psi_{1x}}^2}{2U} + \psi_{2yy}\psi_{1y} - U\psi_{1xx} - U_y\psi_{1y} - U\psi_{1yy} \\
+\psi_{1yy}\psi_{2y} - \frac{\psi_{1yy}{\psi_{1x}}^2}{2U} + \psi_{1y}\psi_{2yy} + 2\psi_{1x}\psi_{2xy} + 2\psi_{1x}\psi_{1\xi y} \\
+2\psi_{2x}\psi_{1xy} + 2\psi_{1\xi}\psi_{1xy} + \frac{{\psi_{1x}}^2\psi_{1xx}}{U} - U_y\psi_{1y} - \psi_{1yy}U)dy = 0. \qquad (6.31)
\end{aligned}$$

Performing the integration with respect to y in (6.31) we obtain the Ginzburg-Landau equation in the form

$$A_\tau = \sigma A + \delta A_{\xi\xi} + \mu |A|^2 A. \qquad (6.32)$$

The complex coefficients σ, δ and μ have the form

$$\sigma = \frac{\sigma_1}{\beta}, \quad \delta = \frac{\delta_1}{\beta}, \quad \mu = \frac{\mu_1}{\beta}. \qquad (6.33)$$

where

$$\beta = \int_{-\infty}^{\infty} \varphi_1^a(\varphi_{1yy} - k_c^2\varphi_1)\,dy, \tag{6.34}$$

$$\sigma_1 = \frac{s_c}{2}\int_{-\infty}^{\infty} \varphi_1^a(2u_0\varphi_{1yy} + 2u_{0y}\varphi_{1y} - k_c^2u_0\varphi_1)\,dy, \tag{6.35}$$

$$\begin{aligned}\delta_1 = \int_{-\infty}^{\infty} \varphi_1^a\Big[&\varphi_{2yy}^{(1)}(c_g - u_0) + \varphi_2^{(1)}(-k_c^2c_g - 2k_c^2c + 3k_c^2u_0 \\ &+ u_{0yy} - ik_cu_0S_c) + \varphi_1(2ik_cc_g + ik_cc - 3ik_cu_0 - \frac{u_0S_c}{2})\Big]\,dy,\end{aligned} \tag{6.36}$$

$$\begin{aligned}\mu_1 = \int_{-\infty}^{\infty} &\varphi_1^a\{6ik_c^3\varphi_2^{(2)}\varphi_{1y}^* - 2ik_c\varphi_{1y}^*\varphi_{2yy}^{(2)} + 3ik_c^3\varphi_1^*\varphi_{2y}^{(2)} \\ &+ 2ik_c^3\varphi_1\varphi_{2y}^{(0)} - 2ik_c\varphi_{1yy}\varphi_{2y}^{(0)} + ik_c\varphi_{2y}^{(2)}\varphi_{1yy}^* \\ &- ik_c\varphi_1^*\varphi_{2yyy}^{(2)} + 2ik_c\varphi_1\varphi_{2yyy}^{(0)} + 2ik_c\varphi_{1yyy}^*\varphi_2^{(2)} \\ &- \frac{s_c}{2}[-2k_c^2\varphi_1\varphi_{2y}^{(0)} + 3k_c^2\varphi_1^*\varphi_{2y}^{(2)} - \frac{3k_c^4}{2u_0}\varphi_1^2\varphi_1^* \\ &+ 4\varphi_{1yy}\varphi_{2y}^{(0)} + 2\varphi_{1yy}^*\varphi_{2y}^{(2)} + 4\varphi_{1y}\varphi_{2yy}^{(0)} \\ &+ 2\varphi_{2yy}^{(2)}\varphi_{1y}^*]\}\,dy.\end{aligned} \tag{6.37}$$

6.4 Discussion

The equation (6.32) governs evolution of perturbation amplitude. It has a variety of solutions, depending on values of coefficients. In particular if the real part of the coefficient μ is negative, then a saturation of amplitude can occur and a finite-amplitude equilibrium is possible.

Coefficients δ, σ and μ can be calculated as follows:

First, function ψ_1 is calculated from (6.7). The calculation is performed using a numerical method based on Chebyshev polynomials. The function ϕ_1 is sought in the form of Chebyshev polynomial series (please, refer to Chapter 5 for details). The generalized eigenvalue problem (7.15) is solved and the set of eigenvalues λ is obtained for various values of stability parameter s. The point is to find the value of s where at least one λ has the negative real part λ_r. The search starts at a high s value, where all λ_r are positive. Then the value of s is decreased step by step. As soon as the point is reached where one λ_r becomes negative, the search is stopped and the eigenvector is calculated. The eigenvector is normalized to it's maximal value and later used for defining the coefficients of the Chebyshev polynomial series in order to approximate ψ_1.

The adjoint function ψ_1^a is calculated in similar way from (6.29).

As functions ψ_1 and ψ_1^a are found, the group velocity c_g can be calculated using (6.30).

Knowing the group velocity c_g and functions ψ_1, ψ_1^a we can obtain functions $\psi_1^{(0)}$, $\psi_1^{(1)}$, $\psi_2^{(2)}$ from equations (6.24), (6.25) and (6.26) respectively.

Having all the above-mentioned functions found, we can calculate the integrals (6.34) - (6.37) and obtain the coefficients σ, δ and μ. The integrals are calculated by a numerical integration method, using procedure QUANDC8 described in [11].

7 NUMERICAL METHOD

The present chapter describes numerical methods that are used to perform stability analysis for flows with and without the ”rigid-lid” assumption. In both cases a numerical method is based on Chebyshev polynomials, although the way of solution differs. The numerical procedure used for calculation of Ginzburg-Landau coeficients is also described.

7.1 Introduction

Solutions for differential equations used in this thesis are obtained by means of numerical methods. The choice of suitable numerical method is very important for accurate results.

The present chapter describes the numerical method used for solving a modified Rayleigh equation that governs development of perturbation for a flow modelled with ”rigid-lid” assumption as well as the method applied for solution of a system of differential equations derived for a flow with free surface. Both methods are based on Chebyshev polynomials of the first kind. The Chebyshev polynomials of the first kind (usually denoted as T_n) are polynomials of degree n and the sequence of Chebyshev polynomials of either kind composes a polynomial sequence.

The Chebyshev polynomials of the first kind are defined by the recurrence relation [32]:

$$T_0(x) = 1,$$

$$T_1(x) = x,$$

$$T_{n+1}(x) = 2xT_n(x) - T_{n-1}(x).$$

For example:

$$T_2(x) = 2x^2 - 1,$$

$$T_3(x) = 4x^3 - 3x,$$

$$T_4(x) = 8x^4 - 8x^2 + 1.$$

The Chebyshev polynomials of the first kind can be defined by the trigonometric identity:

$$T_n(x) = \cos(n \arccos x),$$

hence:

$$T_n(\cos(\theta)) = \cos(n\theta).$$

A Chebyshev polynomial of the first kind with degree n has n different simple roots, called Chebyshev roots, in the interval $[-1,1]$. The roots are sometimes called Chebyshev nodes because they are used as nodes in polynomial interpolation. Using the trigonometric definition and the fact that

$$\cos(\frac{\pi}{2}(2k+1)) = 0,$$

one can easily prove that the roots of T_n are

$$x_k = \cos(\frac{\pi}{2}\frac{2k-1}{n}), k = 1, ..., n.$$

The extremas of the Chebyshev polynomials are

$$x_k = \cos(\frac{\pi k}{N+1}), k = 1, ..., n.$$

Chebyshev polynomials are important in approximation theory because the roots of the Chebyshev polynomials of the first kind, which are also called Chebyshev nodes, are used as nodes in polynomial interpolation. The resulting interpolation polynomial provides an approximation that is close to the polynomial of best approximation to a continuous function under the maximum norm [32].

If a collocation method is used, the roots or extremas of Chebyshev polynomials are often selected as collocation points.

7.2 Numerical method (rigid-lid assumption)

The ”rigid-lid” approach allows to reduce the Saint-Venant equations (4.2) - (4.4) to a single equation (5.30), called the modified Rayleigh equation. The modified Rayleigh equation

$$\phi_1''[(2\beta_1-\beta_2)U-c+\frac{c_f}{ikh}U]+U_y(2\beta_1-2\beta_2 +\frac{c_f}{ikh})\phi_1'+(k^2c-\beta_2U_{yy}-k^2\beta_2U-\frac{c_f}{2ih}kU)\phi_1=0 \tag{7.1}$$

with boundary conditions

$$\phi_1(\pm\infty)=0 \tag{7.2}$$

is solved by a collocation method based on Chebyshev polynomials.

The function ϕ_1 is defined at infinite domain. In order to map infinite region into interval $[-1;1]$ a variable x is introduced, defined by expression:

$$x=\frac{2}{\pi}\arctan(y), \tag{7.3}$$

and we seek the solution of equation (7.1) in the form Chebyshev polynomial series

$$\phi_1(x)=\sum_{k=0}^{N-1}a_k(1-x^2)T_k(x), \tag{7.4}$$

where N is number of terms in the series, and $T_k(x)$ is a k-order Chebyshev polynomial.
The term $(1-x^2)$ enables the boundary conditions $\phi_1(\pm1)=0$ to be automaticaly satisfied.
According to the chain rule, derivatives of the function $\phi_1(x)$ where x is defined by (7.3) are

$$\frac{d\phi_1}{dy}=\frac{d\phi_1}{dx}\frac{dx}{dy}=\frac{2}{\pi(1+y^2)}\frac{d\phi_1}{dx}=\frac{2}{\pi}\cos^2\left(\frac{\pi x}{2}\right)\frac{d\phi_1}{dx}, \tag{7.5}$$

$$\frac{d^2\phi_1}{dy^2}=\frac{4}{\pi^2}\cos^4\frac{\pi x}{2}\frac{d^2\phi_1}{dx^2}-\frac{4}{\pi}\sin\frac{\pi x}{2}\cos^3\frac{\pi x}{2}\frac{d\phi_1}{dx}, \tag{7.6}$$

$$\frac{d\phi_1}{dx}=\sum_{k=0}^{N-1}a_k(-2xT_k(x)+(1-x^2)T_k'(x)), \tag{7.7}$$

$$\frac{d^2\phi_1}{dx^2}=\sum_{k=0}^{N-1}a_k(-2T_k(x)-4xT_k'(x)+(1-x^2)T_k''(x)). \tag{7.8}$$

Taking extremas of Chebyshev polynomials $x_j=\cos\left(\frac{\pi j}{N+1}\right)$ as collocation points, we get

$$T_k(x_j) = \cos\left(k \arccos\left(\cos\frac{\pi j}{N+1}\right)\right) = \cos\frac{k\pi j}{N+1}, \tag{7.9}$$

$$T_k'(x_j) = \frac{k}{\sqrt{1-x_j^2}} \sin\left(k \arccos\left(\cos\frac{\pi j}{N+1}\right)\right) = \frac{k \sin\frac{k\pi j}{N+1}}{\sin\frac{\pi j}{N+1}}, \tag{7.10}$$

$$T_k''(x_j) = \frac{k\cos\frac{\pi j}{N+1}}{\sin^3\frac{\pi j}{N+1}} - \frac{k^2\cos\frac{k\pi j}{N+1}}{\sin^2\frac{\pi j}{N+1}}. \tag{7.11}$$

So

$$\phi_{1k}(x_j) = a_k(1-{x_j}^2)\cos\frac{k\pi j}{N+1}, \tag{7.12}$$

$$\frac{d\phi_{1k}(x_j)}{dy} = a_k\frac{2}{\pi}\cos^2\frac{\pi x}{2}\left(-2x\cos\frac{k\pi j}{N+1} + (1-x^2)\frac{k\sin\frac{k\pi j}{N+1}}{\sin\frac{\pi j}{N+1}}\right), \tag{7.13}$$

$$\begin{aligned}\frac{d^2\phi_{1k}(x_j)}{dy^2} = \frac{4}{\pi^2}\cos^4\frac{\pi x}{2}a_k\Bigg(&-2\cos\frac{k\pi j}{N+1} - 4x\frac{k\sin\frac{k\pi j}{N+1}}{\sin\frac{\pi j}{N+1}} \\ &+(1-x^2)\left(\frac{k\cos\frac{\pi j}{N+1}}{\sin^3\frac{\pi j}{N+1}} - \frac{k^2\cos\frac{k\pi j}{N+1}}{\sin^2\frac{\pi j}{N+1}}\right)\Bigg) \\ -\frac{4}{\pi}\sin\frac{\pi x}{2}\cos^3\frac{\pi x}{2}a_k&\left(-2x\cos\frac{k\pi j}{N+1} + (1-x^2)\frac{k\sin\frac{k\pi j}{N+1}}{\sin\frac{\pi j}{N+1}}\right).\end{aligned} \tag{7.14}$$

Using the collocation method and taking into account (7.12 - 7.14) we obtain a system of linear equations with respect to coefficients a_k:

$$(A - cB)a = 0, \tag{7.15}$$

where

$$a = [a_0, a_1, a_2, ..., a_{N-1}]^T$$

is a vector containing coefficients a_k, and A and B are two comlex-valued matrices.

The element $A[j,k]$ of the matrix A is given by the expression

$$A_{j,k} = \frac{4}{\pi^2}\cos^4\frac{\pi x}{2}\left(-2\cos\frac{k\pi j}{N+1} - 4x\frac{k\sin\frac{k\pi j}{N+1}}{\sin\frac{\pi j}{N+1}}\right.$$

$$+(1-x^2)\left(\frac{k\cos\frac{\pi j}{N+1}}{\sin^3\frac{\pi j}{N+1}}-\frac{k^2\cos\frac{k\pi j}{N+1}}{\sin^2\frac{\pi j}{N+1}}\right)\Bigg)$$
$$-\frac{4}{\pi}\sin\frac{\pi x}{2}\cos^3\frac{\pi x}{2}\Bigg(-2x\cos\frac{k\pi j}{N+1}$$
$$+(1-x^2)\frac{k\sin\frac{k\pi j}{N+1}}{\sin\frac{\pi j}{N+1}}\Bigg)\left((2\beta_1-\beta_2)U+\frac{c_f}{ikh}U\right)$$
$$+U_y\left(2\beta_1-2\beta_2+\frac{c_f}{ikh}\right)\frac{2}{\pi}\cos^2\left(\frac{\pi x}{2}\right)\Bigg(-2x\cos\frac{k\pi j}{N+1}$$
$$+(1-x^2)\frac{k\sin\frac{k\pi j}{N+1}}{\sin\frac{\pi j}{N+1}}\Bigg)+\Bigg(-\beta_2U_{yy}-k^2\beta_2U$$
$$-\frac{c_f}{2ih}kU\Bigg)(1-{x_j}^2)\cos\frac{k\pi j}{N+1}. \tag{7.16}$$

The element $B[j,k]$ of the matrix B is given by the expression

$$B[j,k]=(1-{x_j}^2)\cos\frac{k\pi j}{N+1}k^2c-c\Bigg(\frac{4}{\pi^2}\cos^4\frac{\pi x}{2}\Bigg(-2\cos\frac{k\pi j}{N+1}$$
$$-4x\frac{k\sin\frac{k\pi j}{N+1}}{\sin\frac{\pi j}{N+1}}+(1-x^2)\left(\frac{k\cos\frac{\pi j}{N+1}}{\sin^3\frac{\pi j}{N+1}}-\frac{k^2\cos\frac{k\pi j}{N+1}}{\sin^2\frac{\pi j}{N+1}}\right)\Bigg)$$
$$-\frac{4}{\pi}\sin\frac{\pi x}{2}\cos^3\frac{\pi x}{2}\left(-2x\cos\frac{k\pi j}{N+1}+(1-x^2)\frac{k\sin\frac{k\pi j}{N+1}}{\sin\frac{\pi j}{N+1}}\right)\Bigg). \tag{7.17}$$

7.3 Numerical method (flows with free surface)

For flows with free surface, a system of ordinary differential equations, derived from the Saint-Venant equations, is analyzed:

$$\frac{H_0}{b}ik\hat{u}+ikU\hat{h}+\frac{H_0}{b}\frac{d\hat{v}}{dy}-\lambda\hat{h}=0, \tag{7.18}$$

$$[(2\beta_1-1)ikU+sU]\hat{u}+[(\beta_1-1)\frac{ikU^2b}{H_0}+\frac{ik}{Fr^2}-\frac{sU^2b}{2H_0}]\hat{h}$$
$$+(\beta_2-1)U\frac{d\hat{v}}{dy}+\beta_2vU_y-\lambda\hat{u}=0, \tag{7.19}$$

$$\frac{1}{Fr^2}\frac{d\hat{h}}{dy}+(ik\beta_2U+\frac{s}{2}U)\hat{v}-\lambda\hat{v}=0, \tag{7.20}$$

with the boundary conditions

$$v(\pm\infty) = 0. \tag{7.21}$$

Using a substitution

$$x = \frac{2}{\pi}\arctan(y)$$

in order to map infinite domain into the region $[-1;1]$, we represent the functions $v(x)$, $u(x)$ and $h(x)$ in the form of fundamental interpolation polynomials:

$$u(x) = \sum_{k=1}^{n} a_k \frac{T_n(x)}{(x-x_k)T_n'(x_k)}, \tag{7.22}$$

$$v(x) = \sum_{k=1}^{n} b_k \frac{(1-x^2)}{(1-x_k^2)} \frac{T_n(x)}{(x-x_k)T_n'(x_k)}, \tag{7.23}$$

$$h(x) = \sum_{k=1}^{n} c_k \frac{T_n(x)}{(x-x_k)T_n'(x_k)}, \tag{7.24}$$

where a_k, b_k and c_k are unknown constants, but $T_n(x)$ is an n-order Chebyshev polynomial that has the form $T_n(x) = \cos(n\arccos(x))$. The points x_k, defined by the expression $x_k = \cos\frac{(2k-1)\pi}{2n}$, are the zeroes of the Chebyshev polynomial of order n, that is, $(T_n(x_k) = 0)$. It is obvious that the term $\frac{T_n(x)}{(x-x_k)T_n'(x_k))}$ is equal to zero, if $x = x_j$, where x_j is a zero of an n-order Chebyshev polynomial, and $j \neq k$. If $x = x_k$ then using the Taylor series expansion of $T_n(x)$ about the point $x = x_k$ we obtain:

$$\begin{aligned} &\frac{T_n(x)}{(x-x_k)T_n'(x_k))} \\ &= \frac{T_n(x_k) + (x-x_k)T_n'(x_k) + \frac{(x-x_k))^2}{2}T_n''(x_k) + \ldots}{(x-x_k)T_n'(x_k)} \\ &= 1 + \frac{(x-x_k)}{2}\frac{T_n''(x_k)}{T_n'(x_k)} + \ldots \end{aligned} \tag{7.25}$$

The derivaties are:

$$T_k(x_j) = \cos(k\arccos(x_j)) = \cos(k\arccos(\cos\frac{(2k-1)\pi}{2n}))$$

$$= \cos(\frac{(2k-1)k\pi}{2n}), \tag{7.26}$$

$$T_k'(x_j) = (cos(k\arccos(x_j)))' = \frac{k}{\sqrt{1-x_j^2}}\sin(k\arccos(x_j))$$

$$= \frac{k}{\sqrt{1-(\cos\frac{(2k-1)\pi}{2n})^2}}\sin(k\arccos(\cos\frac{(2k-1)\pi}{2n}) = \frac{k\sin(\frac{(2k-1)k\pi}{2n})}{\sin(\frac{(2k-1)\pi}{2n})}, \tag{7.27}$$

$$T_k''(x_j) = (\frac{k}{\sqrt{1-x_j^2}}\sin(k\arccos(x_j)))'$$

$$= \frac{k}{(\sqrt{1-x_j^2})^3}\sin(k\arccos(x_j))$$

$$-\frac{k^2}{(\sqrt{1-x_j^2})^2}cos(k\arccos(x_j)) = \frac{k\cos\frac{\pi j}{N+1}}{\sin^3\frac{\pi j}{N+1}} - \frac{k^2\cos\frac{k\pi j}{N+1}}{\sin^2\frac{\pi j}{N+1}}. \tag{7.28}$$

Hence,

$$\frac{T_n(x)}{(x-x_k)T_n'(x_k))} = \begin{cases} 0, & \text{if } x = x_j,\ j \neq k, \\ 1, & \text{if } x = x_j,\ j = k. \end{cases} \tag{7.29}$$

Using the collocation method and choosing zeroes of Chebyshev polynomials as the collocation points we obtain

$$(A - \lambda B)d = 0, \tag{7.30}$$

where A and B are two complex-valued matrices. Vector d has the form

$d = (a_1, a_2, ..., a_n, b_1, b_2, ..., b_n, c_1, c_2, ..., c_n)^T$.

Solving the generalized eigenvalue problem (7.30), for given s and k we obtain a set of eigenvalues λ.

7.4 Resonantly forced boundary value problems

In cases where the boundary value problem for ordinary differential equation is resonantly forced the corresponding nonhomogeneous problem has a solution if and only if some solvability conditions are satisfied. In order to calculate the coefficients of the Ginzburg-Landau equation we have to solve several boundary value problems for ordinary differential equations. One of these

problems (6.25) is resonantly forced. Using method of Chebyshev polynomials to discretize the problem we obtain the system of linear algebraic equations of the form

$$Ax = b, \tag{7.31}$$

where A is the coefficient matrix and b is the right-hand side. Note that for critical values of the parameters of the linear stability problem the corresponding homogeneous equation $Ax = 0$ has a nontrivial solution.

Numerical solution of (7.31) is sought by means of the singular value decomposition method (SVD). The idea of the method is briefly explained below (see [17] for details).

A matrix $Q \in \mathbf{R}^{n\times n}$ is said to be unitary if

$$Q^H Q = QQ^H = E, \tag{7.32}$$

where E is the $n \times n$ identity matrix and Q^H is the conjugate transpose of Q (also called the Hermitian adjoint of Q).

If A is a complex-valued matrix then there exist unitary matrices $U \in \mathbf{R}^{n\times n}$ and $V \in \mathbf{R}^{n\times n}$ such that

$$U^H AV = \Sigma, \tag{7.33}$$

where $\Sigma = diag(\sigma_1, \sigma_2, \ldots, \sigma_n)$ is the diagonal matrix whose diagonal entries are the singular value of the matrix A. Equation (7.33) is called the singular value decomposition of A.

Using orthogonality condition (7.32) we transform (7.33) to the form

$$U^H AV = \Sigma \Rightarrow AV = U\Sigma \Rightarrow A = U\Sigma V^H. \tag{7.34}$$

Assume that $r = n - 1 = rank(A)$. In this case $\sigma_1 \geq \sigma_2 \geq \ldots \geq \sigma_{n-1} > \sigma_n = 0$. Thus, we delete the last column of U and the last row of V^H from the analysis. Using Z as a new U, W^H for the new V^H and T for the new Σ, equation (7.31) becomes

$$ZTW^H x = b. \tag{7.35}$$

The matrix T in (7.35) is ivertible so that the solution x can be written in the form

$$x = \sum_{i=1}^{n-1} \frac{u_i^H b v_i}{\sigma_i}, \tag{7.36}$$

where u_i and v_i, $i = 1, 2, \ldots, n-1$ are the columns of the matrices U and V, respectively. The SVD is computed by means of the IMSL routine LSVCR, which provides the matrix Σ as well as the matrices U and V.

8 STABILITY ANALYSIS OF THO-PHASE FLOWS

The present chapter considers stability of a shallow two-phase flow. A two-phase flow is a flow of fluid that contains particles. Influence of particle loading on stability of the flow has been considered by means of linear and weakly non-linear analyses. It has been found that presence of particles enhances flow stability and decreases perturbation magnitude [25] [27] [28].

8.1 Introduction

A two phase flow is a flow of fluid that contains particles. It is obvious that presence of particles should affect perturbation behaviour and influence flow stability.

The analysis of a two-phase flow is performed under the following assumptions [42]:

1. The flow is of constant density and zero viscosity.
2. The particles have spherical shape. The size of the particles is small compared to large-scale structures.
3. The initial distribution of the particles is uniform.
4. The particles have no dynamic interaction with the flow. Small parturbations imposed on the flow have no effect on the particles during the initial moment.

The other assumptions of a shallow flow model are also applied.

8.2 Linear stability analysis

The governing equations for the two-phase flow have additional term $A(u^p - u)$ [41] describing interaction between the flow and the particles. The equations are:

$$\frac{\partial H_0}{\partial t} + \frac{\partial}{\partial x}(uH_0) + \frac{\partial}{\partial y}(vH_0) = 0, \tag{8.1}$$

$$\begin{aligned}\frac{\partial u}{\partial t} + (2\beta_1 - 1)u\frac{\partial u}{\partial x} + [(\beta_1 - 1)\frac{u^2}{H_0} + g]\frac{\partial H_0}{\partial x} + (\beta_2 - 1)u\frac{\partial v}{\partial y} + \\ + (\beta_2 - 1)\frac{uv}{H_0}\frac{\partial H_0}{\partial y} + \beta_2 v\frac{\partial u}{\partial y} - S_{0x} + \frac{c_f u\sqrt{u^2+v^2}}{2H_0} \\ -F(y) - A(u^p - u) = 0,\end{aligned} \tag{8.2}$$

$$\begin{aligned}\frac{\partial v}{\partial t} + \beta_2 u\frac{\partial v}{\partial x} + (\beta_2 - 1)v\frac{\partial u}{\partial x} \\ + (\beta_2 - 1)\frac{uv}{H_0}\frac{\partial H_0}{\partial x} + (2\beta_3 - 1)v\frac{\partial v}{\partial y} + \\ + [(\beta_3 - 1)\frac{v^2}{H_0} + g]\frac{\partial H_0}{\partial y} - S_{0y} + \frac{c_f v\sqrt{u^2+v^2}}{2H_0} - A(v^p - v) = 0,\end{aligned} \tag{8.3}$$

where A is the particle loading parameter, u^p is velocity of particles. The particle loading parameter is defined by the expression:

$$A = \frac{\rho_p}{\rho_f}\frac{f\tau_f}{\tau_A}, \tag{8.4}$$

where ρ_p is the bulk density of the particles, ρ_f is the density of the fluid, f is the ratio of actual drag on the particles to Stokes drag, τ_f is the flow characteristic time, τ_A is the particle aerodynamic response time.

The drag F_d on the particle that is moving through the fluid with velocity v is defined by the formula:

$$F_d = -\tilde{b}v,$$

where $\tilde{b}$ is a constant for a particular case of small spherical objects moving through a viscous fluid the constant is defined by the expression derived by George Gabriel Stokes [37]:

$$\tilde{b} = 6\pi\eta r,$$

where r is radius of the particle, η is the fluid viscosity.

As it has been shown previously, the ”rigid-lid” assumption is applicable for small Froude numbers (that is typical for two-phase shallow flows in nature). So, the equations (8.1) - (8.3) are transformed as follows:

- Water depth H_0 is assumed to be constant.

- Measures of length, time and velocity are given by b, $\frac{b}{U_a}$ and U_a respectively. The characteristic length b usually represents the wake half-width for wake flows.
- The equations are transformed to dimensionless form.
- The gravity-driven flow is replaced by pressure-driven flow, namely $\frac{\partial p}{\partial x} = -\frac{S_{0x}}{Fr^2}$, $\frac{\partial p}{\partial y} = -\frac{S_{0y}}{Fr^2}$.

After all above-mentioned transformations we get

$$\frac{\partial u}{\partial x} + \frac{\partial v}{\partial y} = 0, \tag{8.5}$$

$$\frac{\partial u}{\partial t} + (2\beta_1 - 1)u\frac{\partial u}{\partial x} + (\beta_2 - 1)u\frac{\partial v}{\partial y} + \beta_2 v\frac{\partial u}{\partial y} = \tilde{F}(y) - \frac{\partial p}{\partial x} - \frac{c_f}{2h}u\sqrt{u^2+v^2} + A(u^p - u), \tag{8.6}$$

$$\frac{\partial v}{\partial t} + (\beta_2 - 1)v\frac{\partial u}{\partial x} + \beta_2 u\frac{\partial v}{\partial x} + (2\beta_3 - 1)v\frac{\partial v}{\partial y} = -\frac{\partial p}{\partial y} - \frac{c_f}{2h}v\sqrt{u^2+v^2} + A(v^p - v), \tag{8.7}$$

where x and y are the spatial coordinates, t is the time, u and v are the depth-averaged velocity components in the x and y directions respectively, p is pressure, $h = \frac{H_0}{b}$ is dimensionless water depth, $\tilde{F}(y) = \frac{bF(y)}{U_a^2}$ is the forcing function.

The bottom friction coefficient c_f is defined by the equation [14]:

$$\frac{1}{\sqrt{c_f}} = -4\log\left(\frac{1.25}{4Re\sqrt{c_f}}\right).$$

where Re is the Reynolds number.

Denoting partial derivatives by subscripts we can rewrite the equations (8.5)-(8.7) in the form:

$$u_x + u_y = 0, \tag{8.8}$$

$$u_t + (2\beta_1 - 1)uu_x + (\beta_2 - 1)uv_y + \beta_2 vu_y = \tilde{F}(y) - p_x - \frac{c_f}{2h}u\sqrt{u^2+v^2} + A(u^p - u), \tag{8.9}$$

$$v_t + (\beta_2 - 1)vu_x + \beta_2 uv_x + (2\beta_3 - 1)vv_y = -p_y - \frac{c_f}{2h}v\sqrt{u^2+v^2} + A(v^p - v). \tag{8.10}$$

We seek u, v and p in the form:

$$u = U(y) + u'(x,y,t) = U + u', \tag{8.11}$$

$$v = v'(x,y,t) = v', \tag{8.12}$$

$$p = p_0 + p', \tag{8.13}$$

$$u^p = U^p(y) = U^p, \tag{8.14}$$

$$v^p = 0. \tag{8.15}$$

Here $U(y)$ is the base flow solution. The function $U(y)$ in the present chapter is chosen in the form

$$U(y) = 1 + \frac{2R}{1-R}\frac{1}{\cosh^2(\alpha y)}, \tag{8.16}$$

where $R = \dfrac{U_c - U_a}{U_c + U_a}$ is the velocity ratio, $\alpha = sinh^{-1}(1)$, U_c is the velocity on the centerline and U_a is the ambient velocity. The profile (8.16) is suggested by Monkewitz [29] after careful analysis of experimental data for single-phase wake flows and is adopted in present chapter.

Substituting (8.11)-(8.15) into (8.8)-(8.10) we get:

$$(U+u')_x + (v')_y = 0, \tag{8.17}$$

$$\begin{aligned}(U+u')_t + (2\beta_1 - 1)(U+u')(U+u')_x + (\beta_2 - 1)(U+u')(v')_y \\ +\beta_2(v')(U+u')_y = \tilde{F}(y) \\ -(p_0+p')_x - \frac{c_f}{2h}(U+u')\sqrt{(U+u')^2 + (v')^2} + A(U^p - U - u'),\end{aligned} \tag{8.18}$$

$$\begin{aligned}(v')_t + (\beta_2 - 1)(v')(U+u')_x + \beta_2(U+u')(v')_x \\ +(2\beta_3 - 1)(v')(v')_y = -(p_0+p')_y \\ -\frac{c_f}{2h}(v')\sqrt{(U+u')^2 + (v')^2} + A(-v'),\end{aligned} \tag{8.19}$$

or, neglecting the quadratic terms:

$$u'_x + v'_y = 0, \tag{8.20}$$

$$u'_t + (2\beta_1 - 1)Uu'_x + (\beta_2 - 1)Uv'_y + \beta_2 v'U_y = \tilde{F}(y)$$

$$-p_{0x} - p'_x - \frac{c_f}{2h}(U+u')\sqrt{(U^2+2Uu')} + A(U^p - U - u'), \tag{8.21}$$

$$v'_t + \beta_2 U v'_x = -p_{0y} - p'_y - \frac{c_f}{2h}(v')\sqrt{(U^2+2Uu')} + A(-v'). \tag{8.22}$$

The term containing the square root is linearized as follows:

$$\begin{aligned}(U+u')\sqrt{(U^2+2Uu')} &= (U+u')U\sqrt{(1+\frac{2u'}{U})} = |(1+x)^\varepsilon = 1+\varepsilon x| \\ &= (U+u')U(1+\frac{u'}{U}) = (U+u')(U+u') = (U+u')^2 = U^2+2Uu'. \end{aligned}\tag{8.23}$$

By substituting (8.23) into (8.20)-(8.22) we get

$$u'_x + v'_y = 0, \tag{8.24}$$

$$u'_t + (2\beta_1 - 1)Uu'_x + (\beta_2 - 1)Uv'_y + \beta_2 v' U_y = \tilde{F}(y)$$

$$-p_{0x} - p'_x - \frac{c_f}{2h}(U^2 + 2Uu') + A(U^p - U - u'), \tag{8.25}$$

$$v'_t + \beta_2 U v'_x = -p_{0y} - p'_y - \frac{c_f}{2h}Uv' + A(-v'). \tag{8.26}$$

Taking into account that $U^P = U$ we get the following system of equations:

$$u'_x + v'_y = 0, \tag{8.27}$$

$$u'_t + (2\beta_1 - 1)Uu'_x + (\beta_2 - 1)Uv'_y + \beta_2 v' U_y = \tilde{F}(y)$$

$$-p_{0x} - p'_x - \frac{c_f}{2h}U^2 - \frac{c_f}{h}Uu' - Au', \tag{8.28}$$

$$v'_t + \beta_2 U v'_x = -p_{0y} - p'_y - \frac{c_f}{2h}Uv' - Av'. \tag{8.29}$$

Keeping in mind that dimensionless water depth $h = \frac{H_0}{b}$, introducing the stability parameter defined by the expression

$$s = \frac{c_f b}{H_0},$$

and assuming that the forcing function $\tilde{F}(y)$ is equal to $\frac{c_f}{2h}U^2$ (this means that $\tilde{F}(y) - \frac{c_f}{2h}U^2 = 0$) we get

$$u'_x + v'_y = 0, \tag{8.30}$$

$$u'_t + (2\beta_1 - 1)Uu'_x + (\beta_2 - 1)Uv'_y + \beta_2 v' U_y$$

$$+p_{0x}+p'_x+SUu'+Au'=0, \tag{8.31}$$

$$v'_t+\beta_2 Uv'_x+p_{0y}+p'_y+\frac{s}{2}Uv'+Av'=0. \tag{8.32}$$

To eliminate pressure the equation (8.31) is differentiated with respect to y and the equation (8.31) is differentiated with respect to x. We obtain:

$$\begin{aligned} &u'_{ty}+(2\beta_1-1)U_y u'_x+(2\beta_1-1)Uu'_{xy}\\ &+(\beta_2-1)U_y v'_y+(\beta_2-1)Uv'_{yy}+\beta_2 v'_y U_y+\beta_2 v'U_{yy}\\ &+p_{0xy}+p'_{xy}+SU_y u'+SUu'_y+Au'_y=0, \end{aligned} \tag{8.33}$$

$$v'_{tx}+\beta_2 Uv'_{xx}+p_{0xy}+p'_{xy}+\frac{s}{2}Uv'_x+Av'_x=0. \tag{8.34}$$

By substracting the equation (8.33) from (8.34) we get

$$\begin{aligned} &u'_{ty}+(2\beta_1-1)U_y u'_x+(2\beta_1-1)Uu'_{xy}+(\beta_2-1)U_y v'_y\\ &+(\beta_2-1)Uv'_{yy}+\beta_2 v'_y U_y+\beta_2 v'U_{yy}+SU_y u'+SUu'_y\\ &+Au'_y-v'_{tx}-\beta_2 Uv'_{xx}-\frac{s}{2}Uv'_x-Av'_x=0. \end{aligned} \tag{8.35}$$

Introducing the stream function ψ defined by the relations

$$u'=\psi_y, \tag{8.36}$$

$$v'=-\psi_x, \tag{8.37}$$

and assuming ψ of the form

$$\psi=\phi(y)e^{-\lambda t+ikx}, \tag{8.38}$$

we get

$$\begin{aligned} &-\lambda\phi_{yy}+(2\beta_1-1)Uik\phi_{yy}-(\beta_2-1)Uik\phi_{yy}-\beta_2 ik\phi_y U_y\\ &-\beta_2 ik\phi U_{yy}+SU_y\phi_y+SU\phi_{yy}+A\phi_{yy}+k^2\lambda\phi\\ &-\beta_2 Uik^3\phi-\frac{s}{2}Uk^2\phi-Ak^2\phi=0, \end{aligned} \tag{8.39}$$

with boundary conditions

$$\phi(\pm\infty) = 0. \tag{8.40}$$

8.3 Weakly non-linear analysis

The effect of nonlinearity on behavoir of the most unstable mode can be investigated by applying some of the methods of weakly nonlinear theory (see for example [36] or [14]) in order to derive the amplitude evolution equation for the case where s is slightly smaller than the critical value s_c.

In order to facilitate the derivation, a stream function ψ is introduced by the expressions (8.36) - (8.37) and the equations (8.8) - (8.10) are rewritten in the form (in a way similar to derivation of equation (5.18)):

$$\begin{aligned}(\Delta\psi)_t + \psi_y(\Delta\psi)_x - \psi_x(\Delta\psi)_y + \frac{c_f}{2h}\Delta\psi\sqrt{\psi_x^2+\psi_y^2} \\ + \frac{c_f}{2h\sqrt{\psi_x^2+\psi_y^2}}(\psi_y^2\psi_{yy} + 2\psi_x\psi_y\psi_{xy} + \psi_x^2\psi_{xx}) + A\Delta\psi = 0.\end{aligned} \tag{8.41}$$

Consider a perturbed solution to (8.41) in the form:

$$\psi = \psi_0(y) + \varepsilon\psi_1(x,y,t) + \varepsilon^2\psi_2(x,y,t) + \varepsilon^3\psi_3(x,y,t)... \tag{8.42}$$

Substituting (8.42) into (8.41) and neglecting the terms of order ε^2 we obtain:

$$L\psi_1 = 0, \tag{8.43}$$

where

$$\begin{aligned}L\psi_1 = \psi_{1xxt} + \psi_{1yyt} + \psi_{0y}(\psi_{1xxx} + \psi_{1yyx}) - \psi_{0yyy}\psi_{1x} \\ + \frac{c_f}{2h}((\psi_{1xx} + 2\psi_{1yy})\psi_{0y} + 2\psi_{1y}\psi_{0yy}) + A(\psi_{1xx} + \psi_{1yy}).\end{aligned} \tag{8.44}$$

Linear analysis implies that the function ψ_1 in (8.43) has the form

$$\psi_1(x,y,t) = \phi_1(y)\exp[ik(x-ct)], \tag{8.45}$$

where $\phi_1(y)$ is the amplitude of the normal perturbation (8.45).

Weakly non-linear analysis method considers flow stability at the point where s is slightly below the critical value s_c, namely $s = s_c(1-\varepsilon^2)$, where ε is a small parameter. Slow time τ and the stretched lengthwise variable ξ are introduced in the form:

$$\tau = \varepsilon^2 t, \xi = \varepsilon(x - c_g t), \tag{8.46}$$

where c_g is the group velocity.

Weakly nonlinear theory is therefore applied in vicinity of the critical point (see Figure 8.1).

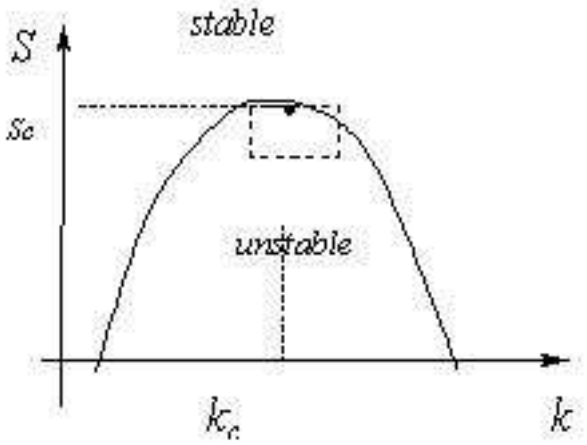

Figure 8.1: Schematic diagram of the critical values of the bed friction number versus k. The dashed rectangle shows the region where weakly nonlinear theory is applicable.

The differential operators $\frac{\partial}{\partial t}$ and $\frac{\partial}{\partial x}$ are then replaced by

$$\frac{\partial}{\partial t} \to \frac{\partial}{\partial t} - \varepsilon c_g \frac{\partial}{\partial \xi} + \varepsilon^2 \frac{\partial}{\partial \tau}, \tag{8.47}$$

$$\frac{\partial}{\partial x} \to \frac{\partial}{\partial x} + \varepsilon \frac{\partial}{\partial \xi}. \tag{8.48}$$

The function ψ_1 in (8.44) is represented in the form

$$\psi_1(x,y,t) = \bar{A}(\xi,\tau)\phi_1(y)\exp[ik(x-ct)] + c.c., \tag{8.49}$$

where $\bar{A}$ is a slowly varying amplitude, $\phi_1(y)$ is the eigenfunction of the linear stability problem (8.39) - (8.40), the values of k and c correspond to the critical state, and $c.c.$ means complex conjugate. In order to find an amplitude evolution equation for $\bar{A}$ we need to consider higher terms of the perturbation expansion (8.42). Substituting (8.42) into (8.41) and collecting terms of order ε^2, we obtain:

$$\begin{aligned} L\psi_2 = c_g(\psi_{1xx\xi} + \psi_{1yy\xi}) - 2\psi_{1x\xi t} - \psi_{0y}(3\psi_{1xx\xi} + \psi_{1yy\xi}) \\ -\psi_{1y}(\psi_{1xxx} + \psi_{1yyx}) + \psi_{1x}(\psi_{1xxy} + \psi_{1yyy}) + \psi_{1\xi}\psi_{0yyy} \\ -s[(\psi_{1xx} + \psi_{1yy})\psi_{1y} + 2\psi_{1x\xi}\psi_{0y} + \psi_{1yy}\psi_{1y} - 2\psi_{0y}\psi_{0yy} \\ +2\psi_{1x}\psi_{1xy}] - 2A\psi_{1x\xi}. \end{aligned} \tag{8.50}$$

Substituting (8.42) into (8.41) and collecting terms of order ε^3 we get:

$$\begin{aligned} L\psi_3 = c_g(\psi_{2xx\xi} + 2\psi_{1x\xi\xi} + \psi_{2yy\xi}) - \psi_{1xxt} - \psi_{1yyt} - 2\psi_{2x\xi t} - \psi_{1\xi\xi t} \\ -3\psi_{0y}(\psi_{2xx\xi} + \psi_{1x\xi\xi}) - \psi_{1y}(\psi_{2xxx} + 3\psi_{1xx\xi}) - \psi_{2y}(\psi_{1xxx} + \psi_{1yyx}) \\ -\psi_{1y}(\psi_{2yyx} - \psi_{1\xi yy}) - \psi_{0y}\psi_{2\xi yy} + \psi_{2x}\psi_{1xxy} + \psi_{1\xi}\psi_{1xxy} \\ +\psi_{1x}\psi_{2xxy} + 2\psi_{1x}\psi_{1xy\xi} + \psi_{1x}\psi_{2yyy} + \psi_{2x}\psi_{1yyy} \\ +\psi_{1\xi}\psi_{1yyy} + \psi_{2\xi}\psi_{0yyy} \\ -s[\psi_{2y}(\psi_{1xx} + \psi_{1yy}) + 2\psi_{2yy}\psi_{1y} + \frac{3}{2}\frac{\psi_{1xx}\psi_{1x}^2}{\psi_{0y}} \\ +\psi_{2xx}\psi_{1y} + 2\psi_{1x\xi}\psi_{1y} + 2\psi_{0y}\psi_{2x\xi} + \psi_{1\xi\xi}\psi_{0y} - \psi_{1xx}\psi_{0y} \\ -2\psi_{0yy}\psi_{1y} - 2\psi_{0y}\psi_{1yy} - \psi_{1yy}\psi_{2y} - \psi_{1y}\psi_{2yy} + 2\psi_{1x}\psi_{2xy} \\ +2\psi_{1x}\psi_{1yy} + 2\psi_{2x}\psi_{1xy} + 2\psi_{1\xi}\psi_{1xy}] - A(2\psi_{2x\xi} + \psi_{1\xi\xi}). \end{aligned} \tag{8.51}$$

The form of right-hand side of (8.50) and formula (8.49) suggest that the function ψ_2 should be sought in the form

$$\psi_2 = \bar{A}\bar{A}^*\phi_2^{(0)}(y) + A_\xi\phi_2^{(1)}(y)\exp[ik(x-ct)] + \bar{A}^2\phi_2^{(2)}(y)\exp[2ik(x-ct)] + c.c., \tag{8.52}$$

where $\bar{A}^*$ denotes complex conjugate of $\bar{A}$ and the functions $\phi_2^{(0)}(y)$, $\phi_2^{(1)}(y)$ and $\phi_2^{(2)}(y)$ are to be determined.

Substituting (8.49) for ψ_1 and (8.52) for ψ_2 into (8.50) and collecting the terms that are proportional to $\bar{A}\bar{A}^*$ gives

$$\begin{aligned} 2S(U\phi_{2yy}^{(0)} + U_y\phi_{2y}^{(0)}) + 2A\phi_{2yy}^{(0)} = ik(\phi_{1y}\phi_{1yy}^* - \phi_{1y}^*\phi_{1yy} \\ +\phi_1\phi_{1yyy}^* - \phi_1^*\phi_{1yyy}) - s(k^2\phi_1\phi_{1y}^* + k^2\phi_1^*\phi_{1y} \\ +2\phi_{1yy}\phi_{1y}^* + 2\phi_{1yy}^*\phi_{1y}), \end{aligned} \tag{8.53}$$

with the boundary conditions

$$\phi_2^{(0)}(\pm\infty) = 0. \tag{8.54}$$

Similarly, collecting the terms that are proportional to $A_\xi \exp[ik(x-ct)]$ we obtain

$$\begin{aligned} (ikU - ikc)\phi_{2yy}^{(1)} + (ik^3c - ik^3U - ikU_{yy})\phi_2^{(1)} + s[2U\phi_{2yy}^{(1)} \\ +2Uy\phi_{2y}^{(1)} - k^2U\phi_2^{(1)}] + A[\phi_{2yy}^{(1)} - k^2U\phi_2^{(1)}] = (c_g - U)\phi_{1yy} \\ +[-2k^2c + 3k^2U + U_{yy} - k^2c_g - ikUS - 2ikA]\phi_1. \end{aligned} \tag{8.55}$$

The boundary conditions are

$$\phi_2^{(1)}(\pm\infty) = 0. \tag{8.56}$$

Comparing (8.39) - (8.40) and (8.55) - (8.56) we see that the solution to (8.55), (8.56), namely, the function $\phi_2^{(1)}$, is resonantly forced since the homogeneous equation which corresponds to (8.55) is satisfied at $s = s_c$, $k = k_c$ and $c = c_c$. Thus (8.55) - (8.56) has a solution if and only if the right-hand side of (8.55) is ortogonal to all eigenfunctions of the corresponding adjoint problem. The adjoint operator, L^a, and the adjoint eigenfunction, ϕ_1^a, are defined as follows:

$$\int_{-\infty}^{+\infty} \phi_1^a L(\phi_1)dy = \int_{-\infty}^{+\infty} \phi_1 L^a(\phi_1^a)dy = 0. \tag{8.57}$$

The adjoint eigenfunction ϕ_1^a satisfies the equation

$$\begin{aligned}(ikU+2SU+A)(\phi_1^a)''+(2ikU_y+2SU_y)(\phi_1^a)'\\ -(ik^3U+Uk^2S+Ak^2)\phi_1^a+ikc[(\phi_1^a)''-k^2\phi_1^a]=0,\end{aligned} \tag{8.58}$$

with the boundary conditions

$$\phi_1^a(\pm\infty)=0. \tag{8.59}$$

Applying the solvability condition for equation (8.55) we obtain the group velocity, c_g, in the form

$$c_g=\frac{I_1}{I_2}, \tag{8.60}$$

where

$$I_1=\int_{-\infty}^{+\infty}[U\phi_{1yy}-\phi_1(3k^2U+U_{yy}-2k^2c-2ikUS-2Aik)]\phi_1^a dy, \tag{8.61}$$

and

$$I_2=\int_{-\infty}^{+\infty}\phi_1^a(\phi_{1yy}-k^2\phi_1)dy. \tag{8.62}$$

Finally, collecting the terms that are proportional to $\bar{A}^2$ we obtain the following equation for the function $\phi_2^{(2)}$:

$$\begin{aligned}2(ikU-ikc)\phi_{2yy}^{(2)}+(8ik^3c-8ik^3U-2ikU_{yy})\phi_2^{(2)}+s[2U\phi_{2yy}^{(2)}\\ +2U\phi_{2y}^{(2)}-4k^2U\phi_2^{(2)}]+A[\phi_{2yy}^{(2)}-4k^2\phi_2^{(2)}]=ik(\phi_!\phi_{1yyy}-\phi_{1y}\phi_{1yy})\\ -s(2\phi_{1y}\phi_{1yy}-2k^2\phi_1\phi_{1y}),\end{aligned} \tag{8.63}$$

with the boundary conditions

$$\phi_2^a(\pm\infty)=0. \tag{8.64}$$

The amplitude evolution equation for $\bar{A}$ is obtained from the solvability condition for equation (8.51) and has the form

$$\frac{\partial \bar{A}}{\partial \tau} = \sigma \bar{A} + \delta \frac{\partial^2 \bar{A}}{\partial \xi^2} + \mu |\bar{A}|^2 \bar{A}, \tag{8.65}$$

where

$$\sigma = \frac{\sigma_1}{\gamma_1}, \tag{8.66}$$

$$\delta = \frac{\delta_1}{\gamma_1}, \tag{8.67}$$

$$\mu = \frac{\mu_1}{\gamma_1}. \tag{8.68}$$

The coefficients $\sigma = \sigma_r + i\sigma_i, \delta = \delta_r + i\delta_i, \mu = \mu_r + i\mu_i$ are complex. Equation (8.65) is the Ginzburg-Landau equation.

The coefficients γ_1, σ_1, δ_1 and μ_1 are given by

$$\gamma_1 = \int_{-\infty}^{+\infty} \phi_1^a (\phi_{1yy} - k^2 \phi_1) dy, \tag{8.69}$$

$$\sigma_1 = s \int_{-\infty}^{+\infty} \phi_1^a (2U\phi_{1yy} + 2U_y \phi_{1y} - k^2 U \phi_1) dy, \tag{8.70}$$

$$\begin{aligned} \delta_1 = \int_{-\infty}^{+\infty} \phi_1^a [\phi_{2yy}^{(1)} (c_g - U) \\ + \phi_2^{(1)} (-k^2 c_g - 2k^2 c + 3k^2 U + U_{yy} - 2ikUS - 2ikA) \\ + \phi_1 (2ikc_g + ikc) - 3ikU - US - A)] dy, \end{aligned} \tag{8.71}$$

$$\begin{aligned} \mu_1 = \int_{-\infty}^{+\infty} \phi_1^a \{ 6ik^3 \phi_2^{(2)} \phi_{1y}^* - 2ik\phi_{1y}^* \phi_{2yy}^{(2)} \\ + 3ik^3 \phi_1^* \phi_{2y}^{(2)} + ik^3 \phi_1 (\phi_{2y}^{(0)} + \phi_{2y}^{*(0)}) - ik\phi_{1yy} (\phi_{2y}^{(0)} \\ + \phi_{2y}^{*(0)}) + ik\phi_{2y}^{(2)} \phi_{1yy}^* - ik\phi_1^* \phi_{2yyy}^{(2)} \\ + ik\phi_1 (\phi_{2yyy}^{(0)} + \phi_{2yyy}^{*(0)}) + 2ik\phi_{1yyy}^* \phi_2^{(2)} - 2S[-k^2 \phi_1 (\phi_{2y}^{(0)} \\ + \phi_{2y}^{*(0)}) + 3k^2 \phi_1^* \phi_{2y}^{(2)} - \frac{1.5k^4 \phi_1^2 \phi_1^*}{U} \\ + 2\phi_{1yy} (\phi_{2y}^{(0)} + \phi_{2y}^{*(0)}) + 2\phi_{1yy}^* \phi_{2y}^{(2)} + 2\phi_{1y} (\phi_{2yy}^{(0)} \\ + \phi_{2yy}^{*(0)}) + 2\phi_{2yy}^{(2)} \phi_{1y}^*] \} dy. \end{aligned} \tag{8.72}$$

The right-hand side of equation (8.65) contains three terms corresponding to linear amplification, diffusion and nonlinear saturation, respectively. The coefficients of (8.65) have the following

physical meaning:

- The real part of σ, namely, σ_r, gives the rate of amplification of an unstable perturbation.
- The imaginary part of σ, that is, σ_i, reflects the angular frequency of the oscillation.
- The dependence of the instability growth rate and oscillation frequency on the wavelength is represented by the coefficients δ_r and δ_i, respectively.
- The coefficient μ determines whether saturation of instabilities is possible.

If $\mu_r < 0$ then the nonlinearities tend to saturate the instability. Such a situation is referred to as "supercritical instability" in the hydrodynamic stability literature. On the other hand, if $\mu_r > 0$, then higher order terms on the right-hand side of (8.65) are also important and (8.65) is much less informative. Such a case is known as "subcritical instability". One example of subcritical instability is given in [36] for the case of a plane Poiseuille flow. The constant μ_r in equation (8.65) is usually referred to as the Landau constant in the hydrodynamic stability literature.

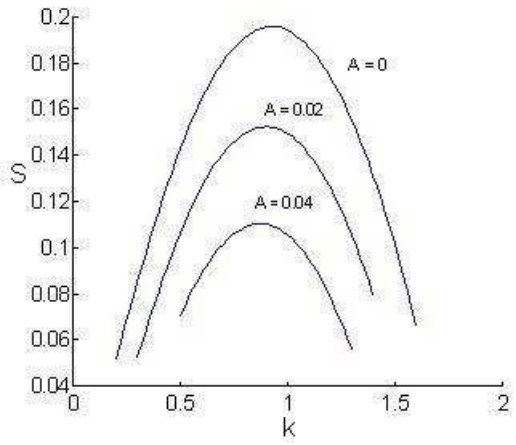

Figure 8.2: Neutral stability curves for different values of A at $R = -0.5$.

8.4 Results

Figure 8.2 plots neutral stability curves for the parameter s versus k for $R = -0.5$ and different values of the particle loading parameter A. The values of A have been chosen in the range of prac-

tical interest [41]. Each stability curve separates stability and instability domains. The instability domain is below the curve. As can be seen from the figure, lower stability curves correspond to higher values of A. This means that higher A enhances stability of the flow.

The value of the stability parameter s at the top of the curve s_c, namely the critical value of s, can be taken as a reference point characterizing the stability of the flow. For values of s above s_c the flow is stable for all wavenumbers k. The dependence s_c on A at $R = -0.5$ is shown in Figure 8.3. Stabilizing effect of the particle loading parameter is clearly seen in the figure since the critical values of s are decreasing almost linearly as the parameter A increases.

Figure 8.4 plots the growth rates for the most unstable mode in unstable regime for different values of A. As the particle loading parameter increases, the growth rates decrease.

Parameter A is defined by (8.4). The value of A depends on various parameters such as particle bulk density, drag on the particles, and aerodynamic response time of the particles. The bulk density is the mass of many particles divided by the volume they occupy. So one can conclude that the presence of particles enhances flow stability. The higher is bulk density of the particles, drag and the lower is the aerodynamic response time the more stable the flow is. This result is consistent with data of Yang et al. [41].

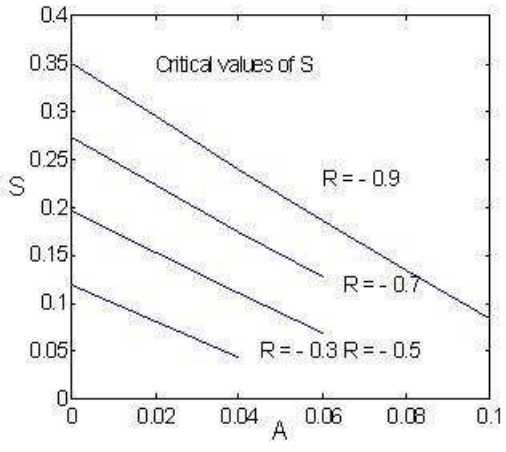

Figure 8.3: Critical values of s versus A for different values of R.

In order to evaluate the coefficients of the Ginzburg-Landau equation numerically, one needs to find the critical values of k, s and c from the linear stability problem (8.39) - (8.40). Then the corresponding eigenfunction ϕ_1^a of the adjoint problem (8.58) - (8.59) is calculated. Next, three

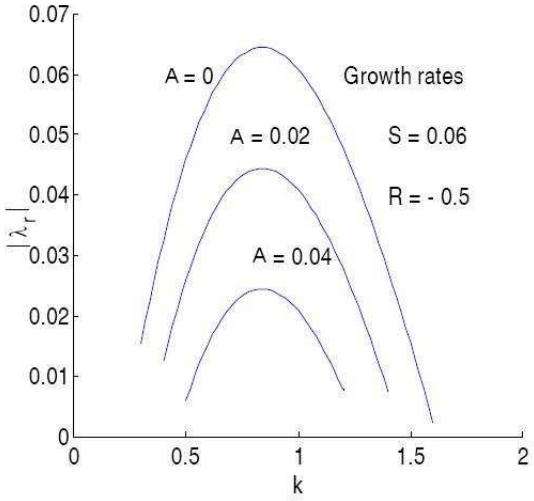

Figure 8.4: Growth rates for the most unstable mode for different values of A.

Table 8.1: The coefficients of the Ginzburg-Landau equation for different values of A.

A	σ	δ	μ
0.0	0.0899+0.0004i	0.1150-0.1834i	-4.5212-11.6033i
0.02	0.0716+0.0001i	0.1116-0.2131i	-4.8302-11.7427i
0.04	0.0529-0.0000i	0.1062-0.2438i	-5.3386-11.6620i
0.06	0.0300-0.0002i	0.0986-0.2819i	-6.6213-11.8045i

boundary value problems (8.53) - (8.56), (8.63) are solved and the functions $\phi_2^{(0)}$, $\phi_2^{(1)}$ and $\phi_2^{(2)}$ are calculated. Finally the group velocity c_g is computed from the solvability condition (8.60). In all cases pseudospectral method based on Chebyshev polynomials is used. The coefficients of the complex Ginzburg-Landau equation (8.65) are then evaluated numerically by means of (8.66)-(8.72). The results are shown in Table 8.1 for $R = -0.5$.

As can be seen from Table 8.1, the real part of μ (known as the Landau constant in the literature) is negative, therefore, finite amplitude equilibrium is possible and the instability is supercritical. Thus, the Ginzburg-Landau equation may be used for the analysis of shallow wake two-phase flows in convectively unstable regime. Note that in cases where the real part of μ is positive, the higher powers of $\bar{A}$ (which are neglected in (8.65)) become also important, and the Ginzburg-Landau model cannot be used for the analysis. In such cases a finite equilibrium state is

Table 8.2: The amplitude $\bar{A}_0$ and the frequency ω for different values of A at $R = -0.5$.

A	ω	$\bar{A}_0$
0.0	0.230	0.141
0.02	0.174	0.122
0.04	0.116	0.100

not possible. This means that the disturbances are linearly unstable and grow unbounded; that is, the instability is subcritical. An example of such case is given in [36] for plane Poiseuille flow.

Consider unmodulated (independent on ξ) equilibrium amplitude solution of (8.65) of the form

$$\bar{A} = \sqrt{\frac{\sigma_r}{\mu_r}} \exp[i\tau(\sigma_i - \frac{\mu_i}{\mu_r}\sigma_r)], \tag{8.73}$$

where the amplitude $\bar{A}_0$ and the frequency ω are given by

$$\bar{A}_0 = \sqrt{\frac{\sigma_r}{\mu_r}}, \omega = \sigma_i - \frac{\mu_i}{\mu_r}\sigma_r. \tag{8.74}$$

It is seen from (8.74) that both the amplitude and the frequency of the most unstable mode are modified by nonlinear effects. The values of $\bar{A}_0$ and ω for different values of A are calculated for the case $R = -0.5$ and are shown in Table 8.2.

As can be seen from Table 8.2, the stabilizing effect of the particle loading parameter A is obvious also in weakly nonlinear regime: the finite amplitude is getting smaller as A increases.

Using the substitutions

$$\begin{aligned} \tilde{\tau} &= \tau\sigma_r, \\ \tilde{\xi} &= \xi\sqrt{\frac{\sigma_r}{\delta_r}}, \\ \tilde{A} &= \bar{A}\sqrt{\mu_r}\sigma_r \exp(-ic_0\sigma_r\tau), \end{aligned} \tag{8.75}$$

we transform (8.65) to the form

$$\tilde{A}_{\tilde{\tau}} = \tilde{A} + (1+ic_1)\tilde{A}_{\tilde{\xi}\tilde{\xi}} - (1+ic_2)|\tilde{A}|^2\tilde{A}, \tag{8.76}$$

where

Table 8.3: The coefficients of the Ginzburg-Landau equation (8.76) for different values of A.

A	c_0	c_1	c_2
0.0	0.004	- 1.595	2.566
0.02	0.001	- 1.906	2.431
0.04	0.000	- 2.296	2.184
0.06	-0.007	- 2.859	1.783

$$c_0 = \frac{\sigma_i}{\sigma_r}, c_1 = \frac{\delta_i}{\delta_r}, c_2 = \frac{\mu_i}{\mu_r}. \tag{8.77}$$

It can easily be shown (see, for example, [1]) that (8.76) has a plane wave solution of the form

$$\tilde{A} = C\exp[i(K\tilde{\xi} - \Omega\tilde{\tau})]. \tag{8.78}$$

Stability of solutions (8.78) is studied in [5] where it is shown that a sufficient condition for instability is

$$1 + c_1 c_2 < 0, \tag{8.79}$$

Instability described by (8.79) is referred to as the Benjamin-Feir instability. Using the numerical values of the coefficients of (8.65) given in Table 8.1 we have calculated the coefficients c_0, c_1, and c_2. The results are presented in Table 8.3.

As can be seen from Table 8.3, for all values of A the instability condition (8.79) is satisfied. This means that pure periodic waves (8.78) are unstable (and, therefore, are not observable).

8.5 Conclusion

Linear and weakly nonlinear stability of two-phase shallow wake flow is analyzed in the present chapter. Linear stability analysis is performed under the following simplifying assumptions: (1) the mean velocity profile of the two-phase flow is assumed to be identical to that of a single-phase flow, (2) the particle concentration is assumed to be uniform, (3) small perturbations imposed on the flow have no effect on the particles during initial moment. Calculations show that particle loading parameter stabilizes the flow. In addition, bottom friction also enhances the stability of

the flow. Methods of weakly nonlinear theory are used to derive the amplitude evolution equation for the most unstable mode. It is shown that the development of the most unstable mode in weakly nonlinear regime is governed by the complex Ginzburg-Landau equation. The coefficients of the Ginzburg-Landau equation are calculated numerically for different values of the parameters of the problem. It is shown that the particle loading parameter has a stabilizing effect on the flow also in the weakly nonlinear regime: the saturation amplitude is getting smaller as the particle loading parameter increases. In addition, it is shown that pure periodic solutions of the Ginzburg-Landau equation are unstable (and, therefore, not observable).

9 STABILITY ANALYSIS OF NON-PARALLEL FLOW

Stability of a non-parallel flow is considered in the present chapter. A weakly non-linear method is used for the stability analysis that implies the base flow weakly depends on downstream coordinate. An equation of perturbation amplitude and a leading order approximation for the perturbation stream function have been achieved [26].

9.1 Introduction

Stability analysis of shallow wake or mixing layer flow is usually implies the assumption that the velocity profile of the flow does not change downstream (parallel flow assumption). From mathematical point of view this means that the base flow is independent on the lengthwise coordinate. In real flows, however, the flow velocity profile slowly alters downstream. The non-uniformity of the flow velocity distribution across transverse coordinate ususally declines with the fluid travelling downstream. Effectively that means that the base flow weakly depends on the lengthwise coordinate.

As the base flow is a function of the lengthwise coordinate, the stability analysis should be modified. Weakly-nonlinear analysis can be performed in order to take into account slow variation of the base flow.

The current chapter makes an attempt to analyse stability of the flow if base flow weakly depends on the lengthwise coordinate.

9.2 Derivation of Governing Equations

The governing equations for the nonparallel flow are derived from the ”rigid-lid” flow equation (5.18) taking into account that the base flow function Ψ_0 weakly depends on x (see Figure 9.1).

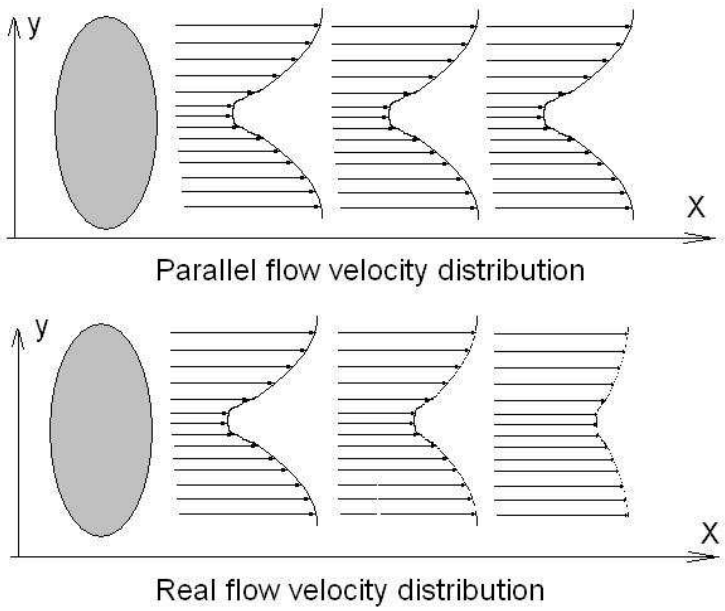

Figure 9.1: Parallel and non-parallel flow velocity profiles.

We seek solution of the equation (5.18) in the form:

$$\Psi(x,y,t) = \Psi_0(y,X) + \psi(x,y,t), \tag{9.1}$$

where

$$X = \varepsilon x$$

is a slowly varying coordinate, ε is the small dimensionless parameter that characterizes the non-parallelism of the base flow, $\Psi_{0y}(y,X)$ is the base flow, $\psi(x,y,t)$ is a perturbation.

Substituting (9.1) into (5.18) we get:

$$\begin{aligned}
(\Delta\Psi_0)_t + (\Delta\psi)_t + (2\beta_1 - \beta_2)((\Psi_{0y} + \psi_y)(\Psi_{0xy} + \psi_{xy}))_y \\
-\beta_2((\Psi_{0x} + \psi_x)(\Psi_{0yy} + \psi_{yy}))_y \\
+(\beta_2 - 1)((\Psi_{0x} + \psi_x)(\Psi_{0xy} + \psi_{xy}))_x \\
+\beta_2((\Psi_{0xx} + \psi_{xx})(\Psi_{0y} + \psi_y))_x \\
-(2\beta_3 - 1)((\Psi_{0x} + \psi_x)(\Psi_{0xx} + \psi_{xx}))_y \\
+\frac{c_f}{2h}(\Delta\Psi_0 + \Delta\psi)\sqrt{(\Psi_{0x} + \psi_x)^2 + (\Psi_{0y} + \psi_y)^2} \\
+\frac{c_f}{2h\sqrt{(\Psi_{0x} + \psi_x)^2 + (\Psi_{0y} + \psi_y)^2}}((\Psi_{0y} + \psi_y)^2(\Psi_{0yy} + \psi_{yy})
\end{aligned}$$

$$+2(\Psi_{0x}+\psi_x)(\Psi_{0y}+\psi_y)(\Psi_{0xy}+\psi_{xy})$$
$$+(\Psi_{0x}+\psi_x)^2(\Psi_{0xx}+\psi_{xx}))=0, \tag{9.2}$$

or

$$\begin{aligned}
&(\Delta\psi)_t+(2\beta_1-\beta_2)((\Psi_{0y}+\psi_y)(\varepsilon\Psi_{0Xy}+\psi_{xy}))_y\\
&-\beta_2((\varepsilon\Psi_{0X}+\psi_x)(\Psi_{0yy}+\psi_{yy}))_y\\
&+(\beta_2-1)((\varepsilon\Psi_{0X}+\psi_x)(\varepsilon\Psi_{0Xy}+\psi_{xy}))_x\\
&+\beta_2(\psi_{xx}(\Psi_{0y}+\psi_y))_x-(2\beta_3-1)((\varepsilon\Psi_{0X}+\psi_x)\psi_{xx})_y\\
&+\frac{c_f}{2h}(\Psi_{0yy}+\Delta\psi)\sqrt{(\varepsilon\Psi_{0X}+\psi_x)^2+(\Psi_{0y}+\psi_y)^2}\\
&+\frac{c_f}{2h\sqrt{(\varepsilon\Psi_{0X}+\psi_x)^2+(\Psi_{0y}+\psi_y)^2}}((\Psi_{0y}+\psi_y)^2(\Psi_{0yy}+\psi_{yy})\\
&+2(\varepsilon\Psi_{0X}+\psi_x)(\Psi_{0y}+\psi_y)(\varepsilon\Psi_{0Xy}+\psi_{xy})+(\varepsilon\Psi_{0X}+\psi_x)^2(\psi_{xx}))=0.
\end{aligned} \tag{9.3}$$

Keeping in mind that Ψ_{0t} is equal to zero as $\Psi_0=\Psi_0(y,X)$, and neglecting terms of ψ^2 and ε^2 we get:

$$\begin{aligned}
&(\Delta\psi)_t+(2\beta_1-\beta_2)((\Psi_{0yy}+\psi_{yy})(\varepsilon\Psi_{0Xy}+\psi_{xy})\\
&+(\Psi_{0y}+\psi_y)(\varepsilon\Psi_{0Xyy}+\psi_{xyy}))\\
&-\beta_2((\varepsilon\Psi_{0Xy}+\psi_{xy})(\Psi_{0yy}+\psi_{yy})+(\varepsilon\Psi_{0X}+\psi_x)(\Psi_{0yyy}+\psi_{yyy}))\\
&+(\beta_2-1)(\psi_{xx}(\varepsilon\Psi_{0Xy}+\psi_{xy})+(\varepsilon\Psi_{0X}+\psi_x)(\psi_{xxy}))\\
&+\beta_2(\psi_{xxx}(\Psi_{0y}+\psi_y)+\psi_{xx}(\varepsilon\Psi_{0Xy}+\psi_{xy}))\\
&-(2\beta_3-1)((\varepsilon\Psi_{0Xy}+\psi_{xy})\psi_{xx}+(\varepsilon\Psi_{0X}+\psi_x)\psi_{xxy})\\
&+\frac{c_f}{2h}(\Psi_{0yy}+\Delta\psi)\sqrt{2\varepsilon\Psi_{0X}\psi_x+\Psi_{0y}^2+\Psi_{0y}2\psi_y}\\
&+\frac{c_f}{2h\sqrt{2\varepsilon\Psi_{0X}\psi_x+\Psi_{0y}^2+2\Psi_{0y}\psi_y}}((\Psi_{0y}^2+2\Psi_{0y}\psi_y)(\Psi_{0yy}+\psi_{yy})\\
&+2(\varepsilon\Psi_{0X}+\psi_x)(\Psi_{0y}+\psi_y)(\varepsilon\Psi_{0Xy}+\psi_{xy})+2\varepsilon\Psi_{0X}\psi_x\psi_{xx})=0.
\end{aligned} \tag{9.4}$$

Simplifying, we get

$$\begin{aligned}
&(\Delta\psi)_t+(2\beta_1-\beta_2)((\varepsilon\Psi_{0Xy}\Psi_{0yy}+\varepsilon\Psi_{0Xy}\psi_{yy}+\psi_{xy}\Psi_{0yy})\\
&+(\varepsilon\Psi_{0Xyy}\Psi_{0y}+\varepsilon\Psi_{0Xyy}\psi_y+\Psi_{0y}\psi_{xyy}))
\end{aligned}$$

$$
\begin{aligned}
&-\beta_2((\varepsilon\Psi_{0Xy}\Psi_{0yy}+\Psi_{0yy}\psi_{xy}+\varepsilon\Psi_{0Xy}\psi_{yy})\\
&+(\varepsilon\Psi_{0X}\Psi_{0yyy}+\Psi_{0yyy}\psi_x+\varepsilon\Psi_{0X}\psi_{yyy}))\\
&+(\beta_2-1)(\psi_{xx}\varepsilon\Psi_{0Xy}+\varepsilon\Psi_{0X}\psi_{xxy})+\beta_2(\psi_{xxx}\Psi_{0y}+\psi_{xx}\varepsilon\Psi_{0Xy})\\
&-(2\beta_3-1)(\varepsilon\Psi_{0Xy}\psi_{xx}+\varepsilon\Psi_{0X}\psi_{xxy})\\
&+\frac{c_f}{2h}(\Psi_{0yy}+\Delta\psi)\sqrt{2\varepsilon\Psi_{0X}\psi_x+\Psi_{0y}^2+\Psi_{0y}2\psi_y}\\
&+\frac{c_f}{2h\sqrt{2\varepsilon\Psi_{0X}\psi_x+\Psi_{0y}^2+2\Psi_{0y}\psi_y}}((\Psi_{0y}^2\Psi_{0yy}+2\Psi_{0y}\Psi_{0yy}\psi_y+\Psi_{0y}^2\psi_{yy})\\
&+2(\varepsilon\Psi_{0X}\Psi_{0y}\psi_{xy}+\varepsilon\Psi_{0Xy}\Psi_{0y}\psi_x+\varepsilon\Psi_{0Xy}\Psi_{0y}\psi_x))=0. \qquad (9.5)
\end{aligned}
$$

The term $\sqrt{2\varepsilon\Psi_{0X}\psi_x+\Psi_{0y}^2+\Psi_{0y}2\psi_y}$ is linearized as follows:

$$
\begin{aligned}
\sqrt{\Psi_{0y}^2+2\varepsilon\Psi_{0X}\psi_x+\Psi_{0y}2\psi_y}&=\sqrt{\Psi_{0y}^2(1+\varepsilon\frac{2\Psi_{0X}\psi_x}{\Psi_{0y}^2}+\psi_y\frac{2\Psi_{0y}}{\Psi_{0y}^2})}\\
&=\Psi_{0y}\sqrt{1+\varepsilon\frac{2\Psi_{0X}\psi_x}{\Psi_{0y}^2}+\psi_y\frac{2\Psi_{0y}}{\Psi_{0y}^2}}=|(1+\varepsilon)^\alpha=1+\alpha\varepsilon+...|\\
&=\Psi_{0y}(1+\varepsilon\frac{\Psi_{0X}\psi_x}{\Psi_{0y}^2}+\psi_y\frac{\Psi_{0y}}{\Psi_{0y}^2})=\Psi_{0y}+\varepsilon\frac{\Psi_{0X}\psi_x}{\Psi_{0y}}+\psi_y\\
&=\frac{\Psi_{0y}^2}{\Psi_{0y}}+\varepsilon\frac{\Psi_{0X}\psi_x}{\Psi_{0y}}+\frac{\psi_y\Psi_{0y}}{\Psi_{0y}}=\frac{\Psi_{0y}^2+\varepsilon\Psi_{0X}\psi_x+\psi_y\Psi_{0y}}{\Psi_{0y}}. \qquad (9.6)
\end{aligned}
$$

The term $\frac{1}{\sqrt{2\varepsilon\Psi_{0X}\psi_x+\Psi_{0y}^2+\Psi_{0y}2\psi_y}}$ is transformed in the following way:

$$
\begin{aligned}
\frac{1}{\sqrt{2\varepsilon\Psi_{0X}\psi_x+\Psi_{0y}^2+\Psi_{0y}2\psi_y}}&=\frac{1}{\sqrt{\Psi_{0y}^2(1+\varepsilon\frac{2\Psi_{0X}\psi_x}{\Psi_{0y}^2}+\psi_y\frac{2\Psi_{0y}}{\Psi_{0y}^2})}}\\
&=\frac{1}{\Psi_{0y}}\frac{1}{\sqrt{1+\varepsilon\frac{2\Psi_{0X}\psi_x}{\Psi_{0y}^2}+\psi_y\frac{2\Psi_{0y}}{\Psi_{0y}^2}}}=|(1+\varepsilon)^\alpha=1+\alpha\varepsilon+...|\\
&=\frac{1}{\Psi_{0y}}(1-\varepsilon\frac{\Psi_{0X}\psi_x}{\Psi_{0y}^2}-\psi_y\frac{\Psi_{0y}}{\Psi_{0y}^2})=\frac{1}{\Psi_{0y}}-\varepsilon\frac{\Psi_{0X}\psi_x}{\Psi_{0y}^3}-\psi_y\frac{\Psi_{0y}}{\Psi_{0y}^3}\\
&=\frac{\Psi_{0y}^2-\varepsilon\Psi_{0X}\psi_x-\psi_y\Psi_{0y}}{\Psi_{0y}^3}. \qquad (9.7)
\end{aligned}
$$

So, the linearized form of the term $(\Psi_{0yy}+\Delta\psi)\sqrt{2\varepsilon\Psi_{0X}\psi_x+\Psi_{0y}^2+\Psi_{0y}2\psi_y}$ is:

$$
(\Psi_{0yy}+\Delta\psi)\sqrt{2\varepsilon\Psi_{0X}\psi_x+\Psi_{0y}^2+\Psi_{0y}2\psi_y}
$$

$$
\begin{aligned}
&= (\Psi_{0yy} + \psi_{xx} + \psi_{yy}) \frac{\Psi_{0y}^2 + \varepsilon\Psi_{0X}\psi_x + \psi_y\Psi_{0y}}{\Psi_{0y}} \\
&= \frac{1}{\Psi_{0y}} (\Psi_{0yy}\Psi_{0y}^2 + \psi_{xx}\Psi_{0y}^2 + \psi_{yy}\Psi_{0y}^2 + \Psi_{0yy}\varepsilon\Psi_{0X}\psi_x \\
&+ \psi_{xx}\varepsilon\Psi_{0X}\psi_x + \psi_{yy}\varepsilon\Psi_{0X}\psi_x + \Psi_{0yy}\psi_y\Psi_{0y} + \psi_{xx}\psi_y\Psi_{0y} + \psi_{yy}\psi_y\Psi_{0y}) \\
&= \frac{1}{\Psi_{0y}} (\Psi_{0yy}\Psi_{0y}^2 + \psi_{xx}\Psi_{0y}^2 + \psi_{yy}\Psi_{0y}^2 + \Psi_{0yy}\varepsilon\Psi_{0X}\psi_x + \Psi_{0yy}\psi_y\Psi_{0y}) \\
&= \Psi_{0yy}\Psi_{0y} + \psi_{xx}\Psi_{0y} + \psi_{yy}\Psi_{0y} + \frac{\Psi_{0yy}\varepsilon\Psi_{0X}\psi_x}{\Psi_{0y}} + \Psi_{0yy}\psi_y. \qquad (9.8)
\end{aligned}
$$

The term

$$
\begin{aligned}
&\frac{1}{\sqrt{2\varepsilon\Psi_{0X}\psi_x + \Psi_{0y}^2 + 2\Psi_{0y}\psi_y}} ((\Psi_{0y}^2\Psi_{0yy} + 2\Psi_{0y}\Psi_{0yy}\psi_y + \Psi_{0y}^2\psi_{yy}) \\
&\qquad + 2(\varepsilon\Psi_{0X}\Psi_{0y}\psi_{xy} + \varepsilon\Psi_{0Xy}\Psi_{0y}\psi_x + \varepsilon\Psi_{0Xy}\Psi_{0y}\psi_x)) \qquad (9.9)
\end{aligned}
$$

is linearized as follows:

$$
\begin{aligned}
&\frac{1}{\sqrt{2\varepsilon\Psi_{0X}\psi_x + \Psi_{0y}^2 + 2\Psi_{0y}\psi_y}} ((\Psi_{0y}^2\Psi_{0yy} + 2\Psi_{0y}\Psi_{0yy}\psi_y + \Psi_{0y}^2\psi_{yy}) \\
&\qquad + 2(\varepsilon\Psi_{0X}\Psi_{0y}\psi_{xy} + \varepsilon\Psi_{0Xy}\Psi_{0y}\psi_x + \varepsilon\Psi_{0Xy}\Psi_{0y}\psi_x)) \\
&= \frac{1}{\Psi_{0y}^3} (\Psi_{0y}^2 - \varepsilon\Psi_{0X}\psi_x - \psi_y\Psi_{0y}) ((\Psi_{0y}^2\Psi_{0yy} + 2\Psi_{0y}\Psi_{0yy}\psi_y + \Psi_{0y}^2\psi_{yy}) \\
&\qquad + (2\varepsilon\Psi_{0X}\Psi_{0y}\psi_{xy} + 2\varepsilon\Psi_{0Xy}\Psi_{0y}\psi_x + 2\varepsilon\Psi_{0Xy}\Psi_{0y}\psi_x)) \\
&= \frac{1}{\Psi_{0y}^3} (\Psi_{0y}^4\Psi_{0yy} + 2\Psi_{0y}^3\Psi_{0yy}\psi_y + \Psi_{0y}^4\psi_{yy} + 2\varepsilon\Psi_{0X}\Psi_{0y}^3\psi_{xy} \\
&+ 2\varepsilon\Psi_{0Xy}\Psi_{0y}^3\psi_x + 2\varepsilon\Psi_{0Xy}\Psi_{0y}^3\psi_x - \varepsilon\Psi_{0X}\psi_x\Psi_{0y}^2\Psi_{0yy} - \psi_y\Psi_{0y}^3\Psi_{0yy}) \\
&= \Psi_{0y}\Psi_{0yy} + 2\Psi_{0yy}\psi_y + \Psi_{0y}\psi_{yy} + 2\varepsilon\Psi_{0X}\psi_{xy} \\
&\quad + \varepsilon\Psi_{0Xy}\psi_x + 2\varepsilon\Psi_{0Xy}\psi_x - \frac{\varepsilon\Psi_{0X}\psi_x\Psi_{0yy}}{\Psi_{0y}} - \psi_y\Psi_{0yy}. \qquad (9.10)
\end{aligned}
$$

Substituting the linearized terms (9.8) and (9.10) into (9.5) we obtain

$$
\begin{aligned}
&(\Delta\psi)_t + (2\beta_1 - \beta_2)((\varepsilon\Psi_{0Xy}\Psi_{0yy} + \varepsilon\Psi_{0Xy}\psi_{yy} + \psi_{xy}\Psi_{0yy}) \\
&\qquad + (\varepsilon\Psi_{0Xyy}\Psi_{0y} + \varepsilon\Psi_{0Xyy}\psi_y + \Psi_{0y}\psi_{xyy})) \\
&\qquad - \beta_2((\varepsilon\Psi_{0Xy}\Psi_{0yy} + \Psi_{0yy}\psi_{xy} + \varepsilon\Psi_{0Xy}\psi_{yy}) \\
&\qquad + (\varepsilon\Psi_{0X}\Psi_{0yyy} + \Psi_{0yyy}\psi_x + \varepsilon\Psi_{0X}\psi_{yyy})) \\
&\qquad + (\beta_2 - 1)(\psi_{xx}\varepsilon\Psi_{0Xy} + \varepsilon\Psi_{0X}\psi_{xxy})
\end{aligned}
$$

$$
\begin{aligned}
&+\beta_2(\psi_{xxx}\Psi_{0y}+\psi_{xx}\varepsilon\Psi_{0Xy})-(2\beta_3-1)(\varepsilon\Psi_{0Xy}\psi_{xx}+\varepsilon\Psi_{0X}\psi_{xxy})+\\
&+\frac{c_f}{2h}(\Psi_{0yy}\Psi_{0y}+\psi_{xx}\Psi_{0y}+\psi_{yy}\Psi_{0y}+\frac{\Psi_{0yy}\varepsilon\Psi_{0X}\psi_x}{\Psi_{0y}}+\Psi_{0yy}\psi_y\\
&+\Psi_{0y}\Psi_{0yy}+2\Psi_{0yy}\psi_y+\Psi_{0y}\psi_{yy}+2\varepsilon\Psi_{0X}\psi_{xy}\\
&+2\varepsilon\Psi_{0Xy}\psi_x+2\varepsilon\Psi_{0Xy}\psi_x-\frac{\varepsilon\Psi_{0X}\psi_x\Psi_{0yy}}{\Psi_{0y}}-\psi_y\Psi_{0yy})=0.
\end{aligned}
\tag{9.11}
$$

Simplifying the expression (9.11) and grouping the terms, we get:

$$
\begin{aligned}
&(\Delta\psi)_t+(2\beta_1-\beta_2)(\psi_{xy}\Psi_{0yy}+\Psi_{0y}\psi_{xyy})\\
&-\beta_2(\Psi_{0yy}\psi_{xy}+\Psi_{0yyy}\psi_x)+\beta_2\psi_{xxx}\Psi_{0y}\\
&+\frac{c_f}{2h}(2\Psi_{0yy}\Psi_{0y}+\psi_{xx}\Psi_{0y}+2\psi_{yy}\Psi_{0y}+2\Psi_{0yy}\psi_y)\\
&+\varepsilon((2\beta_1-\beta_2)(\Psi_{0Xy}\Psi_{0yy}+\Psi_{0Xy}\psi_{yy}+\Psi_{0Xyy}\Psi_{0y}+\Psi_{0Xyy}\psi_y)\\
&-\beta_2(\Psi_{0Xy}\Psi_{0yy}+\Psi_{0Xy}\psi_{yy}+\Psi_{0X}\Psi_{0yyy}+\Psi_{0X}\psi_{yyy})\\
&+(\beta_2-1)(\psi_{xx}\Psi_{0Xy}+\Psi_{0X}\psi_{xxy})+\beta_2(\psi_{xx}\Psi_{0Xy})\\
&-(2\beta_3-1)(\Psi_{0Xy}\psi_{xx}+\Psi_{0X}\psi_{xxy})\\
&+\frac{c_f}{2h}(2\Psi_{0X}\psi_{xy}+2\Psi_{0Xy}\psi_x+2\Psi_{0Xy}\psi_x))=0.
\end{aligned}
\tag{9.12}
$$

Denoting Ψ_{0y} as U and $-\Psi_{0X}$ as V we can rewrite (9.12) as follows:

$$
\begin{aligned}
&(\Delta\psi)_t+(2\beta_1-\beta_2)(\psi_{xy}U_y+U\psi_{xyy})\\
&-\beta_2(U_y\psi_{xy}+U_{yy}\psi_x)+\beta_2\psi_{xxx}U\\
&+\frac{c_f}{2h}(2U_yU+\psi_{xx}U+2\psi_{yy}U+2U_y\psi_y)\\
&+\varepsilon((2\beta_1-\beta_2)(U_XU_y+U_X\psi_{yy}+U_{Xy}U+U_{Xy}\psi_y)\\
&-\beta_2(U_XU_y+U_X\psi_{yy}-VU_{yy}-V\psi_{yyy})\\
&+(\beta_2-1)(\psi_{xx}U_X-V\psi_{xxy})+\beta_2(\psi_{xx}U_X)\\
&-(2\beta_3-1)(U_X\psi_{xx}-V\psi_{xxy})+\frac{c_f}{2h}(2U_X\psi_x-2V\psi_{xy}+2U_X\psi_x))=0.
\end{aligned}
\tag{9.13}
$$

Linearizing (9.5) in the neighborhood of the base flow, dropping the subscript ”f” and retaining

only the terms of order ε we obtain

$$\begin{aligned}\psi_{xxt}+\psi_{yyt} \quad + \quad & (2\beta_1-\beta_2)(U_y\psi_{xy}+U\psi_{xyy})-\beta_2(U_y\psi_{xy}+U_{yy}\psi_x)+\beta_2 U\psi_{xxx} \\ & +\frac{c_f}{2h}\Big[U(\psi_{xx}+2\psi_{yy})+2U_y\psi_y\Big] \\ & +\varepsilon\Big\{(2\beta_1-\beta_2)(U_X\psi_{yy}+U_{Xy}\psi_y)-\beta_2(U_X\psi_{yy}-V\psi_{yyy}) \\ & +(\beta_2-1)(U_X\psi_{xx}-V\psi_{xxy})+\beta_2 U_X\psi_{xx} \\ & -(2\beta_3-1)(U_X\psi_{xx}-V\psi_{yy}) \\ & +\frac{c_f}{2h}\Big[2U_X\psi_x-2V\psi_{xy}+V\psi_x U_y/U\Big]\Big\}=0, \end{aligned} \tag{9.14}$$

where $U=\psi_{0y}$ and $V=-\psi_{0X}$.

The method of normal modes is a classical method of stability analysis of parallel steady flows (see, for example, [8]). In such cases the stream function is represented in the form

$$\psi(x,y,t)=\varphi(y)\exp\left[i(kx-\omega t)\right], \tag{9.15}$$

where k is the wavenumber of a perturbation and ω is the frequency of oscillation. An arbitrary perturbation consists of a superposition of perturbed components of the form (9.15) over the range of all wavenumbers. However, in order to find a necessary condition for instability, it is enough to consider only one component of the form (9.15) (see, for example, [19]). If the base flow is slightly non-parallel, then the perturbation stream function $\psi(x,y,t)$ is decomposed into a slowly varying amplitude function $\varphi(y,X,\omega)$ and a fast varying phase function $\theta(X,\omega)/\varepsilon$ [19]:

$$\psi(x,y,\omega,t)=\varphi(y,X,\omega)\exp\left[i\left(\frac{\theta(X,\omega)}{\varepsilon}-\omega t\right)\right]. \tag{9.16}$$

We also assume that $\varphi(y,X,\omega)$ can be represented by a power series in ε in the form

$$\varphi(y,X,\omega)=\varphi_1(y,X,\omega)+\varepsilon\varphi_2(y,X,\omega)+\ldots \tag{9.17}$$

Substituting (9.16) and (9.17) into (9.14) and collecting the terms that do not contain ε we obtain

$$L\varphi_1=0, \tag{9.18}$$

where

$$
\begin{aligned}
L[\varphi_1] &= \varphi_1''\left[(2\beta_1-\beta_2)U-\frac{\omega}{k}-\frac{ic_fU}{kh}\right] \\
&\quad +\varphi_1'\left[2(\beta_1-\beta_2)U_y-\frac{ic_fU_y}{kh}\right] \\
&\quad +\varphi_1\left(\omega k-\beta_2U_{yy}-\beta_2k^2U+\frac{ic_fkU}{2h}\right). \qquad (9.19)
\end{aligned}
$$

The primes in (9.19) represent the derivatives with respect to y and $k=k(X,\omega)=\theta_X$. Thus, equation (9.18) is the modified Rayleigh equation which is obtained in [22] under parallel flow approximation. Equation (9.18) together with zero boundary conditions forms an eigenvalue problem (where the eigenvalues are $k=k(X,\omega)$). The values of $k=k(X,\omega)=\theta_X$ can be obtained as a result of the numerical solution of the eigenvalue problem. In addition, a normalized eigenfunction of the linear stability problem, $\Phi(y,X,\omega)$, can be calculated. Note that the coordinate X appears in (9.18) as a parameter.

In order to obtain the equation for the amplitude of a perturbation we assume that

$$\varphi_1(y,X,\omega)=A(X,\omega)\Phi(y,X,\omega), \qquad (9.20)$$

where $A(X,\omega)$ is an unknown complex amplitude and $\Phi(y,X,\omega)$ is a normalized eigenfunction of the linear stability problem.

Substituting (9.16), (9.17) and (9.20) into (9.14) and collecting the terms containing ε we obtain

$$L[\varphi_2]=g, \qquad (9.21)$$

where

$$
\begin{aligned}
g &= \frac{i}{k}\frac{dA}{dX}\Big\{2\omega k\Phi + (2\beta_1-\beta_2)(U_y\Phi^{'}+U\Phi^{''}) \\
&\quad -\beta_2[U_y\Phi^{'}+U_{yy}\Phi+3U\Phi k^2]+\frac{ic_fUk\Phi}{h}\Big\} \\
&\quad -\frac{i}{k}A\Big\{2\omega k\Phi_X+\omega\frac{dk}{dx}\Phi+(2\beta_1-\beta_2)[U_y\Phi_X^{'}+U\Phi_X^{''}+U_X\Phi^{''}+U_{Xy}\Phi^{'}] \\
&\quad -\beta_2[U_y\Phi_X^{'}+U_{yy}\Phi_X+3Uk^2\Phi_X \\
&\quad +3U\Phi k\frac{dk}{dX}+U_X\Phi^{''}-V\Phi^{'''}+U_Xk^2\Phi] \\
&\quad +(\beta_2-1)(Vk^2\Phi^{'}-k^2U_X\Phi)-(2\beta_3-1)[k^2V\Phi^{'}-k^2U_X\Phi] \\
&\quad +\frac{c_f}{2h}\Big[2iUk\Phi_X+iU\Phi\frac{dk}{dX} \\
&\quad +2ikU_X\Phi-2ikV\Phi^{'}+i\frac{V}{U}U_yk\Phi\Big]\Big\}. \qquad (9.22)
\end{aligned}
$$

An amplitude evolution equation for $A(X,\omega)$ is obtained from Fredholm's alternative, namely, equation (9.21) has a solution if and only if the function g is orthogonal to all eigenfunctions $\tilde{\Phi}$ of the corresponding adjoint problem. Using the solvability condition

$$\int_{-\infty}^{\infty} g\tilde{\Phi}\,dy = 0, \qquad (9.23)$$

we obtain the equation for the function $A(X,\omega)$ in the form

$$M(X,\omega)\frac{dA}{dX}+N(X,\omega)A=0, \qquad (9.24)$$

where

$$
\begin{aligned}
M(X,\omega) &= \frac{i}{k}\int_{-\infty}^{\infty}\Big\{2\omega k\Phi+(2\beta_1-\beta_2)(U_y\Phi^{'}+U\Phi^{''}) \\
&\quad -\beta_2[U_y\Phi^{'}+U_{yy}\Phi+3U\Phi k^2]+\frac{ic_fUk}{h}\Phi\Big\}\tilde{\Phi}\,dy, \qquad (9.25)
\end{aligned}
$$

$$
\begin{aligned}
N(X,\omega) \;=\; & \frac{i}{k}\int_{-\infty}^{\infty}\Big\{2\omega k\Phi_X+\omega\frac{dk}{dX}\Phi+(2\beta_1-\beta_2)[U_y\Phi_X^{'}+U\Phi_X^{''} \\
& +U_X\Phi^{''}+U_{Xy}\Phi^{'}]-\beta_2[U_y\Phi_X^{'}+U_{yy}\Phi_X+3Uk^2\Phi_X \\
& +3U\Phi k\frac{dk}{dX}+U_X\Phi^{''}-V\Phi^{'''}+U_Xk^2\Phi] \\
& +(\beta_2-1)[Vk^2\Phi^{'}-k^2U_X\Phi]-(2\beta_3-1)[k^2V\Phi^{'}-k^2\Phi U_X] \\
& \frac{c_f}{2h}\Bigg[2ikU\Phi_X+iU\frac{dk}{dX}\Phi \\
& +2ikU_X\Phi-2ikV\Phi^{'}+i\frac{V}{U}U_yk\Phi\Bigg]\Big\}\tilde{\Phi}\,dy. \qquad (9.26)
\end{aligned}
$$

Thus, using the WKB method, the leading order approximation of the stream function $\psi(x,y,\omega,t)$ has the form

$$
\psi(x,y,\omega,t)\sim A(X,\omega)\Phi(y,X,\omega)\exp\left[i\left(\frac{1}{\varepsilon}\int_0^X k(X,\omega)\,dX-\omega t\right)\right]. \qquad (9.27)
$$

9.3 Discussion

Formula (9.27) provides the connection between local parallel flow approximations and takes into account slow streamwise variation of the base flow. Following [6], a few important conclusions can be drawn from (9.27). First, all the three terms on the right-hand side of (9.27) contain information related to the amplitude and phase of the perturbation. Second, the growth rate and phase speed of the perturbation at any given downstream station depends on the choice of the perturbed quantities. Finally, the growth rate and phase speed depend even on the location where these quantities are calculated. In particular, it is shown in [6] that for any given flow variable Q one can define a local wavenumber k_l by the formula

$$
k_l(x,y|Q)=-i\frac{\partial}{\partial x}\ln Q(x,y), \qquad (9.28)
$$

where $k_l=k_{lr}+ik_{li}$ and the values of k_{lr} and k_{li} are interpreted as the local phase speed and local spatial growth rate. Thus, in order to make a meaningful comparison of the weakly nonlinear model (9.27) with experimental data one needs to choose a particular flow quantity Q (say, pressure or streamwise velocity), then measure it at a particular point and evaluate the right-hand side of (9.28) at the same point. In other words, in order to validate the weakly nonlinear model one needs to have either detailed experimental data or, alternatively, numerical solution of nonlinear two-dimensional shallow water equations.

10 CONCLUSION

The research work presented in this thesis can be divided into five parts:

1. Linear stability analysis of flows with free surface.
2. Linear stability analysis of a flow under the ”rigid-lid” assumption.
3. Weakly non-linear analysis of a flow under the ”rigid-lid” assumption and derivation of Ginzburg-Landau equation.
4. Linear and weakly non-linear stability analysis of two-phase flows.
5. Stability analysis of a non-parallel flow.

Conclusions for each of these parts are presented in each of the following sections.

10.1 Stability analysis of free surface flows

A flow with unbounded surface was analyzed in the chapter. Saint-Venant equations with momentum correction coefficients were used as a starting point for derivation of a system of equations that governs behavoir of perturbation. The system was derived as follows:

- Small perturbations of pressure and velocity components in both transverse and downstream directions were imposed on the flow.
- The equations were linearized in the neighbourhood of the base flow by neglecting quadratic terms of perturbation expansion.
- The method of normal modes was employed. The perturbation function was sought as product of a function that depends on transverse coordinate only and a wave with a complex frequency propagating in downstream direction.

The obtained system of ordinary differential equations together with boundary conditions formed an eigenvalue problem. It was solved by a numerical method based on Chebyshev polynomials. The solution was sought in the form of fundamental interpolation polynomials. As a result of the solution, a set of eigenvalues was obtained. Each eigenvalue represented the complex frequency of a mode. The eigenvalues determine stability of a flow. As frequency is complex, perturbation growth or decay is possible.

It was found that bottom friction had a dramatic effect on the stability of the flow. In compliance with Chen&Jirka [2], the stability parameter, that included the bottom friction coefficients, was considered as a defining factor for flow stability.

The conditions were found when the transition from stable to unstable flow took place. The search for the conditions was performed by obtaining solutions of the perturbation equations while varying the two parameters:

- The stability parameter taking into account vertical and transverse scale of the flow as well as bottom friction coeffcient.
- The wavenumber of a perturbation mode.

The transition to unstable flow takes place at certain value of stability parameter that is referred to as the critical value. As long as the critical value is known we are able to predict whether a specific flow is stable or unstable. The stability parameter for the specific flow needs to be calculated and compared to the critical value. If the calculated stability parameter value falls in the range below the critical one, then the flow is unstable. If the calculated value exceeds the critical one, the flow is stable.

Analysis of shallow flow usually implies numerous assumptions introduced to simplify the problem. The assumptions may affect accuracy of determination of the critical value.

The effect on accuracy of calculations was evaluated for two assumptions:

- The assumption of uniform velocity distribution in vertical direction.
- The assumption of constant depth (”rigid-lid” assumption).

The assumption of uniform velocity distribution was tested by employing momentum correction coefficients. The momentum correction coefficients were used to take into account the vertical

non-uniformity of a real flow. For an uniform flow the momentum correction coefficients were equal to unity, while they deviated from unity for non-uniform flow and the deviation is larger for flows with higher non-uniformity.

The ”rigid-lid” assumption was tested by employing the Froude number. The Froude number was effectively ratio of gravity and inertia forces. The case when the Froude number was close to zero corresponded to ”rigid-lid” assumption; the higher was the Froude number the larger was the deviation of the flow from the assumption.

The critical value of the stability parameter was found for different values of the Froude number and the momentum correction coefficients. The effect of variation of the two parameters on the results was evaluated. The range of variaton of the parameters was selected to match the range in nature and experiments [40], [34].

It was found that deflection of the Froude number from zero did not have a dramatic influence on the stability analysis results as long as the Froude number stayed within limits typical for shallow flows in nature ($0.1 - 0.2$). It was shown that for this case the application of the ”rigid-lid” assumption introduced a relatively small error into analysis that did not exceed 2%.

The momentum correction coefficients, in turn, had higher influence on stability analysis results. For flows abundant in nature, the values of momentum correction coefficients were high enough to introduce error about 10%. Depending on whether transverse or downstream velocity component was considered, neglection of a momentum correction coefficient might lead to either underestimation or overestimation of the stability of the flow.

The neutral stability curves were constructed for various values of momentum correction coefficients and for various values of the Froude number.

10.2 Linear stability analysis of a flow under ”rigid-lid” assumption

The stability of a flow was analyzed by a linear method employing the ”rigid-lid” assumption. The essense of the ”rigid-lid” assumption was that water depth is considered to be constant, thus enabling reduction of the system of equations to a single equation.

Momentum correction coefficients were used to compensate for vertical non-uniformity of a flow and influence of momentum correction coefficients on stability analysis results was analyzed.

The governing equations for shallow water flow (Saint-Venant) equations were modified taking into account that the flow depth was constant. Then the equations governing transverse and downstream velocity components were added up and the flow function was introduced. Thus a single equation was obtained. The equation was transformed as follows:

- The solution was sought in a form of series expansion in powers of a small parameter.
- The equation was linearized by neglecting quadratic expansion terms.
- The method of normal modes was applied in order to transform the equation into ordinary differential equation that forms an eigenvalue problem.

In compliance with method of normal modes, the solution was sought as a product of a function of transverse coordinate and a wave packet with each mode having a wavenumber and a wavespeed. The wavespeed was complex and defined stability of a mode: negative imaginary part led to amplification of a mode while positive imaginary part led to supression of a mode.

The eigenvalue problem was solved by pseudospectral collocation method based on Chebyshev polynomials and a set of eigenvalues was obtained. The value of a bottom friction coefficient was adjusted in order to find the threshold where a transition from stable to unstable flow took place. Later, the procedure was repeated for various wavenumber values and a stability curve was constructed.

A set of stability curves was obtained for various values of momentum correction coefficients. The obtained curves were compared together and it was found that the area below the curve (instability region) tended to increase as vertical non-uniformity of downstream velocity grows. Transverse velocity component had opposite effect on flow stability: as it's non-uniformity increased, the instability domain diminished.

It was found that for velocity non-uniformity expected in natural shallow wake flows the error due to neglection of momentum correction coefficients could reach 10%. Evaluation of vertical non-uniformity of the flow velocity might be essential for obtaining accurate stability analysis results.

10.3 Weakly non-linear analysis

Weakly non-linear analysis was performed in order to see how the perturbation is evolving. The idea of weakly non-linear analysis was to consider perturbation amplitude that was weakly dependent on time and coordinate. The ”slow” time and ”streched” coordinate moving with group velocity were introduced using a small scaling parameter ε.

Following the same procedure as for linear stability analysis, the Saint-Venant equations were used as a starting point. The governing equation for the perturbation amplitude was derived by following the procedure:

- The ”rigid-lid” assumption was used.
- The equations governing downstream and transverse velocity components were differentiated with respect to transverse and downstream coordinates respectively. The equations were added up and pressure was eliminated.
- The stream function was introduced. The velocity equation was transformed to an ordinary differential equation with the stream function as unknown function.
- The solution was sought in a form of power series expansion in powers of a small parameter ε.
- The terms proportional to the fourth power of ε were neglected.

The obtained equation contained terms proportional to the first, second and third power of ε. The terms proportional to ε^1 formed the previously obtained linear eqigenvalue problem. However, the solution of this first-order equation was sought in a form including an additional term that was the perturbation amplitude weakly depending on time and downstream coordinate. By collecting higher terms, two non-linear non-homogenious equations were obtained. It was shown that the two equations were resonantly forced, as corresponding homogenious equations had non-trivial solutions. According to Fredholm’s alternative, the non-homogenious equations have solutions if certain solvability conditions are satisfied.

The solvability conditions have yielded an equation that governed growth of perturbation amplitude. It was shown that perturbation amplitude was governed by the Ginzburg-Landau equation.

The Ginzburg-Landau equation included a perturbation growth term, a dispersive term, and a nonlinear term. The complex coefficients for the terms defined perturbation amplitude growth, amplitude dispersion and non-linear effects respectively. The non-linear term coefficient (often referred to as the Landau constant) determined whether an amplitude saturation is possible. If the real part of the coefficient was negative, then amplitude tended to saturate instability and finite-amplitude equillibrium was possible.

The coefficients of Ginzburg-Landau equation could be calculated by means of numerical methods. The numerical method suitable for calculation of the coefficients was developed and described in the chapter.

10.4 Stability analysis of two-phase flows

Stability of a two-phase flow was analysed in the chapter by means of linear and weakly non-linear method. The governing equations were derived from the Saint-Venant equations with an additional term describing particle-fluid interaction. The interaction was characterized by the particle loading parameter. The particle loading parameter took into account ratios of the bulk density of the particles to density of the fluid, actual drag on the particles to Stokes drag and flow aerodynamic response time to particle aerodynamic response time.

Linear stability analysis was performed in order evaluate effect of particles on the stability of the flow. The ”rigid-lid” assumption was used. The equations were linearized by imposing a small perturbation on the solution and neglecting quadratic terms. The method of normal modes was also employed and a modified Rayleigh equation was obtained.

The equation was solved by a numerical spectral collocation method based on Chebyshev polynomials. Critical value of the stability parameter was calculated and stability curves were obtained for various values of the particle loading parameter. It was found that presence of particles enhanced flow stability. The critical value of stability parameter was found to decrease linearly with growth of the particle loading parameter.

Weakly non-linear analysis was performed in order to see the influence of particle loading on perturbation growth. The Ginzburg-Landau equation was derived as a governing equation for perturbation growth. A numerical method was employed in order to calculate the coefficients for

the Ginzburg-Landau equation. The numerical method involved determination of eigenfunctions and group velocity by solving several boundary value problems numerically and calculation of coefficients by numerical integration.

The coefficients of the Ginzburg-Landau equation were calculated for various values of the particle loading parameter. Special attention was paid to the nonlinear term coefficient, the so-called ”Landau constant”, as it defined whether finite-amplitude equilibrium and flow stabilization was possible.

Calculations showed that for values of particle loading parameter that were of practical interest [41] for flows abundant in nature and engineering the Landau constant allowed possibility for the finite-amplitude equillibrium and stabilization of a secondary flow. It was also found that the particle loading parameter affected finite-amplitude value. The amplitude decreased as the particle loading parameter grew.

It has also been found that finite-equillibrium state might have a plane-wave solution, however, analysis showed that the solution would not be stable.

10.5 Analysis of non-parallel flow

The chapter considered stability of a non-parallel flow, when the base-flow profile changed downstream.

The solution for the Saint-Venant equations was sought in a form of a superposition of a base flow that was weakly dependent on downstream coordinate and a perturbation. The solution was substituted into the equation and the equation was linearized by neglecting quadratic perturbation terms.

The method of normal modes is usually applied in order to transform the linearized equation to ordinary differential equation. The method of normal modes usually implies that the solution is sought as a product of a perturbation function and a wave.

In case of non-parallel flow the solution was decomposed into a slowly varying function ϕ and a fast varying phase function. The function ϕ was sought in a form of power series expansion in the small parameter ε. By collecting the terms proportional to ε^0 a modified Rayleigh equation was obtained for function ϕ that formed a stability problem together with boundary conditions.

The solution of the modified Rayleigh equation was sought in a form of a product of a complex amplitude and a normalized eigenfunction of the linear stability problem. The equation for the complex amplitude was derived, that allowed to find the leading order approximation of the perturbation stream function.

The expression of leading order approximation contained three terms: the complex amplitude, the normalized eigenfunction of the linear stability problem and the exponential term.

The form of the leading order approximation allowed to make several important conclusions. First, all the three terms contained information related to the amplitude and phase of the perturbation. Second, the growth rate and phase speed of the perturbation at any given downstream station depended on the choice of the perturbed quantities (e. g. velocity components). Finally, the growth rate and phase speed depended even on the location where these quantities were calculated.

In other words, in order to validate the weakly nonlinear model one would need to have either detailed experimental data or, alternatively, numerical solution of nonlinear two-dimensional shallow water equations.

List of Figures

List of Tables

Bibliography

[1] Aranson L.S., Kramer L. The world of the complex Ginzburg-Landau equation// Rev. Mod. Phys. - 2002. - Vol.74. - pp. 99.-143.

[2] Chen D., Jirka G. H. Absolute and convective instabilities of plane turbulent wakes in a shallow water layer// Journal of Fluid Mechanics. - 1997. - Vol.338. - pp. 157.-172.

[3] Chen D., Jirka G. H. Experimental study of plane turbulent wake in a shallow water layer// Fluid Dynamic Research. - 1995. - Vol.16. - pp. 11.-41.

[4] Chu V.H., Wu J.H., Khayat R. E. Stability of transverse shear flows in shallow open chanels// Journal of Hydraulic Engineering - 1999. - Vol.117. - No.10. - pp. 1370.-1388.

[5] Couairon A., Chomaz J.-M. Primary and secondary nonlinear global instability// Physica D. - Vol. 132. - pp. 428.-456.

[6] Crighton D. G., Gaster M. Stability of slowly diverging jet flow// Journal of Fluid Mechanics. - Vol.77. - Part 2. - pp. 397.-413.

[7] Dimas A. A., Kiger K. T. Linear instability of a particle-laden mixing layer with a dynamic dispersed phase// Physics of Fluids. - 1998. - Vol.10. - No.10. - pp. 2539.-2557.

[8] Drazin P. G., Reid W. H. Hydrodinamic Stability. Second Edition. - Cambridge University Press, 2004.

[9] El-Hady M. N. Nonparallel instability of supersonic and hypersonic boundary layers// Physics of Fluids. - 1991. - Vol.3. - No.9. - pp. 2164.-2178.

[10] Falques A., Iranzo V. Numerical simulation of vorticity waves in the nearshore// Journal of Geophysical Research. - 1994 - Vol.99. - pp. 825. - 841.

[11] Forsythe G. E., Malcolm M. A., Moler C. B. Computer Methods for Mathematical Computations. - Prentice-Hall Inc., 1977.

[12] Gaster M., Kit E., Wygnanski I. Large-scale structures in a forced turbulent mixing layer// Journal of Fluid Mechanics. - 1985 - Vol.150. - pp. 23.-39.

[13] Ghidaoui M., Kolyshkin A. A. Linear stability analysis of lateral motions in compound open channels// Journal of Hydraulic Engineering. - 1999 - Vol.125. - pp. 871.-880.

[14] Ghidaoui M., Kolyshkin A. A. Stability analysis of shallow wake flows// Journal of Fluid Mechanics. - 2003 - Vol.494. - pp. 355.-377.

[15] Ghidaoui M. S., Kolyshkin A. A. Weakly nonlinear spatial stability analysis of shallow water flows// 4th International Symposium on Environmental Hydraulics. - Hong Kong, 2004.

[16] Ghidaoui M., Kolyshkin A. A., Yen B. C. Influence of momentum correction coefficients on linear stability analysis of open-channel flows// Proc. of XXVIII IAHR Congress,Theme E5. - 1999 (on CD).

[17] Golub G.H., Van Loan C.F. Matrix computations. Third edition. - London: The Johns Hopkins University Press, 1996.

[18] Grubisic V., Smith R. B. The effect of bottom friction on Shallow-water flow past an isolated obstacle// Journal of the Atmospheric Sciences. - 1985 - Vol.52. - No 11.

[19] Huerre P., Rossi M. Hydrodynamic instabilities in open flows, in Hydrodynamics and Nonlinear Instabilities. - Cambridge University Press., 1998.

[20] Ingram R. G., Chu V. H. Flow around islands in Rupert Bay: An investigation of the bottom friction effect// Journal of Geophysical Research. - 1987 - Vol.92. - pp. 14521.-14533.

[21] Kolyshkin A. A., Nazarovs S. On the Stability of Wake Flows in Shallow Water// Proceedings of the 10th International Conference MMA2005&CMAM2. - Trakai (on CD).

[22] Kolyshkin A. A., Nazarovs S. Significance of Averaging Coefficients in Stability Analysis of Shallow Wake Flows// Mathematical Modelling and Analysis. - 2007 - Vol.12. - No.2. - pp. 1.-12.

[23] Kolyshkin A. A., Nazarovs S. Influence of averaging coefficients on weakly nonlinear stability of shallow flows// IASME Transactions. - 2005. - Vol.2. - pp. 86.-91.

[24] Kolyshkin A. A., Nazarovs S. Calculations of the coefficients of the Ginzburg-Landau equation for shallow water flows// Scientific Proceedings of the Riga Technical University, Series - Computer Science. - 2005. - Vol.47. - pp. 48.-53.

[25] Kolyshkin A. A., Nazarovs S. Linear and Weakly Nonlinear Analysis of Two-Phase Shallow Wake Flows// WSEAS Transactions on Mathematics. - Vol.6. - pp. 1.-9.

[26] Kolyshkin A. A., Nazarovs S. Stability of Slowly Diverging Flows In Shallow Water// Mathematical Modelling and Analysis. - 2007 - Vol.12. - No.1. - pp. 101.-106.

[27] Kolyshkin A. A., Nazarovs S. Stability of particle-laden shallow flows: linear and weakly nonlinear analysis// Book of abstracts.International conference on approximation methods and numerical modelling in environment and natural sciences. - Spain, Granada, 2007, July 11.-13. - pp. 285.-290.

[28] Kolyshkin A. A., Nazarovs S. The Effect of Particles on Linear and Weakly Nonlinear Instability of a Two-Phase Shallow Flows// Progress in Industrial Mathematics at ECMI 2006. - Springer, 2008. - pp. 784.-792.

[29] Monkewitz P.A. The absolute and convective nature of instability in two-dimensional wakes at low Reynolds numbers// Phys. Fluids. - 1988 - Vol.31. - pp. 999.-1006.

[30] Nazarovs S. Stability analysis of shallow wake flows with free surface// Acta Universitatis Apulensis - No.10. - pp. 345.-354.

[31] van Prooijen B. C., Uijttewaal W. S. J. A linear approach for the evolution of coherent structures in shallow mixing layers// Physics of Fluids. - 2002 - Vol.14. - pp. 4105.-4114.

[32] Rivlin T. J. The Chebyshev polynomials. - Wiley, 1974.

[33] Schmid P. J. Henningson D. S. Stability and transition in shear flows. - Springer, 2001.

[34] Socolofsky S. A., Carmer C., Jirka G. H. Shallow turbulent wakes: linear stability analysis compared to experemental data// Shallow flows. - A.A.Balkema Publishers., 2003.

[35] Socolofsky S. A., Jirka G. H. Large scale flow structures and stability in shallow flows// J. Environmental Engineering and Science, Can. Soc. Civ. Eng. - Vol.3. - pp. 451-462

[36] Stewartson K., Stuart J. T. A non-linear instability theory for a wave system in plane Poiseuille flow// Journal of Fluid Mechanics. - 1971 - Vol.48. - pp. 529.-545.

[37] Streeter V. L., Wylie E. B., Bedford K. W. Fluid Mechanics. - McGraw Hill, 1998.

[38] Van Dyke M. An album of Fluid Motion. - The Parabolic Press, 1982.

[39] Wen F., Evans J. Linear instability of a two-layer flow with differential particle loading// Physics of Fluids. - 1994. - December,No.12. - pp. 3893.-3905.

[40] Xia R., Yen B. C. Significance of averaging coefficients in open-channel flow equations// Journal of Hidraulic Engineering. - 1994 - Vol.120. - pp. 169.-189.

[41] Yang Y., Chung J. N., Troutt T. R., Crowe C. T. Influence of particles on the spatial stability of two-phase layers// Physics of Fluids A2(10). - 1990. - October - pp. 1839.-1845.

[42] Yang Y., Chung J. N., Troutt T. R., Crowe C. T. The effects of particles on the stability of a two-phase wake flow// Internation Journal of Multiphase Flow. - Vol.19. - No.1. - pp 137.-149.

[43] Yen B. C. Open-channel flow equations revisited.// Journal of the engineering mechanics division. - 1973 - Vol.99. - pp. 979.-1009.

[44] Yen B. C., Wenzel H. G., Yoon Y. N. Resistance coefficients for steady spatially varied flow// Journal of the hydraulics division. - 1972 - August - pp. 1395.-1410.

[45] Zwillinger D. Handbook of differential equations. - Academic Press, 1998.

S. Nazarovs
Institute of Engineering Mathematics
Riga Technical University
1 Meza street, Riga, Latvia
email:*nazarow@yahoo.com*